UNIVERSITY
OF OSLO

Mari Dahl Eggen

Stochastic differential equations with memory and relations

Modelling of stratospheric dynamics

Thesis submitted for the degree of Philosophiae Doctor

Department of Mathematics
Faculty of Mathematics and Natural Sciences

This PhD grant was funded by NORSAR.

2023

Series of dissertations submitted to the
Faculty of Mathematics and Natural Sciences, University of Oslo
No. 2645

ISSN 1501-7710

Cover: UiO.
Print production: Graphic center, University of Oslo.

"we're all mad here. I'm mad. You're mad."
-Lewis Carroll

Acknowledgements

Thank you Fred Espen Benth for tremendous support, both on a theoretical and motivational level. Your door is always open for good advice, and you have gracefully pushed me forwards. Thank you Sven Peter Näsholm for introducing me to stratospheric research, and for giving clever strategical advice throughout these three years. Thank you Kristina Rognlien Dahl for a valuable on-boarding to my PhD project including tips, tricks, and guidance to my first publication. It has been a pleasure to share knowledge and perspectives with Alise Danielle Midtfjord, leading to two research papers that would not possibly exist without you. Thank you Ekaterina Vorobeva for your efficiency and great adapting skills in our interdisciplinary collaboration. I very much appreciate the time you have put down for support and inputs to the work of this thesis, Steffen Mæland, Ismael Vera Rodriguez and Quentin Brissaud. A special thanks to Paul Eisenberg for welcoming me to WU Vienna, and for sharing your impressive and intuitive understanding of mathematics. Also a big thanks to Aleksander Grochowicz for input on this thesis' introduction, and to Andreas Petterson for pointing me in the direction of a valuable reference. I'm also very thankful for having welcoming colleagues both at Niels Henrik Abels hus and at NORSAR.

This PhD thesis would not have become a reality without unconditional support and understanding from my one and only, Rollef. Thank you for helping me to orientate when I'm lost, and for always supporting my choices. Thank you Mom and Ellen Sofie for being my safe haven, where I can share joys and complaints. Thank you to my university pals Sejla, Ingrid, Pernille, Vilde, Elisabeth, Helene and Helle for exciting discussions and coffee breaks during our studies, and for continued friendship and support during these three years. A big thanks to Marthe, Katrine and Amalie for always showing devoted interest for my work and well-being. I would also like to thank Edvard for our occasional, still way to seldom, coffee breaks.

At last but not at least, I'm very grateful to the independent research institution NORSAR for enabling this PhD project through funding.

Mari Dahl Eggen
Oslo, May 2023

Summary

This thesis is a collection of five scientific papers, each referred to in this summary as Paper I – Paper V respectively.

Industry and society depend on accurate weather forecasting, with examples ranging from retail sales numbers and sunny hikes in the mountains, to pricing within the electricity markets and public safety during weather hazards. The importance of weather drives a continuous effort within the field of geophysics to improve both short- and long-term numerical weather prediction.

The atmosphere has a layered structure, where the troposphere and stratosphere are two of five major layers. Closest to the Earth's surface lays the troposphere that stretches from the ground up to about 10km altitude, whereas the overlaying stratosphere reaches up to about 50km. Probing of the stratosphere could be key in enhancing long-term weather forecasts on Earth's surface. The stratosphere is challenging to monitor, in particular its dynamics, meaning that successful remote sensing strategies are essential to develop. Research indicates that ground-based measurements of low-frequency inaudible sound waves called infrasound has potential as a remote sensing technique for the stratosphere. Motivated by findings in stratospheric and infrasonic research; the goal of this work is to develop a stochastic mathematical modelling framework able to relate the characteristics of infrasound detections to the state of the stratosphere.

To model stratospheric weather variables using infrasound it is essential to find a modelling framework able to represent weather variables well. Statistical evidence is presented in the literature that the class of Continuous-time Autoregressive Moving Average ((C)ARMA) processes provides a suitable modelling framework for surface temperature and wind variables. In Paper I we seek evidence of this from a mathematical point of view. Based on the physical laws of heat transfer we suggest the Gaussian linear parabolic Stochastic Partial Differential Equation (SPDE) as a stylized model for the time-varying temperature field over a geographical area. The SPDE is assessed as the infinite dimensional Ornstein-Uhlenbeck (OU) process, and we show that sampling of such process naturally admits a type of ARMA processes. Independent convergence results for time and space are derived, connecting the Gaussian linear parabolic SPDE with ARMA processes. A simulation study demonstrates our theoretical results for the stochastic heat equation; that is a special case of the SPDE under consideration. Note that the results implicitly connect Gaussian linear parabolic SPDEs with CARMA processes.

The results from Paper I substantiate using CARMA processes as modelling framework for the stratospheric state. The aim of Paper II is to provide empirical proofs that stratospheric temperature is well-represented by a CARMA model. We show that dynamics of daily-spatial mean values of stratospheric temperature over an Arctic circumpolar area follow a Lévy-driven CAR model (CARMA model without a moving average part) with seasonally varying mean and variance. We also find evidence that the temperature data could be better represented if incorporating stochastic volatility and time-dependent speed of mean reversion.

To add information from infrasound measurements for better representation of the stratospheric state, a multivariate CARMA (MCARMA) process is required as modelling framework. For this purpose, a model estimation methodology for Lévy-driven MCARMA processes is derived in Paper III. This is obtained through solving a discretized version of the MCARMA process recursively. With the goal of giving an empirical example demonstrating the model estimation methodology for a two-dimensional dynamical system of stratospheric temperature and wind, a convergence rate for jump diffusions with jumps of finite variance and infinite variations is derived theoretically. A Lévy-driven MCAR model is fit to the two-dimensional weather system with statistical significance, providing empirical evidence that the stratospheric state might be well-represented by this model.

The results obtained in Paper I – Paper III provide tools to represent a multivariate dynamical system of stratospheric weather variables and variables from ground-based infrasound measurements. The MCARMA processes provide a modelling framework where co-variations between the system variables are modelled in a linear fashion, and the autoregressive part of the model is assumed to be stationary. Empirical results indicate that the linearity and stationarity assumptions should be relaxed. We propose Stochastic Delay Differential Equations (SDDEs) with multiple point delays as a generalized modelling framework, where non-linear and non-stationary interactions between dynamical variables can be represented. The generality of this modelling framework brings additional challenges in model estimation as the exact forms of the non-linear and/or non-stationary model coefficient functions are unknown. Furthermore, if exact model coefficient functions are known (or guessed), proper methods of model estimation must be found.

The work in Paper IV addresses the problem of model estimation of Gaussian SDDEs when the model coefficient functions are unknown. The derived model estimation methodology can also be seen as a novel physics-informed type of machine learning model that we call the Delay-SDE-net. That is, the Delay-SDE-net is a multivariate SDDE with multiple point delays where the model coefficient functions are replaced with neural networks. This makes the model estimation an exercise of training neural networks. When a trained Delay-SDE-net is used to represent a multivariate dynamical system there will be an error compared to the assumed real-world SDDE representation. The theoretical error is derived as the sum of the discretization error and the two-layer neural network approximation error. This deep learning approach is validated in a case study where the model is fit to a two-dimensional system of stratospheric temperature and wind. The Delay-SDE-net model performs better than the MCAR model in Paper III.

In Paper V we explore if the Delay-SDE-net can represent the link between the stratospheric state and ground-based infrasound measurements. A stratospheric wind dataset is constructed as daily-zonal-mean zonal wind from the ECMWF ERA5 reanalysis model product. Furthermore, six infrasound datasets are constructed using infrasound detections from the three northern-most infrasound stations that are part of the International Monitoring System; the variables are daily values of the strongest infrasound amplitude, and the corresponding direction of arrival (called the backazimuth). The Delay-SDE-net is trained to

predict the near real-time zonal wind, solely using the constructed infrasound variables and day of year as input to the neural networks. The results indicate that there is a potential for assimilating infrasound observations into existing atmospheric models as a near real-time source of information about the large-scale stratospheric dynamics.

Sammendrag (Summary in Norwegian)

Denne avhandlingen er en samling av fem forskningsartikler, hvor vi i dette sammendraget refererer til hver av artiklene som Artikkel I – Artikkel V.

Det å levere nøyaktige værprognoser er viktig både for industrien og samfunnet. Dette gjelder for alt fra salgstall innen detaljhandel og solrike fjellturer, til prising innenfor energimarkedet og allmenn trygghet under naturkatastrofer. Viktigheten av vær driver i dag en kontinuerlig innsats innenfor geofysikkmiljøet for å forbedre numeriske korttids- og langtidsprognoser av vær.

Atmosfæren har en lagvis struktur, hvor troposfæren og stratosfæren er to av fem store hovedlag. Troposfæren er det atmosfæriske laget som ligger nærmest Jordens overflate, og dette området strekker seg fra bakken til omtrent 10 kilometers høyde. Det atmosfæriske laget som ligger ovenfor troposfæren kalles stratosfæren, og strekker seg opp til omtrent 50 kilometers høyde. Det å sondere stratosfæren har vist seg å kunne være en nøkkel for å forbedre langdisprognoser av været ved Jordens overflate. Fordi stratosfærens værdynamikk er vanskelig å monitorere, vil gode metoder for fjernmåling av dette området være essensielt å utvikle for vellykket sondering. Forskning indikerer at bakkebaserte målinger av lavfrekvente ikke-hørbare lydbølger, kalt infralyd, har potensiale som en fjernmålingsteknikk for stratosfæren. Motivert av funn rundt dette området innenfor stratosfære- og infralydforskning er et overordnet mål i denne avhandlingen å utvikle et stokastisk-matematisk modelleringsrammeverk som kan beskrive sammenhengen mellom karakteristikker av infralydmålinger og stratosfærens tilstand.

For å modellere stratosfæriske værvariabler ved bruk av informasjon fra infralydmålinger er det essensielt å finne et modelleringsrammeverk som kan representere værvariabler på en god måte. Det er i forskningslitteraturen blitt presentert statistiske resultater som underbygger at klassen av kontinuerlig-tid (diskret-tid) autoregressive og glidende gjennomsnittsprosesser (CARMA (ARMA) prosesser) innbefatter gode modelleringsrammeverk for temperatur- og vindvariabler ved jordoverflaten. I Artikkel I søker vi bevis for dette fra et matematisk ståsted. Basert på fysiske lover for varmeoverføring foreslår vi en Gaussisk lineær parabolsk Stokastisk Partiell Differensiallikning (SPDE) som en stilisert modell for et tidsvariabelt temperaturfelt over et gitt geografisk område. Denne SPDE-en er studert som en uendeligdimensjonal Ornstein-Uhlenbeck (OU) prosess, og vi viser at sampling av slike prosesser tilkjennegir seg som en gitt type av ARMA prosesser. Uavhengige konvergensresultater for tid og rom er utledet, og knytter Gaussiske lineære parabolske SPDE-er til ARMA prosesser. En simuleringsstudie underbygger de teoretiske resultatene for den stokastiske varmelikningen; et modelleringsrammeverk som er et spesialtilfelle av vår studerte klasse av SPDE-er. Resultatene i dette arbeidet gir en implisitt kobling mellom Gaussiske lineære parabolske SPDE-er og CARMA prosesser.

Resultatene fra Artikkel I underbygger det å bruke en CARMA prosess som modelleringsrammeverk for den stratosfæriske tilstanden. Målet i Artikkel II er å finne empiriske bevis på at stratosfærisk temperatur kan representeres ved

bruk av en slik modell. Vi viser at stratosfærisk temperaturdynamikk, studert som daglige gjennomsnittsverdier over et Arktisk sirkumpolart område, følger en Lévy-drevet CAR modell (CARMA modell uten glidende gjennomsnitt) med sesongvarierende gjennomsnitt og varians. Resultatene antyder at det studerte datasettet potensielt sett kan representeres mer nøyaktig ved å inkorporere stokastisk volatilitet og tidsvarierende gjennomsnittlig reverseringshastighet (speed of mean reversion) i modellen.

For å bedre representere den stratosfæriske tilstanden ved hjelp av informasjon fra infralydmålinger trengs en multivariat CARMA (MCARMA) prosess som modelleringsrammeverk. For dette formålet utledes i Artikkel III en modellestimeringsmetode for Lévy-drevne MCARMA prosesser. Metoden er utledet ved å rekursivt løse en diskretisert versjon av MCARMA prosessen. En teoretisk konvergensrate for hoppediffusjoner med endeligdimensjonale hopp og uendelig variasjon utledes videre. Dette resultatet fungerer som en teoretisk støtte for det empiriske eksempelet som demonstrerer den utledede modellestimeringsmetoden. I eksempelet ser vi på et dynamisk system bestående av stratosfæriske temperatur- og vindvariabler, og en Lévy-drevet MCAR modell er tilpasset det to-dimensjonale værsystemet med statistisk signifikans. Resultatet gir en empirisk indikasjon på at den stratosfæriske tilstanden kan representeres godt ved bruk av denne modellen.

Resultatene fra Artikkel I – Artikkel III kan fungere som verktøy for å representere et multivariat dynamisk system av stratosfæriske værvariabler og variabler fra bakkebaserte infralydmålinger. MCARMA modellen gir et modelleringsrammeverk hvor samvariasjonen mellom systemets variabler modelleres lineært, og den autoregressive delen av modellen er antatt å være stasjonær. Empiriske resultater indikerer at antakelsene om lineær og stasjonær samvariasjon er for restriktive. Vi foreslår derfor en Stokastisk Forsinket Differensiallikning (SDDE) med mange punktforsinkelser som et generalisert modelleringsrammeverk, hvor ikke-lineære og ikke-stasjonære interaksjoner mellom variabler kan bli representert. Generaliteten som kommer med dette modelleringsrammeverket, gir utfordringer når en modell skal estimeres fordi den eksakte formen på de ikke-lineære og/eller ikke-stasjonære modellkoeffisientfunksjonene er ukjente. Hvis formen på modellkoeffisientfunksjonene er kjent (eller gjettet) må man likevel klare å finne en passende modellestimeringsmetode.

Arbeidet som er lagt ned i Artikkel IV adresserer problemet med å finne en modellestimeringsmetode for Gaussiske SDDE-er når modellkoeffisientfunksjonene er ukjente. Modellestimeringsmetoden som utledes kan også ansees som en ny type fysikk-informert maskinlæringsmodell, som vi kaller Delay-SDE-net. Dette er fordi modellestimeringen blir en øvelse i å trene neurale nettverk, da Delay-SDE-net-modellen er en multivariat SDDE hvor modellkoeffisientfunksjonene er byttet ut med neurale nettverk. Når et trent Delay-SDE-net brukes til å representere et multivariat dynamisk system vil det finnes en feil i modellen, sammenliknet med den antatt reelle SDDE representasjonen. Den teoretiske feilen er utledet som en sum av diskretiseringsfeilen, og tilnærmingsfeilen som forekommer ved bruk av to-lags neurale nettverk. Denne dyp-lærings-tilnærmingen er validert i en case studie hvor modellen er tilpasset

et to-dimensjonalt værsystem bestående av stratosfæriske temperatur- og vind-variabler. Delay-SDE-net-modellen presterer bedre enn MCAR modellen som brukes i Artikkel III.

I Artikkel V undersøker vi om Delay-SDE-net-modellen kan representere koblingen mellom den stratosfæriske tilstanden og bakkebaserte infralydmålinger. Et datasett med stratosfærisk vind er konstruert som daglig-sonalt-gjennomsnitt av sonal vind fra ECMWF sitt ERA5 reanalyse modellprodukt. Videre konstrueres seks infralyd-datasett ved bruk av infralydmålinger fra de tre nordligste infralyd stasjonene som er del av The International Monitoring System; variablene er daglige verdier av sterkeste infralyd-amplitude, og tilsvarende ankomstretning (også kalt backazimuth). Delay-SDE-net-modellen trenes til å predikere nær-sanntids sonal vind ved bare å bruke informasjon fra konstruerte infralyd-variabler, samt dag i året, som input til de neurale nettverkene. Resultatene indikerer at det er potensiale for å assimilere infralydobservasjoner i eksisterende atmosfæriske modeller som en kilde til nær-sanntids informasjon om storskala stratosfærisk dynamikk.

List of Papers

Paper I

Benth, F.E, Eggen, M.D. and Eisenberg, P. "Ornstein-Uhlenbeck processes in Hilbert space and autoregressive moving-average time series".
Manuscript in preparation for submission.

Paper II

Eggen, M.D., Dahl, K.R., Näsholm, S.P. and Mæland, S. "Stochastic modeling of stratospheric temperature". In: *Math Geosci.* Vol. 54, no. 4 (2022), pp. 651—678. DOI: 10.1007/s11004-021-09990-6.

Paper III

Eggen, M.D. "The multivariate ARMA/CARMA transformation relation".
Review received from Scandinavian Journal of Statistics. Manuscript in preparation for resubmission. Available at ArXiv:2205.05080, 2022.

Paper IV

Eggen, M.D. and Midtfjord, A.D. "Delay-SDE-net: A deep learning approach for time series modelling with memory and uncertainty estimates".
Shared first authorship between the two authors. Review received from Journal of Machine Learning Research. Manuscript in preparation for resubmission. Available at ArXiv:2303.08587, 2023.

Paper V

Eggen, M.D., Vorobeva, E., Midtfjord, A.D., Benth, F.E., Hupe, P., Brissaud, Q., Orsolini, Y. and Näsholm, S.P. "Near real-time stratospheric circulation diagnostics based on high-latitude infrasound data using a stochastics-founded machine learning model".
Shared first authorship between Mari Dahl Eggen and Ekaterina Vorobeva. Manuscript in preparation for submission.

Contents

Chapter 1

Introduction

1.1 Motivation and objectives

Industry and society depend on accurate weather forecasting, with examples ranging from retail sales numbers and sunny hikes in the mountains, to pricing within the electricity markets and public safety during weather hazards. The importance of weather drives a continuous effort within the field of geophysics to improve both short- and long-term numerical weather prediction. This dissertation aims at developing tools that can potentially add value to the study of long-term predictions.

The atmosphere has a layered structure, where the troposphere and stratosphere are two of five major layers. Closest to the Earth's surface lays the troposphere that stretches from the ground up to about 10 km altitude, whereas the overlaying stratosphere reaches up to about 50 km. Probing of the stratosphere could be key in enhancing long-term weather forecasts on Earth's surface. The stratosphere is challenging to monitor, in particular its dynamics, meaning that successful remote sensing strategies are essential to develop. Research indicates that ground-based measurements of low-frequency inaudible sound waves called infrasound has potential as a remote sensing technique for the stratosphere.

Motivated by findings in stratospheric and infrasonic research; the goal of this work is to develop a mathematical modelling framework able to relate the characteristics of infrasound detections to stratospheric temperature and wind. Essential features required for such models are that they do the following: 1) capture variations of stratospheric weather variables; 2) capture variations of relevant infrasound variables; and 3) most importantly, represent the co-variation between stratospheric variables and infrasound characteristics. Furthermore, modelling of uncertainties is key to build robust predictive models. These challenges initiates the pursuit for a stochastic model that exhibits suitable properties.

To address this ambition, novel mathematical results are obtained to substantiate our choice of modelling framework, as well as to develop proper estimation methodologies. Using classical mathematical and stochastic theory, including numerical methods as well as neural networks, we illustrate that Stochastic Differential Equations (SDEs) with memory exhibit the necessary properties for our purpose. The concluding paper in this thesis uses a stochastics-founded machine learning model[1] that defines real-time characteristics of the polar upper stratospheric state solely based on day of year and infrasound measurements at three high-latitude ground-based monitoring stations.

[1] Developed during this PhD work

1.2 Geophysical context

This section introduces relevant aspects of stratospheric research. It is assumed that the reader has little prior knowledge within the field of geophysics. In Section 1.2.1, a popular science text presents the stratospheric polar vortex and its coupling to weather on Earth's surface. The popular science text is based on information from [39], [40], [22], [57], [61] and [65]. Section 1.2.2 elaborates how the stratospheric polar vortex is connected to long-term surface weather forecasting. Section 1.2.3 introduces infrasound acoustics, and gives a brief summary about how infrasound measurements can be used to interpret the state of the stratosphere.

1.2.1 The stratospheric polar vortex

Imagine yourself in an aircraft high up in the air, at altitudes above the highway of common flights. Here, you will spot a wide torus of strong winds centered at the North Pole. You just discovered what we call the Arctic stratospheric polar vortex. Sometimes, these strong and volatile eastward winter winds making up the stratospheric polar vortex are abruptly disrupted. What might follow is a winter-time polar vortex entailing summer-time conditions, with the average circumpolar wind being reversed. This phenomenon is called a sudden stratospheric warming. Even though this phenomenon occurs at high altitudes, you can also observe its consequences during the aircraft's decent, all the way down to Earth's surface.

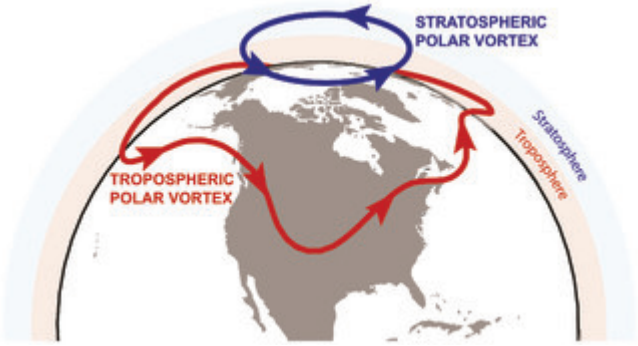

Figure 1.1: An illustration of the stratospheric polar vortex found in [65]. The area below the stratosphere is called the troposphere. The red and wiggly circle is the edge of the tropospheric polar vortex, and is what we refer to as the jet stream. *©American Meteorological Society. Used with permission.*

Just like us living on the Earth's surface can always feel the weather on our bodies, the atmosphere is dynamic also at high altitudes. For example, you might have felt discomfort on a seemingly quiet flight when turbulence suddenly takes hold of the airplane. This happens because of abrupt changes in the surrounding weather. Such situations normally happen around 10 km above the surface, but

abrupt changes in the atmospheric dynamics can happen also at substantially higher altitudes.

The ice-cold area that lays about 10 to 50 km above the surface of the Earth is called the stratosphere, where temperatures range from minus 15 to minus 60 degrees Celsius. Despite these extreme temperature conditions, stratospheric wind conditions are stable compared to the winds closer to the surface. That is, as long as you stay away from the stratospheric poles.

In winter time, the stratospheric winds normally orbit the North Pole at high speed from west to east. The wind speed can reach about 110 m/s, which is far higher than the surface wind speeds recorded from the most powerful tornadoes. In summer time, the direction of the stratospheric polar vortex changes, meaning that the winds are westward. Now the wind speed is also much lower than in the winter. The significant change in wind speed between stratospheric winter and summer time is a natural cycle, just like the seasonal differences that we see at the surface. But what happens if this circulation is abruptly disrupted?

The natural circulation of the stratospheric polar vortex is actually disrupted approximately six times a decade. Before investigating the consequences of this phenomenon, we take a look at what "abruptly disrupted" means in this context.

The gigantic westward vortex of air masses surrounding the North Pole in winter is sensitive to disturbances in the form of large waves forming from, for example, interactions between topography and the more turbulent conditions on Earth's surface. Such bombardment of the stratospheric polar vortex might result in a weakening of the wind speed. If this weakening is severe, the stratospheric polar vortex breaks down, and the average winds might eventually change direction. This phenomenon is called a sudden stratospheric warming.

During a sudden stratospheric warming, the surrounding temperature can increase by up to 50 degrees Celsius in just a few days. A consequence of this natural phenomenon is that the large vortex can move away from the pole, and even split into two independent vortices. Just as the conditions close to Earth can influence the winter time stratospheric polar vortex, the effect of a sudden stratospheric warming can couple downwards in the weather system.

Between the stratosphere and the surface of the Earth there is a stream of winds wiggling around the Northern Hemisphere like a narrow river. This is called the (tropospheric) jet stream. With the jet stream comes storm tracks, consistently moving alongside these wiggly wind streams. The position of the jet stream highly influences the climate at Earth's surface. Since changing wind speeds in the stratosphere influence the position of the jet stream, unusual events in the stratosphere start a chain reaction striking surface weather conditions.

Consequences of sudden stratospheric warmings can range from events of cold Arctic air masses leaking into the more temperate areas of northern Europe and eastern USA, to intensified stormy weather in the Atlantic basin and surroundings. Based on such severe consequences, especially with a weather system in transition due to global warming, it is not hard to acknowledge the importance of better knowledge and understanding of stratospheric weather conditions and how they influence us living on Earth.

1.2.2 Enhanced long-term forecasting of surface weather with better stratospheric data

Weather in the troposphere is chaotic and therefore challenging to predict at longer timescales. As explained in [39], because weather and climate variability is constrained by external factors that vary at slower timescales, the predictability of tropospheric weather can reach approximately 10 days. Examples of such constraining factors are sea-surface temperature and snow cover extent. It is well-established that the stratosphere is another example of such a constraining component. See also [41].

As implied in Section 1.2.1, tropospheric conditions affect stratospheric conditions and vice versa. This phenomenon is referred to as stratosphere-troposphere coupling, and a thorough description is given in [21]. As pointed out in [21], dynamical variability exists on a wide range of timescales in the stratosphere. That is to the extent that the stratosphere's constraints on the troposphere have potential to enhance tropospheric predictability on sub-seasonal to seasonal timescales and beyond.

The dynamic variability of the Northern Hemisphere stratospheric polar vortex is particularly influential on tropospheric weather [4, 47, 49, 58, 66]. In particular, the phenomenon of Sudden Stratospheric Warmings (SSWs) has received a lot of attention because of its pronounced influence on tropospheric weather [5]. Improving SSW forecasting therefore gives the potential for enhanced long-term surface weather predictions. As explained in [53], tropospheric regions affected by SSWs achieve increased predictability up to $3-6$ weeks after extreme stratospheric events. Furthermore, as the probability of SSW occurrences is coupled to other atmospheric phenomena with variability at slow timescales, probabilistic predictability of stratospheric variability may be extended to a few months or longer in the future. Probabilistic predictability of tropospheric weather has the potential to increase analogously.

1.2.3 Probing the stratosphere using infrasound acoustics

A challenge in enhancing stratospheric weather prediction is the sparseness of in-situ observations, in particular for winds beyond 30 km altitude. Model experiments suggest that new observational techniques for monitoring the upper stratosphere might contribute to enhance wintertime forecasting skills [46].

A remote sensing technique that has emerged for the upper stratosphere is based on extracting information from ground-based infrasound measurements, see, e.g., [1, 3, 61]. Infrasound is low-frequency ($< 20\,\mathrm{Hz}$) sound waves that are inaudible to the human ear. Such sound waves originating from sources in the troposphere travel through the atmosphere, and can be reflected back to the surface from different atmospheric levels. Measurements of such ducted infrasound waves carry information from the path of propagation that can be interpreted and used to monitor, for example, the stratosphere. Such information was used to study infrasonic signatures of SSWs in pioneering works already in the 1970s, see [27]. A more thorough explanation of the underlying mechanisms

and a historical overview of studies on infrasonic signatures of SSWs is provided in [61].

A kind of infrasound waves of particular interest for atmospheric probing is called microbaroms. They make up a quasi-continuous field of sound waves generated by nonlinear interactions between counter-propagating ocean waves, typically within the frequency range of $0.1-0.6$ Hz, see, e.g., [9, 26, 64]. Infrasonic signatures for SSWs as noted in early work from the 1970s [27] were found in guided microbaroms, a discovery that is now attracting more attention. For example, [45] found that seasonal trends in measured microbarom amplitude and arrival direction are primarily driven by seasonal reversal (as explained in Section 1.2.1) of stratospheric winds. Furthermore, it has been suggested that there is potential in utilizing microbarom signals to probe stratospheric wind for assimilation of infrasound data into atmospheric models, see [1, 3] for outlooks, as well as Paper V in the current thesis for a related study.

In addition to results indicating that microbaroms can be used to probe the stratosphere, near real-time global data availability of microbarom detections has become reality. The Comprehensive Nuclear-Test-Ban Treaty (CTBT) was signed in 1996, banning all nuclear explosions. As nuclear explosions are a source of infrasound and other measurable signals, the International Monitoring System (IMS) was established for signal detection to monitor worldwide compliance. What is referred to as the IMS infrasound network focuses on measuring infrasound signals and consists of 60 stations distributed globally. Data from the IMS infrasound network have been shown to be valuable in studies of natural infrasound sources and related applications. This is also the case for detection of ocean-generated microbaroms, where the IMS infrasound network record microbarom waves in near real-time that can be used to probe the stratosphere. See, for example, [36], [24] and [52] for more information on CTBT and IMS.

With scientific results indicating that microbarom signals have great potential for use in remote atmospheric sensing, and with near real-time data availability of microbaroms, it is clear that the use of microbarom detections for probing the stratosphere is a promising research topic. However, as the IMS infrasound network is continuously bombarded with microbaroms, it takes proper pre-processing routines, data assessment, and modelling before microbarom detections can be used in applications. Research has been done during the recent years to contribute to these aspects. See, for example, [34], [62] and [64]. An interesting recent work with this respect is done in [35], where systematically processed infrasound data products from 53 stations in the IMS infrasound network are composed and openly provided to the general public. This work facilitates the demonstration of potential use of infrasound detections for applications, as researchers less familiar with infrasound data processing now have the opportunity to easily explore processed IMS infrasound data directly.

The introduction in Section 1.2.2 explains that augmented probing of the stratosphere has potential to enhance long-term forecasting in the future. Still, a lot of research remains to successfully provide real-time measurements of the stratospheric state, and subsequently to incorporate the information into existing weather prediction models. One important piece of the puzzle that remains to

be solved is to properly describe the link between real-time infrasound detections and the current state of the stratosphere. Furthermore, this link would ideally be explicit, such that it can be straightforwardly exploited in future research to better understand stratosphere-troposphere coupling and to enhance long-term weather forecasting.

1.3 Relevant topics in stochastics

This section introduces stochastic models and theory relevant in this thesis. Section 1.3.1 presents particular SDEs with memory, Section 1.3.2 gives an introduction to Wiener processes with values in Hilbert space, and Section 1.3.3 is about methods for assessing the stochastic heat equation. It is assumed that the reader has a solid background within the field of stochastic analysis.

1.3.1 Stochastic differential equations with memory

Many dynamical systems have inherent memory, meaning that their time evolution is dependent on the systems' past states. Some examples of fields where such dynamical systems are relevant to study include biology and medicine [37, 56, 59, 60], geophysics [29, 43, 54] and finance [2, 25, 67]. This section presents SDEs with memory that are applied for the geophysical problem of this thesis. First, we introduce a flexible modelling framework, that is Stochastic Delay Differential Equations (SDDEs) with multiple point delays. Then, modelling frameworks from the family of Autoregressive Moving Average (ARMA) processes are introduced, including continuous-time, multivariate and infinite-dimensional processes.

Unless noted otherwise, we assume given a complete filtered probability space $(\Omega, \mathcal{F}, \{\mathcal{F}_t\}_{t\geq 0}, P)$ under which all stochastic processes $\{X(t)\}_{t\geq 0}$ are defined.

Stochastic delay differential equations

The aim of this section is to introduce SDDEs with multiple point delays.

The class of SDDEs [see for example 55] represents SDEs that are dependent on both current and past states of the dynamical system they describe. This means that SDDEs are non-Markovian processes, and their inherent memory property can be used to give a more accurate representation of the evolution of dynamical systems with memory. As discussed in [6], one cannot use the well-established Markov process theory to study SDDE solutions. The Markov property can be recovered by lifting SDDEs to suitable infinite-dimensional path spaces, where the SDDEs take form as infinite dimensional Stochastic Partial Differential Equations (SPDEs). There exists well-established theory for SPDEs in infinite dimensions, however, some difficulties are encountered as some finite-dimensional properties fail to hold in infinite dimensions. We will not discuss the issue of these theoretical considerations further, as this work focuses on established results for use in applications. For a survey of results related to

SDDEs up to and including the year of 2002, see [38]. More recent results are presented in [6].

Define a back-looking time interval $[-\tau, 0]$, $\tau > 0$, and denote all continuous (d-dimensional) functions on this interval as $C := C([-\tau, 0]; \mathbb{R}^d)$. Given a d-dimensional stochastic process $X(t) : [-\tau, T] \times \Omega \to \mathbb{R}^d$, where $T \in \mathbb{R}^+$, define the corresponding segment process as

$$X_t(u) := X(t+u), \quad u \in [-\tau, 0], \quad t \in [0, T], \tag{1.1}$$

with X_t taking values in C. Early considerations of SDDEs study stochastic processes $X(t)$ satisfying

$$dX(t) = f(X_t)dt + g(X_t)dB(t), \quad t \geq 0 \tag{1.2}$$

where f and g are real-valued continuous drift and diffusion functions on C, respectively, and $\{B(t)\}_{t\geq 0}$ is a (multivariate) standard Brownian motion process. For example, the work in [44], that was published in 1968, presents existence, uniqueness and stability results for the SDDE in Eq. (1.2) involving conditions on the model coefficients and SDDE initial condition. Years later, that is in 1998, [55] considered SDDEs on the form

$$dX(t) = f(t, X_t)dt + g(t, X_t)dB(t), \quad t \geq 0, \tag{1.3}$$

with $\mathcal{F}_0$-measurable continuous initial path $\eta : \Omega \to C$. Note that $X_0 = \eta$. Several topics on non-stationary SDDEs as in Eq. (1.3) are considered in [55], including existence and uniqueness of solutions.

For applications in this thesis, a further developed version of the SDDE in Eq. (1.3) is used, where the segment process (Eq. (1.1)) is projected to represent multiple point delays. This particular SDDE was introduced and studied in [32] and [33][2]. With a framework as given above, we define a projection $\Pi : C \to \mathbb{R}^{dp}$ as

$$\Pi(\eta) := (\eta(u_1), \ldots, \eta(u_p)) \in \mathbb{R}^{dp},$$

where $u_1, \ldots, u_p \in [-\tau, 0]$ are fixed time points. We say that Π is the projection associated to the points $u_1, \ldots, u_p$. Now, given two projections Π_1 and Π_2 with associated time points $u_{1,1}, \ldots, u_{1,p_1} \in [-\tau, 0]$ and $u_{2,1}, \ldots, u_{2,p_2} \in [-\tau, 0]$ respectively, define the multiple point delayed SDDE as

$$dX(t) = f(t, \Pi_1(X_t))dt + g(t, \Pi_2(X_t))dB(t), \quad t \geq 0, \tag{1.4}$$

with $X(t) = \eta(t)$ for $-\tau \leq t < 0$. The SDDE in Eq. (1.4) admits a strong and unique solution, $X(t)$, when required conditions are satisfied. Furthermore, a strong Milstein scheme for such SDDEs is derived in [32] and [33], and the scheme is shown to have a convergence rate of order 1. In this thesis, the Milstein scheme is used for the purpose of approximating multiple point delayed SDDEs as in Eq. (1.4) using neural networks.

[2]Works from 2001 and 2004 respectively, where [32] is a prior version of [33]

ARMA and CARMA processes

The family of autoregressive moving average (ARMA) processes is important in modelling of time series data. Such processes use historic information to explain future values of a time series in a linear fashion. Due to their particular linear structure, the theory for prediction of such time series models is fairy simple, see [18] and [20]. The continuous-time analogue of ARMA processes is the family of continuous-time ARMA (CARMA) processes. That is, ARMA processes are defined by linear difference equations, and CARMA processes are defined using analogous linear differential equations [20]. We will see that CARMA processes have a state-space form admitting a so-called (multivariate) Ornstein-Uhlenbeck (OU) process [28, 51]. In this section, we introduce $\mathbb{R}$-valued Gaussian ARMA and CARMA processes. More flexible models, including multivariate versions and Lévy-driven processes, are introduced and applied in the papers of this thesis[3].

Assume that given a complete filtered probability space $(\Omega, \mathcal{F}, \{\mathcal{F}_n\}_{n\in\mathbb{N}_0}, P)$. Denote by $X(n) : \mathbb{N}\times\Omega \to \mathbb{R}$ a (discrete-time) ARMA process. We define ARMA processes according to the definition given in [20].

Definition 1.3.1 ([20], Definition 3.1.1)**.** $\{X(n)\}_{n\in\mathbb{N}}$ is an ARMA(p, q) process if $\{X(n)\}_{n\in\mathbb{N}}$ is stationary and if for every n,

$$X(n) - \phi_1 - \cdots - \phi_p X(n-p) = Z(n) + \theta_1 Z(n-1) + \cdots + \theta_q Z(n-q),$$

where $Z \coloneqq \{Z(n)\} \sim N(0, \sigma^2)$ and the polynomials $(1 - \phi_1 z - \cdots - \phi_p z^p)$ and $(1 + \theta_1 z + \cdots + \theta_q z^q)$ have no common factors.

In the above definition $N(0, \sigma^2)$ denotes zero mean normal distribution with variance $\sigma^2 \in \mathbb{R}^+$, and $\phi_i, \theta_j \in \mathbb{R}$ for $i = 1, \ldots, p$ and $j = 1, \ldots, q$. Note that the definition in [20] is slightly more general as Z can be white noise with variance $\sigma^2 \in \mathbb{R}^+$. In order to choose the correct orders p and q for ARMA(p, q) processes in applications, the autocorrelation function and partial autocorrelation function of time series is a helpful tool. For more about model selection and other additional information about (vector-valued) ARMA processes, see, for example, [48] and [30].

Now, let $X(t) : \mathbb{R}^+\times\Omega \to \mathbb{R}^p$ be a multivariate OU-process to be defined below, and let $Y(t) = b^\top X(t)$, where $b \coloneqq [b_0, b_1, \ldots, b_{p-2}, b_{p-1}]^\top$, be a (continuous-time) CARMA process. Again inspired by [20] we define CARMA(p, q) processes as follows.

Definition 1.3.2 ([20], Section 11.5.2)**.** $\{Y(t)\}_{t\geq 0}$ is a zero-mean Gaussian CARMA(p, q) process, $0 \leq q < p$, if $\{Y(t)\}_{t\geq 0}$ is a strictly stationary process satisfying the p-th order linear differential equation

$$\begin{aligned} &D^p Y(t) + a_1 D^{p-1} Y(t) + \cdots + a_p Y(t) \\ &= b_0 DB(t) + b_1 D^2 B(t) + \cdots + b_q D^{q+1} B(t), \end{aligned}$$

[3] Vector-valued autoregressive moving average processes are defined in the following section

where D^j denotes j-fold differentiation with respect to t, $\{B(t)\}_{t\geq 0}$ is a standard Brownian motion process, and $a_1, \ldots, a_p$ and $b_0, \ldots, b_q$ are constants. It is assumed that $b_q \neq 0$, $b_j := 0$ for $j > q$, and that the polynomials $(z^p + a_1 z^{p-1} + \cdots + a_p)$ and $(b_0 + b_1 z + \ldots + b_q z^q)$ have no common zeroes.

The CARMA(p, q) processes can be written with a so-called state-space representation that can be used to omit derivatives of the Brownian motion process. That is, we say that $Y(t) = b^\top X(t)$ is the observations equation, and that $X(t)$ solves the state equation

$$dX(t) = AX(t)dt + e_p dB(t), \tag{1.5}$$

where e_p is the p-th unit vector in $\mathbb{R}^p$ and $A \in \mathbb{R}^{p\times p}$ is given by

$$A = \begin{bmatrix} 0 & 1 & 0 & \cdots & 0 \\ 0 & 0 & 1 & \cdots & 0 \\ \vdots & \vdots & \vdots & \ddots & \vdots \\ 0 & 0 & 0 & \cdots & 1 \\ -\alpha_p & -\alpha_{p-1} & -\alpha_{p-2} & \cdots & -\alpha_1 \end{bmatrix}.$$

Using the state-space representation, Gaussian CARMA(p, q) processes can be studied using classical Itô calculus. The state equation in Eq. (1.5) is a multivariate OU-process and, as stated in [20], the multivariate SDE has uniqe solution

$$X(t) = e^{At}X(0) + \int_0^t e^{A(t-u)} e_p dB(u), \quad 0 \geq t < \infty,$$

where $X(0)$ is a normally distributed random vector independent of increments of $B(t)$ and $e^{At} := \sum_{j=0}^{\infty}(A^j/j!)t^j$. For more about (multivariate) CARMA(p, q) processes, see for example [15] and [51].

Note that ARMA and CARMA processes are linked to SDDEs, see [8] and [7].

Autoregressive processes in Hilbert space

In this section we introduce AR processes on a Hilbert space, an extension of the well-known theory of AR processes with values in $\mathbb{R}$ (or $\mathbb{R}^d$ in the multivariate case). This introduction is based on theory from [14]. In the following, $\{X_n\}_{n\in\mathbb{N}_0}$ refers to a sequence of square-integrable random variables defined on the complete filtered probability space $(\Omega, \mathcal{F}, \{\mathcal{F}\}_{n\in\mathbb{N}_0}, P)$. We start this section by recalling the definition of finite-dimensional vector autoregressive moving average (VARMA) processes [see for example 30] as a motivation.

Finite-dimensional vector autoregressive processes of order p, also referred to as VAR(p) processes, are given as a sequence of random variables $X_n \in \mathbb{R}^d$ satisfying

$$X_n = \sum_{j=1}^{p} A_j X_{n-j} + \epsilon_n, \tag{1.6}$$

where $A_j \in \mathbb{R}^{d\times d}$, $j = 1, \ldots, p$, and $\{\epsilon_n\}_{n\in\mathbb{N}_0}$ is a discrete Gaussian process with values in $\mathbb{R}^d$. Further, a sequence of random variables $X_n \in \mathbb{R}^d$ satisfying

$$X_n = \sum_{j=0}^{q} B_j \epsilon_{n-j}, \tag{1.7}$$

where B_0 is the d-dimensional identity matrix, $B_0 = I_d$, with $B_j \in \mathbb{R}^{d\times d}$, $j = 0, \ldots, p$, and where $\{\epsilon_n\}_{n\in\mathbb{N}_0}$ is as above, are called finite-dimensional vector moving average processes of order q, or VMA(q) processes. The VAR(p) process is said to be stationary when $\det(I_d - zA) \neq 0$ with $z \in \mathbb{C}$ such that $|z| \leq 1$. Note that the VMA(q) process is stationary by definition. Combining Eq. (1.6) and (1.7), we obtain the d-dimensional VARMA(p, q) process, that is

$$X_n = \sum_{j=1}^{p} A_j X_{n-j} + \sum_{j=0}^{q} B_j \epsilon_{n-j}.$$

Similarly, given a real-valued separable Hilbert space H, we can define an H-valued process

$$X_n = \rho X_{n-1} + \epsilon_n, \tag{1.8}$$

with $\rho \in \mathcal{L}$, where $\mathcal{L}$ is the class of bounded linear operators, and where $\{\epsilon_n\}_{n\in\mathbb{N}_0}$ is a Q-Wiener process. We call the process in Eq. (1.8) an ARH(1) process. It is clear that ARH(1) processes is a generalization of the VAR(1) process. As explained in Theorem 3.1 of [14], the series

$$X_n = \sum_{j=0}^{\infty} \rho^j(\epsilon_{n-j}), \tag{1.9}$$

is a unique stationary solution of Eq. (1.8) if there exists an integer $j_0 \geq 1$ such that $\|\rho^{j_0}\|_{\text{op}} < 1$, $\|\cdot\|_{\text{op}}$ being the operator norm. Moreover, the the series in Eq. (1.9) converges in $L^2(\Omega, H)$ with probability 1.

Note that once ARH(1) processes are defined, it is straightforward to define the analogue ARH(p) processes. We will, however, not introduce these higher order processes, as ARH(1) are the only AR processes in Hilbert space considered in this thesis.

1.3.2 Q-Wiener processes and Itô integrals

As SPDEs are SDEs evolving in space and time we need to define space-time stochastic forcing. Random fields evolving in time would provide such forcing. In this section, we introduce Gaussian random fields as a motivation. Then we extend this concept to Gaussian processes with values in Hilbert space, namely Q-Wiener processes. The following theory is introduced under a filtered probability space $(\Omega, \mathcal{F}, \{\mathcal{F}_t\}_{t\geq 0}, P)$. We will consider processes of $\mathcal{F}$-measurable Gaussian random variables, X, with values in a separable (measurable) Hilbert

space $(H, \mathcal{B}(H))$, where $\mathcal{B}(H)$ is the Borel σ-algebra on H. We denote the norm and inner product on H as $|\cdot|$ and $\langle \cdot, \cdot \rangle$ respectively. Note that in this setup, we have $X \in L^2(\Omega, H)$. Recall that, given a set $T \subset \mathbb{R}$, $\{X(t)\}_{t \in T}$ is an H-valued stochastic process of random variables $X : T \times \Omega \to H$, and we often write $X(t) \coloneqq X(t, \omega)$, $t \in T$, $\omega \in \Omega$. Finally, $\mathcal{L}$ denotes the space of bounded linear operators.

We assume that the reader is familiar with classical Itô calculus and basic concepts within linear functional analysis (see also Appendix A). For an introduction of random variables and stochastic processes in Hilbert space see Appendix A. This section is exclusively based on theory presented in [50].

Random fields

Define a real-valued random variable $Y : D \times \Omega \to \mathbb{R}$, with $D \subset \mathbb{R}^d$. We write $Y(x) \coloneqq Y(x, \omega)$, for $x \in D$, $\omega \in \Omega$. A random field is defined as follows.

Definition 1.3.3. A random field is the set $\{Y(x)\}_{x \in D}$.

Note that, for fixed $\omega \in \Omega$, $Y(\cdot, \omega)$ is referred to as a realisation of the random field. In the given setup we have $Y(x) \in L^2(\Omega)$ for every $x \in D$, meaning that we have well-defined mean function $\mu(x) \coloneqq E[Y(x)]$ and covariance function

$$C(x, y) \coloneqq \mathrm{Cov}(Y(x), Y(y)) = E[(Y(x) - \mu(x))(Y(y) - \mu(y))], \quad x, y \in D.$$

As we are working with Gaussian random variables, $Y(x) \sim N(\mu, C)$, $x \in D$, we refer to $\{Y(x)\}_{x \in D}$ as a Gaussian random field.

As already noted, random fields evolving in time would provide a suitable forcing for SPDEs. As we are using a semigroup approach to study SPDEs in this thesis, we will not introduce the more complex concept of space-time random fields.

Q-Wiener processes and their approximation

It is often convenient to study SPDEs as stochastic ordinary differential equations (SODEs) with values in a Hilbert space to suppress the spatial dimension. With this approach, the driving random field has to be replaced with an H-valued stochastic process. In this section we introduce the so-called Q-Wiener process, that is a Gaussian random process with values on a separable Hilbert space. We will also show how their sample paths can be approximated.

Let $Q \in \mathcal{L}(H)$ be symmetric positive semi-definite and of trace class, with orthonormal basis $\{e_j : j \in \mathbb{N}\}$ and corresponding eigenvalues $c_j \geq 0$ satisfying $\sum_{j \in \mathbb{N}} c_j < \infty$. The Q-Wiener process is defined as follows.

Definition 1.3.4 ([50], Definition 10.6)**.** An H-valued stochastic process $\{W(t)\}_{t \geq 0}$ is a Q-Wiener process if 1) $W(0) = 0$ a.s.; 2) $W(t)$ is a continuous function $\mathbb{R}^+ \to H$, for each $\omega \in \Omega$; 3) $W(t)$ is $\mathcal{F}_t$-adapted and $W(t) - W(s)$ is independent of $\mathcal{F}_s$ for $s < t$; and 4) $W(t) - W(s) \sim N(0, (t - s)Q)$ for all $0 \leq s \leq t$.

Note that Q is a well defined covariance operator at $t = 1$.

In applications of this work we consider $L^2(D)$-valued Q-Wiener processes for a given domain D. With the presented setup, the Q-Wiener process can always be decomposed as

$$W(t) = \sum_{j=1}^{\infty} \sqrt{c_j} e_j B_j(t), \quad \text{a.s.}, \tag{1.10}$$

where $B_j(t)$ are IID $\mathcal{F}_t$-Brownian motions for each $j \in \mathbb{N}$. As stated in [50, Thm. 10.7], the series converges in $L^2(\Omega, C([0,T], H))$ for any $T > 0$.

As a result of Eq. (1.10), sample paths of Q-Wiener processes can be approximated numerically as a truncated linear combination when the eigenfunctions of Q are known.

Itô integrals with respect to Q-Wiener processes

When studying SPDEs as (Q-Wiener driven) SDEs with values in a Hilbert space, U, it is essential to define Itô integrals with respect to Q-Wiener processes. Note that a requirement would be that the Itô integral takes values in U. As explained in [50], this could be obtained by considering $L_0^2 \coloneqq \mathcal{L}(H_0, U)$-valued integrands, where $H_0 \subset H$ is known as the Cameron-Martin space. We denote the norm on U as $|\cdot|_U$. The space L_0^2 is defined as follows.

Definition 1.3.5 ([50], Definition 10.15)**.** Let $H_0 \coloneqq \{Q^{1/2}v : v \in H\}$ for $Q^{1/2}$ defined by Eq. (A.3). L_0^2 is the set of linear operators $G : H_0 \to U$ such that

$$\|G\|_{L_0^2} \coloneqq \left(\sum_{j=1}^{\infty} |GQ^{1/2} e_j|_U^2 \right)^{1/2} = \|GQ^{1/2}\|_{\mathrm{HS}(H,U)} < \infty,$$

where $\{e_j : j \in \mathbb{N}\}$ is an orthonormal basis for H and $\|\cdot\|_{\mathrm{HS}(H,U)}$ is the Hilbert-Scmidt norm. L_0^2 is a Banach space with norm $\|\cdot\|_{L_0^2}$.

Note that $\{e_j : j \in \mathbb{N}\}$ are eigenfunctions of Q, and that $G \coloneqq \{G(t)\}_{t \geq 0}$ is a L_0^2-valued stochastic process.

Let $\{\hat{e}_k : k \in \mathbb{N}\}$ be an orthonormal basis of U, and let the stochastic process $\langle GQ^{1/2} e_j, \hat{e}_k \rangle_U$ be predictable for each $j, k \in \mathbb{N}$. Then also G is predictable, and we can define the Q-Wiener Itô integral.

Definition 1.3.6 ([50])**.** Let G be an L_0^2-valued predictable stochastic process. Then the U-valued Q-Wiener Itô integral

$$\int_0^t G(s) dW(s) \coloneqq \sum_{j=1}^{\infty} \int_0^t G(s) \sqrt{c_j} e_j dB_j(s), \tag{1.11}$$

is well defined.

As a remark, we note that the J-truncated sum of Eq. (1.11) converge in $L^2(\Omega, U)$ when $J \to \infty$.

1.3.3 The stochastic heat equation

The aim of this section is to introduce theory used to assess the stochastic heat equation as a numerical approximation. We focus on the stochastic heat equation driven by Gaussian noise. That is an SPDE on the form

$$dY(t,x) = \Delta Y(t,x)dt + \sigma dW(t,x), \quad (t,x) \in \mathbb{R}_+ \times D, \tag{1.12}$$

with $D \subset \mathbb{R}^d$, $d \in \mathbb{N}$, and initial condition $Y(0,x) \in \mathbb{R}$, where Δ is the Laplace operator, σ is a scaling acting on the noise and $W(t,x)$ is a space-time Gaussian field. For considerations about existence and uniqueness of solutions, see for example [31]. Note that the stochastic heat equation is a special case of the class of semilinear SPDEs. See [50][4] for a more general review of the theory presented in this section.

A technique for assessing SPDEs is to represent them as SODEs in Hilbert space. That is, instead of considering SPDEs in the classical sense, we consider them as infinite-dimensional systems of SODEs. The theoretical advantage of this approach is that infinite-dimensional systems of SODEs that can be studied using semigroup theory, see Section A.5. The class of numerical methods using this representation is referred to as the method of lines.

In the following we introduce the stochastic heat equation in Hilbert space and present different notions of solutions. As a motivation, the finite difference method for the stochastic heat equation is introduced, that is a finite-dimensional version of the method of lines. Finally, a method of lines called the Galerkin method is presented. This method gives an approximation of the stochastic heat equation via projections and the weak formulation of solutions. By choosing a suitable separable subspace onto which the projection of the stochastic heat equation maps, we call it the spectral Galerkin method.

The stochastic heat equation in infinite dimensions

To follow the notation in Section A.5 we define $A \coloneqq \Delta$. Let H be a Hilbert space of functions of the spatial variable $x \in D$, and let $A : \mathcal{D}(A) \to H$ satisfy Assumption A.3.5, where $\mathcal{D}(A) \subset H$ denotes the domain of A. Now, write the stochastic heat equation in Eq. (1.12) as

$$dY(t) = AY(t)dt + \sigma dW(t), \quad Y(0) \in H, \tag{1.13}$$

where W is a Q-Wiener process in H, and we require $\sigma \in L_0^2$ (see Definition 1.3.5).

Three notions of solutions of the stochastic heat equation in Eq. (1.13) are presented in the following, that is strong, weak and mild solutions. Note that the three definitions below defines solutions of the stochastic heat equation, whereas [50] defines solutions of the more general class of semilinear SPDEs.

[4]The theory presented in this section is based on this reference

Definition 1.3.7 ([50], Definition 10.18)**.** A predictable H-valued process $\{Y(t)\}_{t\in[0,T]}$ is called a strong solution of Eq. (1.13) if

$$Y(t) = Y(0) + \int_0^t AY(s)ds + \int_0^t \sigma dW(s), \quad \forall t \in [0,T].$$

The strong solution requires $Y(t) \in \mathcal{D}(A)$. A less restrictive interpretation of solutions is used in the Galerkin method. We define weak solutions as follows.

Definition 1.3.8 ([50], Definition 10.19)**.** A predictable H-valued process $\{Y(t)\}_{t\in[0,T]}$ is called a weak solution of Eq. (1.13) if

$$\langle Y(t), \nu\rangle = \langle Y(0), \nu\rangle + \int_0^t \langle Y(s), A\nu\rangle ds + \int_0^t \langle \sigma dW(s), \nu\rangle,$$

for $t \in [0,T]$ and $\nu \in \mathcal{D}(A)$, where in the notation of Eq. (1.10)

$$\int_0^t \langle \sigma dW(s), \nu\rangle := \sum_{j=1}^{\infty} \int_0^t \langle \sigma\sqrt{q_j}\chi_j, \nu\rangle dB_j(s).$$

Note that ν in the weak solutions is referred to as a test function. We will see that the Galerkin method uses the fact that the weak formulation reduces the required regularity of the solution $Y(t)$. Finally, the mild solution of the stochastic heat equation is defined.

Definition 1.3.9 ([50], Definition 10.22)**.** A predictable H-valued process is called a mild solution of Eq. (1.13) if for $t \in [0,T]$

$$Y(t) = e^{tA}Y(0) + \int_0^t e^{(t-s)A}\sigma dW(s),$$

where e^{tA} is the semigroup generated by A.

Note that the above holds when A is a bounded operator, which would require an appropriate domain of A. Otherwise, for example if $\mathcal{D}(A) = L^2$, the semigroup $\mathcal{S}(t)$ is unknown, meaning it generally fails to be on the form e^{tA}, see Section A.5. It is expected that strong solutions imply existence of weak solutions, and that weak solutions imply existence of mild solutions. It is important to note that the stochastic heat equation has to be sufficiently regular for the reverse implication to hold. For existence and uniqueness results, see Chapter 10 in [50].

Finite difference method

This section presents the finite difference method for the stochastic heat equation in one dimension on the real line with periodic boundary conditions. The method also works for the more general class of semilinear SPDEs, see [50]. As we will see, the finite-difference method uses classical differentiation theory to derive an approximation of the stochastic heat equation being a finite-dimensional system

of SODEs. Standard time discretization methods, see for example [42], can finally be used to assess the system of SODEs numerically.

By Eq. (1.12), the one-dimensional stochastic heat equation with constant volatility is given as

$$dY(t,x) = Y_{xx}(t,x)dt + \sigma dW(t,x), \quad x \in D \subset \mathbb{R}, \tag{1.14}$$

with initial value $Y(0,x) \in \mathbb{R}$ and volatility $\sigma > 0$, where $\{W(t,x) : (t,x) \in \mathbb{R}^+ \times D\}$ is a Gaussian random field evolving in time. Note that $Y_{xx} \coloneqq \partial^2 Y/\partial x^2$.

Given a domain $D = [0,a)$, we define uniformly spaced grid points $x_j = jh$ for $h = a/J$ and $j = 0,\dots,J$. Let $Y \in C^4(\mathbb{R})$, then by Taylor's theorem (see Theorem A1 in [50]) we have

$$Y_{xx}(t,x_i) = \frac{Y(t,x_{i+1}) - 2Y(t,x_i) + Y(t,x_{i-1})}{h^2},$$

for $i = 1,\dots,J-1$, where the remainder $\mathcal{O}(h^2)$ is suppressed. Define $\boldsymbol{Y}_J(t) \coloneqq [Y_1(t),\dots,Y_{J-1}(t)]^\top \in \mathbb{R}^{J-1}$, where for each $i = 1,\dots,J-1$ the element $Y_i(t)$ is an approximation of the element $Y(t,x_i)$ of the discretized solution $[Y(t,x_1),\dots,Y(t,x_{J-1})]^\top \in \mathbb{R}^{J-1}$. Further, we replace the Gaussian random field with an $L^2(D)$-valued Q-Wiener process $W(t)$, and define the approximation $\boldsymbol{W}_J(t) \coloneqq [W(t,x_1),\dots,W(t,x_{J-1})]^\top \in \mathbb{R}^{J-1}$. The solution $\boldsymbol{Y}_J$ is given by what we call the centered finite difference approximation of the Laplacian. That is, $\boldsymbol{Y}_J$ is the solution of the system of SODEs

$$d\boldsymbol{Y}_J = -A^D \boldsymbol{Y}_J dt + \sigma d\boldsymbol{W}_J(t), \tag{1.15}$$

with initial data $\boldsymbol{Y}_J(0) = [Y_1(0),\dots,Y_{J-1}(0)]^\top$, where the Laplacian is approximated as the $(J-1)\times(J-1)$-matrix

$$A^D \coloneqq \begin{bmatrix} 2 & -1 & 0 & 0 & \cdots & 0 & 1 \\ -1 & 2 & -1 & 0 & \cdots & 0 & 0 \\ 0 & \ddots & \ddots & \ddots & \cdots & 0 & 0 \\ \vdots & \vdots & \ddots & \ddots & \ddots & \vdots & \vdots \\ 1 & 0 & 0 & 0 & \cdots & -1 & 2 \end{bmatrix}.$$

We say that Eq. (1.15) is the method of lines for the finite difference approximation. The periodic boundary condition gives $Y(t,x_0) = Y(t,x_J)$, where $Y(t,x_0)$ and $Y(t,x_J)$ is included in the approximation of $Y(t,x_1)$ and $Y(t,x_{J-1})$ respectively.

Galerkin method

The Galerkin method is based on weak solutions of (S)PDEs. That is, for the stochastic heat equation the method is based on the solution in Definition 1.3.8. For convenience, we assume that Assumption A.3.5 holds throughout this section. The space of approximated solutions is taken as a finite-dimensional subspace

$\tilde{V} \subset \mathcal{D}(A^{1/2})$[5], relaxing the regularity restriction on possible solutions. For this to hold, we choose test functions $\nu \in \tilde{V}$.

The goal is to find an approximation $\tilde{Y}(t) \in \tilde{V}$ to the weak solution $Y(t)$ of the stochastic heat equation. That is, given an orthogonal projection $\tilde{P} : H \to \tilde{V}$ the approximation $\tilde{Y}(t)$ is the solution of[6]

$$\langle \tilde{Y}(t), \nu \rangle = \langle \tilde{Y}(0), \nu \rangle + \int_0^t \langle \tilde{A}^{1/2} \tilde{Y}(s), \tilde{A}^{1/2} \nu \rangle ds + \int_0^t \langle \sigma dW(s), \nu \rangle, \tag{1.16}$$

where $t \in [0, T]$, $\nu \in \tilde{V}$ and $\tilde{Y}(0) = \tilde{P}Y(0)$, and where the linear operator $\tilde{A} : \tilde{V} \to \tilde{V}$ satisfies the relation

$$\langle \tilde{A}\tilde{Y}, \nu \rangle = \langle \tilde{A}^{1/2}\tilde{Y}, \tilde{A}^{1/2}\nu \rangle, \tag{1.17}$$

according to Lemma A.3.6. Note that the left-hand side of Eq. (1.17) might not be well defined, but the right-hand side is because we seek solutions $Y \in \mathcal{D}(A^{1/2})$. The weak formulation in Eq. (1.16) satisfies a $\tilde{V}$-valued SODE on the form

$$d\tilde{Y}(t) = \tilde{A}\tilde{Y}(t)dt + \tilde{P}\sigma dW(t), \quad t \in [0, T],$$

which is called the method of lines for the Galerkin method.

The spectral Galerkin method is an approach to obtain the method of lines by applying a projection directly on the H-valued stochastic heat equation in Eq. (1.13). This projection has to be chosen carefully. By Assumption A.3.5 we know that $\{e_j : j \in \mathbb{N}\}$ is an orthonormal basis for A with corresponding eigenvalues λ_j, $j \in \mathbb{N}$. Now, choose A such that $\{e_j : j \in \mathbb{N}\}$ forms a basis for H, and we can define a Galerkin subspace $V_J \subset H$ with $V_J \coloneqq \operatorname{span}\{e_1, \ldots, e_J\}$. Further, define an orthonormal projection $P_J : H \to V_J$ by

$$P_J Y \coloneqq \sum_{j=1}^{J} \hat{Y}_j e_j, \quad \text{where } \hat{Y}_j \coloneqq \frac{1}{\|e_j\|^2} \langle Y, e_j \rangle \text{ for all } Y \in H.$$

As $\{e_j : j \in \mathbb{N}\}$ is an orthonormal basis for A, we can define $A_J \coloneqq P_J A$. This gives a method of lines approximation

$$dY_J(t) = A_J Y_J(t)dt + P_J \sigma dW(t), \quad t \in [0, T], \tag{1.18}$$

where $Y_J(0) = P_J Y(0)$. The function $Y_J(t)$ is called the spectral Galerkin approximation of the solution $Y(t)$ of the stochastic heat equation in Eq. (1.13). Standard time discretization methods, as found in [42], can be used to assess Eq. (1.18) numerically.

1.4 Outline and progression

As explained in Section 1.1, the aim of this work is to derive a direct link between infrasound measurements and the stratosphere using stochastic models.

[5] Powers of unbounded linear operators is defined in Eq. (A.3)

[6] See Definition 1.3.8

Inspired by prior works within stochastic modelling of surface weather variables, see, for example [23], [10], [11] and [12]; an initial hypothesis for this work was that the class of CARMA processes [15, 16, 17] provide a suitable modelling framework for stratospheric weather variables. Statistical analyses underpinned this hypothesis. Results indicated that dynamics of both stratospheric variables and smoothed infrasound variables could be explained by one-dimensional autoregressive models. This leads to an initial mathematical research question: Is it possible to connect such statistically-founded models with physically-founded models for weather variables?

A well-known physically-founded partial differential equation (PDE) for heat transfer is the heat equation, describing the rate at which heat flows within a medium [63]. By adding a noise term to the heat equation, the model can describe uncertainty in modelling. This extended model is called the stochastic heat equation. In Paper I, a connection between the stochastic heat equation in infinite dimensions and ARMA time series[7] [18], the discrete time analogue to CARMA processes [51], is derived. This result substantiates using CARMA processes as modelling framework for the stratospheric state.

Paper II provides empirical proofs that stratospheric temperature is well represented by a CARMA model. More specifically, we show that daily-spatial mean values of stratospheric temperature over a given area follow a CAR model with seasonally varying mean and variance.

The next challenge was to successfully estimate a multivariate model representing a dynamical system of weather variables. The approach was to find a model able to represent a system of stratospheric temperature and wind. As a test, the one-dimensional CAR model from Paper I was successfully fit to stratospheric wind, confirming results from literature [13, 19]. Furthermore, one can observe crosscorrelations between stratospheric temperature and wind variables. These pieces of empirical evidence motivate to use a multivariate CARMA process as a model.

The estimation methodology for one-dimensional CAR models [10] cannot be used in the multivariate case. In Paper III, an analogue estimation methodology for multivariate CARMA models is derived, which is further used to fit a model to a two-dimensional system of stratospheric temperature and wind. The multivariate CAR model is fit with statistical significance, providing empirical evidence that the stratospheric state might be well-represented by this model.

The goal of deriving a model able to represent stratospheric weather variables and their co-variation is reached, and our attention turns to infrasound data. Is it possible to extract information from infrasound detections for use in prediction of stratospheric weather variables? As discussed in for example [27] and [45], microbaroms ducted to the surface from the stratosphere carry signatures that are possible to decipher. However, it is not straightforward to formulate this link in a model. The estimation methodology from Paper III was used to fit multivariate CARMA models of different orders to a high-dynamical system

[7]The connection is derived for a more general infinite-dimensional stochastic partial differential equation of which the stochastic heat equation is a special case

of stratospheric wind and several infrasound variables. The information from infrasound gave close to none additional explanatory power of the dynamics of stratospheric wind.

The family of CARMA models provides a framework that explains linear autoregressive interactions between variables in a dynamical system. Furthermore, the autoregressive part of the model in Paper II and Paper III is assumed to be stationary. Now, a generalized modelling framework was proposed, being an SDDE with multiple delays. This model can represent both non-linear and non-stationary interactions between dynamical variables. Problems that have to be solved to use this modelling framework: 1) we do not know the exact form of the non-linear and/or non-stationary model coefficient functions; and 2) if exact functions are known (or guessed), proper methods of parameter estimation have to be found. Paper IV addresses these problems, where the Delay-SDE-net is developed.

The Delay-SDE-net uses neural networks as model coefficient functions, making the model parameter estimation an exercise of training these networks. To validate this deep learning approach, the Delay-SDE-net was fit to a two-dimensional system of stratospheric temperature and wind, with the aim of predicting wind up to 7 days forward in time. The validation performed better than the CARMA model approach used in Paper III.

Finally, the study in Paper V explore if the Delay-SDE-net is capable of explaining the link between ground-based infrasound measurements and stratospheric weather variables. This was done by training the neural networks of the Delay-SDE-net model solely using pre-processed infrasound data as features, using circumpolar stratospheric wind as response. The results were affirmative, as the trained Delay-SDE-net was able to replicate the real-time wind profile surprisingly well, only using infrasound measurements as input.

For a more detailed summary of the papers in this thesis, see the following section.

1.5 Summary of Papers

This section elaborates highlights from the collection of research papers in this PhD thesis. The collection includes: 1) "Ornstein-Uhlenbeck Processes in Hilbert Space and Autoregressive Moving-Average Time Series" to be submitted for publication; 2) "Stochastic Modeling of Stratospheric Temperature" that is published in the Springer-journal *Mathematical Geosciences*; 3) "The Multivariate ARMA/CARMA Transformation Relation" that is in preparation for resubmission to *Scandinavian Journal of Statistics*; 4) "Delay-SDE-Net: A Deep Learning Approach for Time Series Modelling with Memory and Uncertainty Estimates" that is in preparation for resubmission to *Journal of Machine Learning Research*. This work has a shared first authorship between the two authors; 5) "Near Real-Time Stratospheric Circulation Diagnostics Based on High-Latitude Infrasound Data Using a Stochastics-Founded Machine Learning Model" to be

submitted for publication. This work has a shared first authorship between Mari Dahl Eggen and Ekaterina Vorobeva.

Paper I: Ornstein-Uhlenbeck Processes in Hilbert Space and Autoregressive Moving-Average Time Series

Key takeaways: *One-dimensional ARMA processes characterizes vector-valued AR(1) processes; Sampled Hilbertian OU-processes admit ARH(1) processes and their evaluations are close to white noise at high sampling frequencies; Spatial convergence of evaluations of finite-dimensional Hilbertian AR(1) processes to evaluations of ARH(1) processes is established*

Based on the physical laws of heat transfer a stylized model for the space-time temperature field over a geographical area is suggested to take the form

$$dY(t,x) = AY(t,x)dt + \sigma dW(t,x), \quad (t,x) \in \mathbb{R}_+ \times \mathbb{R}^2, \tag{1.19}$$

where A is some parabolic operator in space $\mathbb{R}^2$ and W is a Gaussian field, with σ being some scaling acting on the noise. The SPDE in Eq. (1.19) is assessed as an OU-process in a separable Hilbert space, H. The aim is to connect the OU-process in infinite dimensions with one-dimensional ARMA processes.

This work is initiated with motivating results connecting $\mathbb{R}^p$-valued AR(1) time series, $X := \{X_n\}_{n\in\mathbb{N}_0}$, with one-dimensional ARMA time series, $Z := \{Z_n\}_{n\in\mathbb{N}_0}$. That is, with X given by

$$X_{n+1} = BX_n + \epsilon_n,$$

where $B \in \mathbb{R}^{p\times p}$ and $\{\epsilon_n\}_{n\in\mathbb{N}_0}$ is an IID mean zero Gaussian time series with values in $\mathbb{R}^p$, the process $Z_n = w^\top X_n$, for any $w \in \mathbb{R}^p$, is shown to be an one-dimensional ARMA time series. This result is true for a given restriction on the model coefficient B, and a formula for the autoregressive model coefficients of Z is derived as a function of the eigenvalues of B.

Moving to the suggested temperature model, we show that samples of Hilbertian OU-processes admit well defined ARH(1) processes, for which the autoregressive coefficient and the covariance operator are given by the OU-process semigroup. Furthermore, a convergence result in the time dimension is derived for the sampled OU-process, indicating that evaluations of the infinite dimensional ARH(1) processes is close to white noise at high sampling frequency. Next we consider ARH(1) processes projected into a finite-dimensional subspace $V \subset H$. Denote ARH(1) processes living in V by ARV(1). An error representation of the projected ARH(1) process is derived when compared to ARV(1) processes. Further, for a given basis of the finite-dimensional subspace V, a convergence result is derived for an evaluation of the projected ARH(1) process. The convergence result shows that, for fixed equidistant sampling time steps, the evaluated projected ARH(1) process converges to the evaluated ARV(1) process as the dimension of V approaches infinity.

A simulation study is performed with the stochastic heat equation (a special case of the SPDE in Eq. (1.19)) to substantiate the theoretical results. The numerical results indicate that point evaluations of ARH(1) processes approach white noise. Moreover, we see that mean-value[8] evaluations of ARH(1) processes are better represented by one-dimensional autoregressive models of higher orders. This complies with results from prior studies in modelling of weather variables where, for example, daily mean values of such time series are shown to be well represented by autoregressive models of higher orders.

Paper II: Stochastic Modeling of Stratospheric Temperature

Key takeaways: *Deseasonalized stratospheric temperature is well-represented by non-Gaussian CAR(4) model with time-dependent volatility; The model could provide a better representation if the volatility was stochastic; Seasonality is discovered in autoregressive model coefficients of stratospheric temperature*

Motivated by prior results in the literature on stochastic modeling of surface weather variables, a Lévy-driven CAR model is proposed for modelling of temperature dynamics in the Northern Hemisphere stratospheric vortex. More specifically, the stratospheric temperature, $S(t)$, is assumed to be given by

$$S(t) = \Lambda(t) + X_1(t), \tag{1.20}$$

where $\Lambda(t)$ is an additive seasonality function, and $X_1(t)$ is the first component of a stochastic process $\boldsymbol{X}(t) \coloneqq \{\boldsymbol{X}(t)\}_{t\in\mathbb{R}^+}$ taking values in $\mathbb{R}^p$, $p \in \mathbb{N}$. Here, $\boldsymbol{X}(t)$ is given by the multivariate OU-process

$$d\boldsymbol{X}(t) = A\boldsymbol{X}(t)dt + \boldsymbol{e}_p\sigma(t-)dL(t),$$

where A is a constant $p \times p$ coefficient matrix, $\boldsymbol{e}_p$ is the p-th unit vector in $\mathbb{R}^p$, $\sigma(t) : \mathbb{R}^+ \to \mathbb{R}^+$ represents a real valued seasonally varying variance function, and $L(t) = \{L(t)\}_{t\in\mathbb{R}^+}$ is a Lévy process. With this setup, $X_1(t)$ admits a CAR(p) process. Note that the model in Eq. (1.20) explain seasonal and heteroscedastic behaviour in data, as well as linear autoregressive behaviour up to p lags.

With a thoroughly described estimation methodology, the model in Eq. (1.20) is fit to daily zonal (circumpolar) mean stratospheric temperature data at an altitude corresponding to a pressure level of 10 hPa. As suggested by statistical analyses, we used a model of order $p = 4$. The model is fit with statistical significance for the case when the Lévy process generates NIG distributed random variables. Further analyses show that an even better representation of temperature data could be obtained with the volatility $\sigma(t)$ being stochastic, and with the autoregressive coefficient A being time-dependent. The latter innovation is implemented into the model in Eq. (1.20), providing a fit with statistical significance for NIG distributed residuals.

[8]The points of ARH(1) time series is constructed from mean values of simulated data over a given time span

Paper III: The Multivariate ARMA/CARMA Transformation Relation

Key takeaways: *An estimation methodology for multivariate CARMA processes is derived; The Euler convergence rate for NIG-Lévy-driven multivariate CARMA processes is found; A multivariate CAR model is fit to stratospheric temperature and wind*

A connection between model coefficients of multivariate CARMA and ARMA processes is established through an Euler discretization scheme. The derived connection serves as a model estimation methodology for multivariate CARMA processes. To obtain this, consider the state-space representation, $\boldsymbol{Y}(t) \coloneqq \{\boldsymbol{Y}(t)\}_{t\geq 0}$, of the multivariate CARMA process

$$d\boldsymbol{X}(t) = A\boldsymbol{X}(t)dt + \beta d\boldsymbol{L}(t), \quad \boldsymbol{Y}(t) = C\boldsymbol{X}(t), \tag{1.21}$$

where $A \in \mathbb{R}^{pd\times pd}$, $\beta \in \mathbb{R}^{pd\times m}$ and $C \in \mathbb{R}^{d\times pd}$, for $p, d, m \in \mathbb{N}$, and $\boldsymbol{L}(t) \coloneqq \{\boldsymbol{L}(t)\}_{t\geq 0}$ is a Lévy process with values in $\mathbb{R}^m$. Note that the d-dimensional CARMA process, $\boldsymbol{Y}(t)$, is given by a multivariate OU-process, $\boldsymbol{X}(t) \coloneqq \{\boldsymbol{X}(t)\}_{t\geq 0}$, with p and m representing the autoregressive order and the number of independently driving Lévy processes, respectively.

The form of A (see Paper III) makes $\boldsymbol{X}(t)$ a system of pd (number of) SDEs that can be solved recursively. We want to exploit this and define a convenient recursive parameter

$$Q \coloneqq (Q_i^{(l)} \mid k),$$

that is a function of the SDE systems' dimension number $k \in \{1, \ldots, d\}$ and lag number $l \in \{1, \ldots, p\}$. Note that the index i works as a recursive counter. We show that elements of $\boldsymbol{X}(t)$ can be represented by use of Q, and this Q-representation of the multivariate OU-process in Eq. (1.21) is discretized using the Euler scheme. The recursively solved system of discretized SDEs admits a multivariate ARMA process, making a connection between multivariate CARMA and ARMA processes.

To prove convergence of the discretized multivariate CARMA process, the Euler scheme convergence rate for jump diffusions with jumps of finite variance and infinite variations is derived. We chose to study a Lévy process with these specific properties because the case study of this work requires an NIG-Lévy-driven model. The case study is performed to illustrate the derived model estimation methodology for multivariate CARMA processes. That is, we fit a multivariate CAR model to a two-dimensional dynamical system of stratospheric temperature and wind variables.

Paper IV: Delay-SDE-Net: A Deep Learning Approach for Time Series Modelling with Memory and Uncertainty Estimates

Key takeaways: *Phenomena well-represented by an SDDE with multiple delays can be predicted using the Delay-SDE-net; The theoretical L_2-error in*

using a two-layer Delay-SDE-net in place of a real-world SDDE is derived; The Delay-SDE-net performs better in prediction studies than comparing models

In this work we study SDDEs with multiple point delays. That is, let $X(t) : [-\tau, T] \times \Omega \to \mathbb{R}^d$ be a stochastic vector process given by

$$X(t) = \begin{cases} \eta(0) + \int_0^t f(s, \Pi_1(X_s))ds + \int_0^t g(s, \Pi_2(X_s))dW(s), & t \geq 0, \\ \eta(t), & -\tau \leq t < 0, \end{cases} \tag{1.22}$$

where η is a continuous initial process with values in $\mathbb{R}^d$ and $\Pi \in \mathbb{R}^{dp}$ is a projection defining p fixed point delays. Further, X_t is a continuous segment process of $X(t)$, $W(t)$ is a Brownian motion process taking values in $\mathbb{R}^{d_W}$, and $f \in \mathbb{R}^d$ and $g \in \mathbb{R}^{d \times d_W}$ are functions satisfying given conditions.

With the aim of estimating $X(t)$ from the general framework given in Eq. (1.22), we redefine the model coefficients f and g as m-neuron neural networks f_m and g_m, respectively. With this method we will not know the explicit form of the original model coefficients f and g, but f_m and g_m can be trained to give a predicted value of $X(t)$ for given input. We call this model the Delay-SDE-net. To characterize the uncertainty more specifically than simply being a volatility output value from the trained model, we define the neural network volatility as a sum of two neural networks $g_m \coloneqq g_{a,m} + g_{e,m}$. Here, $g_{a,m}$ represents uncertainty accounting for natural randomness in a task, as well as model uncertainty, whereas $g_{e,m}$ account for approximation uncertainty originating from lack of data. A detailed training methodology for the neural networks is described.

The Delay-SDE-net is a physics-informed type of machine learning model, and is derived with a hypothesis that real-world phenomena are well-represented by an SDDE with multiple point delays, as presented in Eq. (1.22). When a trained Delay-SDE-net is used to estimate $X(t)$ there will be an error compared to the real-world SDDE representation. This (L_2-) error is derived theoretically as the sum of the discretization error and the two-layer neural network approximation error. It is evident that the discretization error converges for smaller time discretization steps and that the two-layer neural network error becomes smaller for an increased number of neurons.

Finally, the Delay-SDE-net is studied numerically. A numerical convergence study is performed for the discretization error, and results comply with the applied time discretization scheme. The model prediction performance is tested both on simulated data, and on data from a real-world case study where we consider a two-dimensional dynamical system of stratospheric temperature and wind. The Delay-SDE-net performs better than the comparing models in both tests, where the performance is measured as root mean square error.

Paper V: Near Real-Time Stratospheric Circulation Diagnostics Based on High-Latitude Infrasound Data Using a Stochastics-Founded Machine Learning Model

Key takeaways: *A mapping from ground-based infrasound measurements to stratospheric wind is established; Results indicate that infrasound has potential as a near real-time source of information for stratospheric dynamics*

This study aims to establish a direct mapping from ground-based infrasound measurements to Northern Hemisphere zonal-mean zonal wind at 1 hPa. An SDDE with several point delays is proposed as modelling framework to account for possible non-linear and non-stationary co-variations, as well as memory effects. A proper model is estimated via the Delay-SDE-net, where each of the SDDE model coefficients admits independent neural networks. That is, we train the model

$$\hat{w}_t = f(t, \boldsymbol{x}_{t-p-1}, \ldots, \boldsymbol{x}_t)\Delta t + g(t, \boldsymbol{x}_{t-p-1}, \ldots, \boldsymbol{x}_t)\epsilon_t,$$

where $\Delta t = 1$ is the time step size of 1 day, and ϵ_t is a standard normally distributed random variables. Furthermore, $\boldsymbol{x}_s$, with $s = t - p - 1, \ldots, t$, represents a vector of infrasound variables at time s, the functions f and g represents a trained neural network for the deterministic and stochastic part of the model respectively, and $\hat{w}_t$ represents the corresponding predicted zonal-mean zonal wind.

The stratospheric zonal-mean zonal wind data are constructed from the ECMWFs' ERA5 reanalysis model product. The dataset consists of daily values of zonal-mean zonal wind that are cosine-weighted and averaged between $60°-90°$ latitudes. We use infrasound data from detections at the three northern-most IMS infrasound stations, and the data are pre-processed in an independent research project. The infrasound datasets used in this study are constructed as daily values of the strongest microbarom amplitude and corresponding direction of arrival (called the back-azimuth) for each station. That is, 6 infrasound variables are used as features for the Delay-SDE-net.

The Delay-SDE-net is trained on datasets ranging over the 5 years from 2014 to 2018, and subsequently validated by predicting 1 hPa zonal-mean zonal wind over the years 2019 and 2020. A sensitivity analysis is performed for different combinations of training data to establish the importance of each feature. Performance is measured using the root mean square error between ERA5- and infrasound-based zonal-mean zonal wind. It is evident that the year with a major SSW, that is 2019, performs better with increased number of features. In contrast, the year without a major SSW performs nearly equally well for all combinations of features, indicating that infrasound observations contribute to the prediction less than the day of year. However, predicting wind with a Delay-SDE-net trained solely using the day of year as feature confirms that the additional infrasound features provide enhanced prediction power. The validation demonstrates that the Delay-SDE-net with infrasound input predicts the zonal-mean zonal wind surprisingly well, with a RMSE of 11.3 m/s and 11.9

m/s for 2019 and 2020, respectively, when using all available features. These results indicate that there is a potential for assimilating infrasound observations into existing atmospheric models as a near real-time source of information about the large-scale stratospheric dynamics.

References

[1] Amezcua, J. et al. "Assimilation of atmospheric infrasound data to constrain tropospheric and stratospheric winds". In: *Quarterly Journal of the Royal Meteorological Society* vol. 146, no. 731 (2020), pp. 2634–2653.

[2] Anh, V. and Inoue, A. "Financial markets with memory I: Dynamic models". In: *Stochastic Analysis and Applications* vol. 23, no. 2 (2005), pp. 275–300.

[3] Assink, J. et al. "Advances in Infrasonic Remote Sensing Methods". In: *Infrasound Monitoring for Atmospheric Studies: Challenges in Middle Atmosphere Dynamics and Societal Benefits*. Ed. by Le Pichon, A., Blanc, E., and Hauchecorne, A. Cham: Springer International Publishing, 2019, pp. 605–632.

[4] Baldwin, M. P. and Dunkerton, T. J. "Stratospheric harbingers of anomalous weather regimes". In: *Science* vol. 294, no. 5542 (2001), pp. 581–584.

[5] Baldwin, M. P. et al. "Sudden stratospheric warmings". In: *Reviews of Geophysics* vol. 59, no. 1 (2021).

[6] Baños, D. et al. "Stochastic systems with memory and jumps". In: *Journal of Differential Equations* vol. 266, no. 9 (2019), pp. 5772–5820.

[7] Basse-O'Connor, A. et al. "Stochastic delay differential equations and related autoregressive models". In: *Stochastics* vol. 92, no. 3 (2020), pp. 454–477.

[8] Basse-O'Connor, A. et al. "Multivariate stochastic delay differential equations and CAR representations of CARMA processes". In: *Stochastic Processes and their Applications* vol. 129, no. 10 (2019), pp. 4119–4143.

[9] Benioff, H. and Gutenberg, B. "Waves and currents recorded by electromagnetic barographs". In: *Bulletin of the American Meteorological Society* vol. 20, no. 10 (1939), pp. 421–428.

[10] Benth, F. E., Šaltytė Benth, J., and Koekebakker, S. *Stochastic Modelling of Electricity and Related Markets*. Vol. 11. World Scientific, 2008.

[11] Benth, F. E. and Taib, C. M. I. C. "On the speed towards the mean for continuous time autoregressive moving average processes with applications to energy markets". In: *Energy Economics* vol. 40 (2013), pp. 259–268.

[12] Benth, F. E. et al. "Futures pricing in electricity markets based on stable CARMA spot models". In: *Energy Economics* vol. 44 (2014), pp. 392–406.

[13] Benth, J. Š. and Benth, F. E. "Analysis and modelling of wind speed in New York". In: *Journal of Applied Statistics* vol. 37, no. 6 (2010), pp. 893–909.

[14] Bosq, D. *Linear Processes in Function Spaces: Theory and Applications*. Vol. 149. Springer Science & Business Media, 2000.

[15] Brockwell, P. J. "Lévy-driven CARMA processes". In: *Annals of the Institute of Statistical Mathematics* vol. 53, no. 1 (2001), pp. 113–124.

[16] Brockwell, P. J. "Recent results in the theory and applications of CARMA processes". In: *Annals of the Institute of Statistical Mathematics* vol. 66, no. 4 (2014), pp. 647–685.

[17] Brockwell, P. J. "Representations of continuous-time ARMA processes". In: *Journal of Applied Probability* vol. 41, no. A (2004), pp. 375–382.

[18] Brockwell, P. J. and Davis, R. A. *Time Series: Theory and Methods*. Springer New York, 1991.

[19] Brockwell, P. J., Ferrazzano, V., and Klüppelberg, C. "High-frequency sampling and kernel estimation for continuous-time moving average processes". In: *Journal of Time Series Analysis* vol. 34, no. 3 (2013), pp. 385–404.

[20] Brockwell, P. J. and Davis, R. A. *Introduction to Time Series and Forecasting*. Springer Cham, 2016.

[21] Butler, A. et al. "Sub-Seasonal Predictability and the Stratosphere". In: *Sub-Seasonal to Seasonal Prediction*. Ed. by Robertson, A. and Vitart, F. Elsevier, 2019, pp. 223–241.

[22] Butler, A. H. et al. "Defining sudden stratospheric warmings". In: *Bulletin of the American Meteorological Society* vol. 96, no. 11 (2015), pp. 1913–1928.

[23] Campbell, S. D. and Diebold, F. X. "Weather forecasting for weather derivatives". In: *Journal of the American Statistical Association* vol. 100, no. 469 (2005), pp. 6–16.

[24] Christie, D. R. and Campus, P. "The IMS Infrasound Network: Design and Establishment of Infrasound Stations". In: *Infrasound Monitoring for Atmospheric Studies*. Ed. by Le Pichon, A., Blanc, E., and Hauchecorne, A. Dordrecht: Springer Netherlands, 2009, pp. 29–75.

[25] Chunxiang, A., Shen, Y., and Zeng, Y. "Dynamic asset-liability management problem in a continuous-time model with delay". In: *International Journal of Control* vol. 95, no. 5 (2022), pp. 1315–1336.

[26] De Carlo, M., Ardhuin, F., and Le Pichon, A. "Atmospheric infrasound generation by ocean waves in finite depth: Unified theory and application to radiation patterns". In: *Geophysical Journal International* vol. 221, no. 1 (2020), pp. 569–585.

[27] Donn, W. L. and Rind, D. "Natural infrasound as an atmospheric probe". In: *Geophysical Journal International* vol. 26, no. 1-4 (1971), pp. 111–133.

[28] Fasen, V. “Statistical estimation of multivariate Ornstein–Uhlenbeck processes and applications to co-integration”. In: *Journal of Econometrics* vol. 172, no. 2 (2013), pp. 325–337.

[29] Franzke, C. L. et al. “Stochastic climate theory and modeling”. In: *Wiley Interdisciplinary Reviews: Climate Change* vol. 6, no. 1 (2015), pp. 63–78.

[30] Gómez, V. *Linear Time Series with MATLAB and OCTAVE*. Springer International Publishing: Imprint: Springer, 2019.

[31] Hu, Y., Liu, Y., and Tindel, S. “On the necessary and sufficient conditions to solve a heat equation with general additive Gaussian noise”. In: *Acta Mathematica Scientia* vol. 39, no. 3 (2019), pp. 669–690.

[32] Hu, Y., Mohammed, S.-E. A., and Yan, F. “Discrete-time approximations of stochastic differential systems with memory”. In: *OpenSIUC Preprint* (2001).

[33] Hu, Y., Mohammed, S.-E. A., and Yan, F. “Discrete-time approximations of stochastic delay equations: The Milstein scheme”. In: *The Annals of Probability* vol. 32, no. 1A (2004), pp. 265–314.

[34] Hupe, P. et al. “Assessing middle atmosphere weather models using infrasound detections from microbaroms”. In: *Geophysical Journal International* vol. 216, no. 3 (2019), pp. 1761–1767.

[35] Hupe, P. et al. “International Monitoring System infrasound data products for atmospheric studies and civilian applications”. In: *Earth System Science Data* vol. 14, no. 9 (2022), pp. 4201–4230.

[36] Haak, H., Mykkeltveit, S., and Dahlman, O. *Nuclear test ban: converting political visions to reality*. Springer, 2009.

[37] Ikram, R. et al. “Extinction and stationary distribution of a stochastic COVID-19 epidemic model with time-delay”. In: *Computers in Biology and Medicine* vol. 141 (2022), p. 105115.

[38] Ivanov, A., Kazmerchuk, Y., and Swishchuk, A. “Theory, stochastic stability and applications of stochastic delay differential equations: a survey of results”. In: *Differential Equations Dynam. Systems* vol. 11, no. 1-2 (2003), pp. 55–115.

[39] Karpechko, A., Tummon, F., and WMO Secretariat. “Climate predictability in the stratosphere”. In: *WMO Bulletin* vol. 65, no. 1 (2016).

[40] Kidston, J. et al. “Stratospheric influence on tropospheric jet streams, storm tracks and surface weather”. In: *Nature Geoscience* vol. 8, no. 6 (2015), pp. 433–440.

[41] Kirtman, B. et al. “Prediction from weeks to decades”. In: *Climate Science for Serving Society: Research, Modeling and Prediction Priorities* (2013), pp. 205–235.

[42] Kloeden, P. E. and Platen, E. *Numerical Solution of Stochastic Differential Equations*. Vol. 23. Applications of Mathematics. Berlin: Springer, 1992.

[43] Kondrashov, D. and Berloff, P. “Stochastic modeling of decadal variability in ocean gyres”. In: *Geophysical Research Letters* vol. 42, no. 5 (2015), pp. 1543–1553.

[44] Kushner, H. J. “On the stability of processes defined by stochastic difference-differential equations”. In: *Journal of Differential Equations* vol. 4, no. 3 (1968), pp. 424–443.

[45] Le Pichon, A. et al. “On using infrasound from interacting ocean swells for global continuous measurements of winds and temperature in the stratosphere”. In: *Journal of Geophysical Research: Atmospheres* vol. 111, no. D11 (2006).

[46] Lee, C. et al. “The Potential Impact of Upper Stratospheric Measurements on Sub-seasonal Forecasts in the Extra-Tropics”. In: *Infrasound Monitoring for Atmospheric Studies: Challenges in Middle Atmosphere Dynamics and Societal Benefits*. Ed. by Le Pichon, A., Blanc, E., and Hauchecorne, A. Cham: Springer International Publishing, 2019, pp. 889–907.

[47] Lee, S., Furtado, J., and Charlton-Perez, A. “Wintertime North American weather regimes and the Arctic stratospheric polar vortex”. In: *Geophysical Research Letters* vol. 46, no. 24 (2019), pp. 14892–14900.

[48] Levendis, J. D. *Time Series Econometrics: Learning Through Replication*. Springer International Publishing: Imprint: Springer, 2018.

[49] Liang, Z. et al. “Northern winter stratospheric polar vortex regimes and their possible influence on the extratropical troposphere”. In: *Climate Dynamics* (2022), pp. 1–20.

[50] Lord, G. J., Powell, C. E., and Shardlow, T. *An Introduction to Computational Stochastic PDEs*. Cambridge Texts in Applied Mathematics. Cambridge University Press, 2014.

[51] Marquardt, T. and Stelzer, R. “Multivariate CARMA processes”. In: *Stochastic Processes and Their Applications* vol. 117, no. 1 (2007), pp. 96–120.

[52] Marty, J. “The IMS Infrasound Network: Current Status and Technological Developments”. In: *Infrasound Monitoring for Atmospheric Studies: Challenges in Middle Atmosphere Dynamics and Societal Benefits*. Ed. by Le Pichon, A., Blanc, E., and Hauchecorne, A. Cham: Springer International Publishing, 2019, pp. 3–62.

[53] Merryfield, W. J. et al. “Current and emerging developments in subseasonal to decadal prediction”. In: *Bulletin of the American Meteorological Society* vol. 101, no. 6 (2020), E869–E896.

[54] Michas, G. and Vallianatos, F. “Stochastic modeling of nonstationary earthquake time series with long-term clustering effects”. In: *Physical Review E* vol. 98, no. 4 (2018), p. 042107.

[55] Mohammed, S.-E. A. “Stochastic differential systems with memory: theory, examples and applications”. In: *Stochastic Analysis and Related Topics VI: Proceedings of the Sixth Oslo—Silivri Workshop Geilo 1996*. Springer. 1998, pp. 1–77.

[56] Oelz, D., Schmeiser, C., and Soreff, A. “Multistep navigation of leukocytes: a stochastic model with memory effects”. In: *Mathematical Medicine and Biology* vol. 22, no. 4 (2005), pp. 291–303.

[57] Pedatella, N. et al. “How sudden stratospheric warming affects the whole atmosphere”. In: *Eos* vol. 99 (2018).

[58] Perlwitz, J. and Harnik, N. “Observational evidence of a stratospheric influence on the troposphere by planetary wave reflection”. In: *Journal of Climate* vol. 16, no. 18 (2003), pp. 3011–3026.

[59] Rihan, F. A. *Delay differential equations and applications to biology*. Springer, 2021.

[60] Schlicht, R. and Winkler, G. “A delay stochastic process with applications in molecular biology”. In: *Journal of mathematical biology* vol. 57 (2008), pp. 613–648.

[61] Smets, P., Assink, J., and Evers, L. “The Study of Sudden Stratospheric Warmings Using Infrasound”. In: *Infrasound Monitoring for Atmospheric Studies: Challenges in Middle Atmosphere Dynamics and Societal Benefits*. Ed. by Le Pichon, A., Blanc, E., and Hauchecorne, A. Cham: Springer International Publishing, 2019, pp. 723–755.

[62] Smirnov, A. et al. “Characterizing the oceanic ambient noise as recorded by the dense seismo-acoustic Kazakh network”. In: *Solid Earth* vol. 12, no. 2 (2021), pp. 503–520.

[63] Sobolev, S. L. “Lecture 1 - Derivation of the Fundamental Equations”. In: *Partial Differential Equations of Mathematical Physics*. Pergamon, 1964, pp. 1–21.

[64] Vorobeva, E. et al. “Benchmarking microbarom radiation and propagation model against infrasound recordings: A vespagram-based approach”. In: *Annales Geophysicae* vol. 39, no. 3 (2021), pp. 515–531.

[65] Waugh, D. W., Sobel, A. H., and Polvani, L. M. “What is the polar vortex and how does it influence weather?” In: *Bulletin of the American Meteorological Society* vol. 98, no. 1 (2017), pp. 37–44.

[66] Zhang, J. et al. “Impacts of stratospheric polar vortex changes on wintertime precipitation over the Northern Hemisphere”. In: *Climate Dynamics* (2022), pp. 1–17.

[67] Øksendal, B. and Sulem, A. “A maximum principle for optimal control of stochastic systems with delay, with applications to finance”. In: *Optimal Control and Partial Differential Equations – Innovations and Applications*. Ed. by Menaldi, J. L., Rofman, E., and Sulem, A. IOS Press, 2000, pp. 64–79.

Papers

Paper II

Stochastic modeling of stratospheric temperature

II

Mari Dahl Eggen, Kristina Rognlien Dahl, Sven Peter Näsholm, Steffen Mæland

Published in *Mathematical Geosciences*, January 2022, volume 54, issue 4, pp. 651–678. DOI: 10.1007/s11004-021-09990-6.

Abstract

This study suggests a stochastic model for time series of daily-zonal (circumpolar) mean stratospheric temperature at a given pressure level. It can be seen as an extension of previous studies which have developed stochastic models for surface temperatures. The proposed model is a sum of a deterministic seasonality function and a Lévy-driven multidimensional Ornstein-Uhlenbeck process, which is a mean-reverting stochastic process. More specifically, the deseasonalized temperature model is an order 4 continuous time autoregressive model, meaning that the stratospheric temperature is modeled to be directly dependent on the temperature over four preceding days, while the model's longer-range memory stems from its recursive nature. This study is based on temperature data from the European Centre for Medium-Range Weather Forecasts ERA-Interim reanalysis model product. The residuals of the autoregressive model are well-represented by normal inverse Gaussian distributed random variables scaled with a time-dependent volatility function. A monthly variability in speed of mean reversion of stratospheric temperature is found, hence suggesting a generalization of the 4th order continuous time autoregressive model. A stochastic stratospheric temperature model, as proposed in this paper, can be used in geophysical analyses to improve the understanding of stratospheric dynamics. In particular, such characterizations of stratospheric temperature may be a step towards greater insight in modeling and prediction of large-scale middle atmospheric events, such as for example sudden stratospheric warmings. Through stratosphere-troposphere coupling, the stratosphere is hence a source of extended tropospheric predictability at weekly to monthly timescales, which is of great importance in several societal and industry sectors.

Contents

II.1 Introduction

A thorough understanding of surface weather dynamics is crucial in a wide range of industry and societal sectors. Whether planning marine operations, flights or farming, or managing energy assets, the weather is a key aspect to consider. However, because higher atmospheric layers can couple to levels closer to the surface, in order to understand weather, understanding the dynamics at higher altitudes of the atmosphere is important. The Earth's atmosphere has a layered structure, where each layer has layer-specific properties (see [2] and the references therein for an historical overview). Closest to the surface lays the troposphere, reaching up to around 15 km altitude. Above, up to around 50 km, lays the stratosphere, which is the atmospheric layer of interest in this paper. These two layers interact, and the dynamics in the stratosphere can couple to the troposphere to affect dynamics and predictability at the surface, see for example [21] and [1]. Hence, better probing, modeling, and understanding of stratospheric dynamics has the potential to enhance numerical surface weather prediction, in particular at weekly to monthly timescales.

In the current paper, a novel stochastic model for stratospheric temperature is proposed. The stochastic approach is similar to what has been applied in previous tropospheric temperature and wind dynamics modeling studies (e.g., [11]; [9]; [12]; [15]; [14]).

Temperature tends to revert back to its mean over time [12]. This feature is reflected in what is called the speed of mean reversion, and is captured by autoregressive (AR) processes. AR processes are discrete time stochastic processes having a direct transformation relation with continuous time autoregressive (CAR) processes ([19]; [12]; [14]). This transformation relation allows to introduce a continuous time mathematical model framework based on empirical derivations and analyses. Periodical behaviour is modeled separately from the CAR process. So is a long-term trend in the stratospheric temperature. The reason for the inclusion of a long-term trend in stochastic models for tropospheric temperature, is that it is well known from climate research that there is a long-term warming of the troposphere (e.g., [31]; [37]; [30]). This effect is captured in the surface temperature modeling of [12]. Also in [12], cyclic functions are included through truncated Fourier series which can represent the periodical movements of tropospheric temperature. Similarly, several studies

have shown (e.g., [24]; [25]; [38]) that there is a long-term decreasing trend in stratospheric temperature, and that there are several cyclic (seasonal) patterns ([27]; [35]).

The current empirical analysis and stochastic model study is performed on temperatures as represented in the European Centre for Medium-Range Weather Forecasts (ECMWF) ERA-Interim atmospheric reanalysis model product ([16]; [26]). Full-year daily-zonal mean stratospheric temperature data over 60°N and 10 hPa, from 1979 to 2018, are considered. Similarly as in [12], a seasonality function in the form of a truncated Fourier series is fitted to the stratospheric temperature data to find deseasonalized temperature. Then, an AR model is fitted to the deseasonalized data and thereby subtracted to find the residuals. A search for seasonal heteroskedasticity (variability of variance over time) in the residuals is performed, and such heteroskedasticity is found. Based on this, a time-dependent volatility function, $\sigma(t)$, is defined. The $\sigma(t)$-scaled residuals are proven, with statistical significance, to be normal inverse Gaussian (NIG) distributed random variables. Hence, the results of the data analysis suggest using a Lévy-driven CAR process with a time-varying volatility function to model stratospheric temperature. The residuals contain small memory effects, indicating that it might be reasonable to also consider a stochastic volatility function. This is beyond the scope of this paper.

An individual stability analysis of speed of mean reversion over time is also performed, suggesting that the assumption about constant speed of mean reversion is not fulfilled. The result is twofold; the speed of mean reversion shows large variability from month to month, and it is varying with a seasonal pattern. Similarly, [40] proved that the speed of mean reversion for tropospheric temperature is strongly time-dependent, obtaining a series of daily values of speed of mean reversion through neural networks. However, in contrast to the current paper, they did not observe seasonal patterns. In [8], Ornstein-Uhlenbeck (OU) dynamics are generalized to allow for a stochastic speed of mean reversion, which can incorporate deterministic time dependence as well. However, [8] consider the special case when the Lévy process is a Brownian motion. This is less general than the CAR process proposed for stratospheric temperature modeling in the current paper. Instead of using the aforementioned approaches to include time dependence in the speed of mean reversion of the CAR process, a simpler, approximate approach is suggested: A time-dependent step function with 12 levels is introduced, where the levels represent the months of the year. In this way both the monthly variability and the seasonal behaviour are adjusted for. The procedure of fitting a CAR process to the stratospheric temperature data is repeated for the extended CAR process with time dependence in speed of mean reversion. The inclusion of time dependence does not change the outcome of $\sigma(t)$-scaled residuals: These are still NIG distributed random variables.

The structure of the paper is as follows: In Sect. II.2, a mathematical framework of the stochastic model for stratospheric temperature is proposed. In Sect. II.3, a non-Gaussian CAR process with constant speed of mean reversion and time-dependent volatility function is introduced and proposed to model stratospheric temperature. The methodology for fitting the model to the

stratospheric temperature data is explained. Furthermore, it is shown that the most important features of stratospheric temperature dynamics are explainable through the proposed model. Then, in Sect. II.4 a stability analysis of speed of mean reversion is performed, revealing that the proposed CAR process should be generalized to include a time-dependent speed of mean reversion. Finally, conclusions and suggestions for future work are provided in Sect. II.5.

II.2 The Structure of a Stratospheric Temperature Model

In this section, it is argued that stratospheric temperature exhibits an autoregressive behavior. This motivates the use of autoregressive models. For completeness, the definitions of discrete and continuous time autoregressive processes are recalled. It is also explained how these two kinds of processes are connected.

II.2.1 Autoregressive Behaviour of Stratospheric Temperature Dynamics

Inspection of daily-zonal mean stratospheric temperature data over 60°N and 10 hPa, from now on referred to as the stratospheric temperature data, $S(t)$, clearly indicates a seasonal pattern. This is illustrated in Fig. II.1 which displays 10 years of stratospheric temperature data. The corresponding autocorrelation function (ACF), computed over 1 January 1979 to 31 December 2018 with lags up to 730 days (2 years), is presented in Fig. II.2a. The ACF pattern confirms a stratospheric temperature seasonal behaviour.

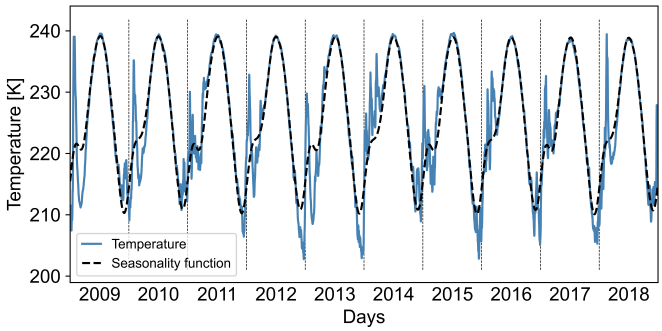

Figure II.1: Daily-zonal mean stratospheric temperature, $S(t)$, over a region R (see Sect. II.3.2) the last 10 years (1 January 2009 to 31 December 2018) with the fitted seasonality function $\Lambda(t)$. The vertical lines represent each of the 10 years

Inspired by prior work in stochastic modeling of surface temperature and wind dynamics, in the context of financial weather contracts (e.g., [11]; [9]; [10]; [12]; [14]), a long-term seasonality and trend function is fit to the stratospheric temperature data, see Sect. II.3.3. The long-term seasonality and trend function is

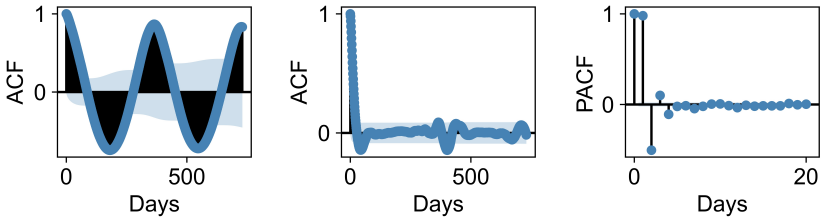

(a) ACF of $S(t)$ (b) ACF of $Y(t)$ (c) PACF of $Y(t)$

Figure II.2: ACF of stratospheric temperature, $S(t)$, and ACF and PACF of deseasonalized stratospheric temperature, $Y(t)$ (see Eq. (II.1))

from now on referred to as the seasonality function. Deseasonalized temperature is obtained by subtracting the fitted seasonality function from the original dataset.

Denote by $Y(t)$ the deseasonalized version of the stratospheric temperature, $S(t)$. Further, define $\Lambda(t) : [0, T] \to \mathbb{R}$ to be a bounded and continuously differentiable (deterministic) seasonality function. Thus, stratospheric temperature is modeled as

$$S(t) = \Lambda(t) + Y(t). \tag{II.1}$$

Note that although the seasonality function $\Lambda(t)$ is deterministic, the stratospheric temperature, $S(t)$, and the deseasonalized temperature, $Y(t)$, are stochastic. Let Ω be a scenario space. Then, both $S(t)$ and $Y(t)$ depend on some scenario $\omega \in \Omega$, that is, $S(t) \triangleq S(t, \omega)$, $Y(t) \triangleq Y(t, \omega)$. For notational convenience, the scenario ω is suppressed from the notation for the remaining part of the paper. In Sect. II.3.3, a review of possible seasonal effects is given prior to the explicit definition of the seasonality function $\Lambda(t)$. There, it will also be shown that a truncated Fourier series with linear trend is an appropriate choice for the seasonality function (see Eq. (II.18)).

Studying the ACF and partial autocorrelation function (PACF) of the deseasonalized temperature data, $Y(t)$, (Figs. II.2b and II.2c) it is found that the deseasonalized temperature dynamics follows an AR process. For completeness, the definition of AR processes is given in the next section. Further, the PACF of the deseasonalized stratospheric temperature (Fig. II.2c) indicates that an AR(4) model should be used to capture significant memory effects (see [34] for an introduction to AR modeling and the interpretation of ACF and PACF plots). This means that the direct memory effects in stratospheric temperature last for four days in this model. However, due to the recursive properties of AR processes, the total memory effect is actually longer. As explained in Sect. II.2.2, there is a transformation relation between (discrete time) AR(p) and (continuous time) CAR(p) processes. This means that, by removing the seasonal behaviour in stratospheric temperature data, the resulting deseasonalized stratospheric temperature data can be modeled by a CAR process. It will be shown that $Y(t)$ can be approximated by a CAR(4) model.

II.2.2 Non-Gaussian CAR(p) Processes and Their Connection to AR(p) Processes

In this section, AR and CAR processes are defined. Motivated by the observed ACF and PACF for the deseasonalized stratospheric temperature data (see Sect. II.2.1), these processes are natural components in a model for stratospheric temperature. They are also part of surface temperature models applied in energy markets contexts (e.g., [11]; [10], Ch. 4; [14]; [12], Ch. 10).

Suppose $(\Omega, \mathcal{F}, \{\mathcal{F}_t\}_{t\geq 0}, P)$ is a complete filtered probability space. Let $\boldsymbol{X}(t) = \{\boldsymbol{X}(t)\}_{t\in\mathbb{R}^+}$ be a stochastic process in $\mathbb{R}^p$, $p \in \mathbb{N}$, defined by a multidimensional non-Gaussian OU process with time-dependent volatility. That is, $\boldsymbol{X}(t)$ is given by the solution of the stochastic differential equation (SDE)

$$d\boldsymbol{X}(t) = A\boldsymbol{X}(t)dt + \boldsymbol{e}_p\sigma(t-)dL(t), \tag{II.2}$$

where $\boldsymbol{e}_p$ is the p-th unit vector in $\mathbb{R}^p$, $\sigma(t) : \mathbb{R}^+ \to \mathbb{R}^+$ is a càdlàg, $\mathcal{F}_t$-adapted function, $L(t) = \{L(t)\}_{t\in\mathbb{R}^+}$ is a Lévy process, and A is the $p \times p$ coefficient matrix

$$A = \begin{bmatrix} 0 & 1 & 0 & \cdots & 0 \\ 0 & 0 & 1 & \cdots & 0 \\ \vdots & \vdots & \vdots & \vdots & \vdots \\ 0 & 0 & 0 & \cdots & 1 \\ -\alpha_p & -\alpha_{p-1} & -\alpha_{p-2} & \cdots & -\alpha_1 \end{bmatrix}, \tag{II.3}$$

where α_k, $k = 1, \ldots, p$, are positive constants. By the multidimensional Itô formula the solution of Eq. (II.2) is given by

$$\boldsymbol{X}(s) = \exp\left(A(s-t)\right)\boldsymbol{x} + \int_t^s \exp(A(s-u))\boldsymbol{e}_p\sigma(u-)dL(u),$$

where $s \geq t \geq 0$ and $\boldsymbol{X}(t) \triangleq \boldsymbol{x} \in \mathbb{R}^p$. Let $p > j > q \in \mathbb{N}$. Then, the Lévy-driven stochastic process $Y(t) = \{Y(t)\}_{t\in\mathbb{R}^+}$ defined as $Y(t) \triangleq \boldsymbol{b}'\boldsymbol{X}(t)$, for a transposed vector $\boldsymbol{b} \in \mathbb{R}^{p\times 1}$ with elements satisfying $b_q \neq 0$ (sometimes, $b_q = 1$ is assumed) and $b_j = 0$, is called a (Lévy-driven) CARMA(p, q) process (e.g., [20]; [17]; [19]; [18]). The simplified version of a CARMA(p, q) process $Y(t)$ where $\boldsymbol{b} = \boldsymbol{e}_1$, meaning $q = 1$ and

$$Y(t) = X_1(t), \tag{II.4}$$

is called a CAR(p) process. Note that p is the direct time lag dependence in $Y(t)$. As seen in for example [11] and [9], the CAR(p) model framework is suitable for capturing surface temperature and wind evolution. Therefore, it is used in modeling of weather dynamics, for example in relation to financial weather contracts. In the current paper, it will be proved that the deseasonalized stratospheric temperature, $Y(t)$, can be modeled by a CAR(p) process as in Eq. (II.4).

Now, for a discrete time framework version, consider an AR(p) process given by

$$X(t) = \beta_1 X(t-1) + \beta_2 X(t-2) + \cdots + \beta_p X(t-p) + e(t), \tag{II.5}$$

where $X(t) \in \mathbb{R}$ is the value of the AR process at times $t = 0, 1, \ldots$, and β_k, $k = 1, \ldots, p$, are constant coefficients and $e(t)$ are i.i.d. random error terms. The dynamics of a Lévy-driven CARMA(p, q) process, see Eq. (II.2), can be expressed as

$$dX_q(t) = \begin{cases} X_{q+1}(t)dt & \text{if } q = 1, \ldots, p-1 \\ -\sum_{q=1}^{p} \alpha_{p-q+1} X_q(t)dt + \sigma(t-)dL(t) & \text{if } q = p. \end{cases} \tag{II.6}$$

By discretization of the expression in Eq. (II.6) ([12]; [14]) a transformation relation between (discrete time) AR(p) processes and the corresponding (continuous time) CAR(p) processes is obtained. That is, a transformation relation between $X(t)$ in Eq. (II.5) and $Y(t)$ in Eq. (II.4). See [12], Ch. 10, for a detailed derivation. Note that the connection between the AR and CAR processes is primarily useful because the continuous version, CAR, allows for deriving analytical results more easily, via stochastic analysis. For instance, [12] uses CAR processes to model surface temperature, which is later used to price options. To the best of our knowledge, financial products based directly on stratospheric data are not commonly available. However, as the state of the stratosphere is connected to long-term surface weather forecasting, the CAR model may be of interest for pricing financial weather contracts with long-term maturity. Further developments may also aim for a stratospheric temperature model where a control is involved. This means a situation where one may affect the stratospheric temperature directly, or indirectly, via for example carbon emissions.

Now consider the special case when $p = 4$, which will be proven to be well suited for modeling of stratospheric temperature, as assumed from observations in Sect. II.2.1. The dynamics of the CAR(4) process, see Eq. (II.2), can be written as

$$\begin{bmatrix} dX_1(t) \\ dX_2(t) \\ dX_3(t) \\ dX_4(t) \end{bmatrix} = \begin{bmatrix} 0 & 1 & 0 & 0 \\ 0 & 0 & 1 & 0 \\ 0 & 0 & 0 & 1 \\ -\alpha_4 & -\alpha_3 & -\alpha_2 & -\alpha_1 \end{bmatrix} \cdot \begin{bmatrix} X_1(t)dt \\ X_2(t)dt \\ X_3(t)dt \\ X_4(t)dt \end{bmatrix} + \begin{bmatrix} 0 \\ 0 \\ 0 \\ \sigma(t-)dL(t) \end{bmatrix}$$

$$= \begin{bmatrix} X_2(t)dt \\ X_3(t)dt \\ X_4(t)dt \\ -\alpha_4 X_1(t)dt - \alpha_3 X_2(t)dt - \alpha_2 X_3(t)dt - \alpha_1 X_4(t)dt + \sigma(t-)dL(t) \end{bmatrix}.$$

Note that the dynamics have the form as described in Eq. (II.6). By the transformation relation between AR(p) processes and CAR(p) processes [12] it

is found that the model coefficients of the CAR(4) process are given by

$$\begin{aligned} \alpha_1 &= 4 - \beta_1, \alpha_2 = -3\beta_1 - \beta_2 + 6, \\ \alpha_3 &= -3\beta_1 - 2\beta_2 - \beta_3 + 4, \alpha_4 = -\beta_1 - \beta_2 - \beta_3 - \beta_4 + 1. \end{aligned} \tag{II.7}$$

The matrix A, see Eq. (II.3), is referred to as the speed of mean reversion throughout the paper. This concept was introduced through half-life computations for Brownian motion-driven (one-dimensional) OU processes in [23], Sect. 2.4. That is, for some $s > t$ and a drift coefficient α the formula

$$s - t = \frac{\ln(2)}{\alpha}, \tag{II.8}$$

gives the time until a shock $X_{(1)}(t)$ away from the process' long-term mean returns half-way back to this long-term mean [14]. For an OU process, the drift coefficient α is the only variable affecting the half-life. As large α gives shorter half-life, and smaller α gives longer half-life, α is referred to as speed of mean reversion. In the current paper, non-Gaussian CAR (CARMA) processes are considered rather than standard OU processes. The half-life formula for non-Gaussian CARMA processes is state-dependent [14], meaning that the time s in Eq. (II.8) is a stopping time. Denote this stopping time by τ. The special case when the non-Gaussian CARMA process is a CAR process (the process considered in the remaining parts of this paper) gives a half-life formula of the form

$$\boldsymbol{e}_1' \left(\exp(A(\tau - t)) - \frac{1}{2} I \right) \boldsymbol{X}(t) = 0, \tag{II.9}$$

[13]. Solving this equation for τ analytically is difficult, and hence it is not clear how the coefficient matrix A affects the process' half-life. The coefficient matrix A will still be referred to as the speed of mean reversion, where each matrix element α_i is assumed to be a contribution to the speed of mean reversion.

A CAR(4) model driven by the multidimensional OU process in Eq. (II.2) assumes constant speed of mean reversion. In Sect. II.4, it will be shown that this assumption is not valid for our dataset. The stratospheric temperature data indicates a seasonal varying pattern in speed of mean reversion from month to month. Based on this observation, an extended model framework is proposed. That is, a CAR(4) model driven by a multidimensional OU process with time varying speed of mean reversion. The theorem below gives an explicit formula for the (unique) solution of the multidimensional OU SDE driven by a Lévy process with time-dependent speed of mean reversion.

Theorem II.2.1. *Let $\boldsymbol{X}(t)$ be given by the multidimensional OU process*

$$d\boldsymbol{X}(t) = A(t)\boldsymbol{X}(t)dt + \boldsymbol{e}_4 \sigma(t-) dL(t), \tag{II.10}$$

where $A(t)$ is the 4×4-matrix

$$A(t) = \begin{bmatrix} 0 & 1 & 0 & 0 \\ 0 & 0 & 1 & 0 \\ 0 & 0 & 0 & 1 \\ -\alpha_4(t) & -\alpha_3(t) & -\alpha_2(t) & -\alpha_1(t) \end{bmatrix}. \tag{II.11}$$

Then

$$\boldsymbol{X}(t) = \exp\left(\int_0^t A(s)ds\right)\left(\boldsymbol{x} + \int_0^t \exp\left(-\int_0^s A(u)du\right)\boldsymbol{e}_4\sigma(s-)dL(s)\right), \tag{II.12}$$

where $\boldsymbol{x} \triangleq \boldsymbol{X}(0)$.

Proof. Rewrite the SDE in Eq. (II.10) by use of the Itô-Lévy decomposition, to find that

$$\begin{aligned} d\boldsymbol{X}(t) =& A(t)\boldsymbol{X}(t)dt + \boldsymbol{e}_4\sigma(t-)\left(adt + bdB(t) + \int_{\mathbb{R}} z\bar{\boldsymbol{N}}(dt,dz)\right) \\ =& \left(A(t)\boldsymbol{X}(t) + \boldsymbol{e}_4 a\sigma(t-)\right)dt + \boldsymbol{e}_4 b\sigma(t-)dB(t) + \boldsymbol{e}_4\sigma(t-)\int_{\mathbb{R}} z\bar{\boldsymbol{N}}(dt,dz). \end{aligned}$$

By definition, $\boldsymbol{X}(t)$ is a multidimensional Itô-Lévy process. Apply the multidimensional Itô formula on $d\boldsymbol{Y}(t) \triangleq d\left(\exp\left(-\int_0^t A(s)ds\right)\boldsymbol{X}(t)\right)$. By defining $Y(t) \triangleq f(t, \boldsymbol{X}(t))$, it is found by the dominated convergence theorem and the fundamental theorem of calculus that

$$\begin{aligned} \frac{\partial f}{\partial t}(t,\boldsymbol{X}(t)) =& \frac{\partial}{\partial t}\sum_{k=1}^{\infty}\frac{1}{k!}\left(-\int_0^t A(s)ds\right)^k \boldsymbol{X}(t) \\ =& -\sum_{k=1}^{\infty}\frac{1}{(k-1)!}\left(-\int_0^t A(s)ds\right)^{k-1} A(t)\boldsymbol{X}(t) \\ =& -\exp\left(-\int_0^t A(s)ds\right)A(t)\boldsymbol{X}(t). \end{aligned}$$

Furthermore, note that

$$\frac{\partial f}{\partial x_i}(t,\boldsymbol{X}(t)) = \exp\left(-\int_0^t A(s)ds\right)\boldsymbol{e}_i \quad \text{and} \quad \frac{\partial^2 f}{\partial x_i \partial x_j}(t,\boldsymbol{X}(t)) = 0,$$

for all i and i,j respectively. The remaining terms coming from the Itô formula are trivial. Thus, one finds that

$$\begin{aligned} & d\boldsymbol{Y}(t)\exp\left(\int_0^t A(s)ds\right) = \\ & -A(t)\boldsymbol{X}(t)dt + \boldsymbol{e}_4 b\sigma(t-)dB(t) + \int_{\mathbb{R}}\left\{\boldsymbol{X}(t-) + \boldsymbol{e}_4\sigma(t-)z - \boldsymbol{X}(t-)\right\}\bar{\boldsymbol{N}}(dt,dz) \\ & + \Big(X_2(t)\boldsymbol{e}_1 + X_3(t)\boldsymbol{e}_2 + X_4(t)\boldsymbol{e}_3 \\ & \quad + (-\alpha_4(t)X_1(t) - \alpha_3(t)X_2(t) - \alpha_2(t)X_3(t) - \alpha_1(t)X_4(t) + a\sigma(t-))\boldsymbol{e}_4\Big)dt \end{aligned}$$

$$
\begin{aligned}
&+\int_{|z|<R}\{\boldsymbol{X}(t-)+\boldsymbol{e}_4\sigma(t-)z-\boldsymbol{X}(t-)-\boldsymbol{e}_4\sigma(t-)z\}\,\nu(dz)dt\\
=&A(t)\boldsymbol{X}(t)-A(t)\boldsymbol{X}(t)+\boldsymbol{e}_4\sigma(t-)\left(adt+bdB(t)+\int_{\mathbb{R}}z\bar{\boldsymbol{N}}(dt,dz)\right)\\
=&\boldsymbol{e}_4\sigma(t-)dL(t).
\end{aligned}
$$

Hence, from the definition of $Y(t)$, when $\boldsymbol{x}\triangleq\boldsymbol{X}(0)$,

$$
\boldsymbol{X}(t)=\exp\left(\int_0^t A(s)ds\right)\left(\boldsymbol{x}+\int_0^t\exp\left(-\int_0^s A(u)du\right)\boldsymbol{e}_4\sigma(s-)dL(s)\right).
$$

■

II.3 Stochastic Modeling of Daily-Zonal Mean Stratospheric Temperature

The aim of the following sections is to fit a CAR model to the daily-zonal mean stratospheric temperature data obtained from the ECMWF ERA-Interim reanalysis product.

II.3.1 Methodology for Deriving and Fitting a Stochastic Model to Stratospheric Temperature Data

This section describes the data analysis applied in Sects. II.3.3-II.3.5 to fit the model in Eq. (II.1) to ERA-Interim stratospheric temperature reanalysis data (described in [16] and specified in Sect. II.3.2). Applying this methodology shows that the model in Eq. (II.1) is suitable to model stratospheric temperature when $Y(t)$ is a non-Gaussian CAR(4) process.

Assume that a dataset of stratospheric temperatures indexed by time is given, and denote this by $\mathcal{S}$. A detailed description of the stratospheric temperature dataset used in this paper will be given in Sect. II.3.2. The main steps of the data analysis of $\mathcal{S}$ are:

1. Fit a deterministic continuous seasonality function $\Lambda(t)$ to $\mathcal{S}$. Subtract $\Lambda(t)$ from $\mathcal{S}$ to obtain a dataset of deseasonalized stratospheric temperatures, denoted $\mathcal{S}_d$.

2. Fit an AR(p) model to $\mathcal{S}_d$ with the choice of p based on the PACF of the dataset. Subtract the fitted AR(p) model from $\mathcal{S}_d$ to obtain a dataset of residuals, $\mathcal{E}$.

3. Compute the empirical expected values of the squared residuals each day over the year (assumed to be 365 days) to construct an approximation of the time-varying volatility function, $\sigma(t)$.

4. Divide $\mathcal{E}$ by $\sigma(t)$ to obtain a dataset of $\sigma(t)$-scaled residuals, denoted $\hat{\mathcal{E}}$. Find the probability distribution of the elements in $\hat{\mathcal{E}}$ (by statistical analysis).

As the goal of this work is to obtain a continuous time stochastic model for stratospheric temperature, notation corresponding to continuous functions will be used in the more detailed explanation that follows.

Assume that the stratospheric temperature, $S(t)$, is given by Eq. (II.1), $Y(t)$ being a CAR(p) process as in Eq. (II.4). The lag $p = 4$ is chosen based on observations in Sect. II.2.1, meaning that the direct memory effect reaches over four days. Then, by the transformation relation between CAR(4) and AR(4) processes in Eq. (II.7), the deseasonalized temperature is given by

$$X(t) = S(t) - \Lambda(t) = \sum_{k=1}^{4} \beta_k X(t-k) + e(t). \tag{II.13}$$

The seasonality function $\Lambda(t)$ is fit by least squares to simulate the seasonal behavior of the stratospheric temperature data in $\mathcal{S}$, and then subtracted from the stratospheric temperature data to find the discrete version of deseasonalized stratospheric temperature. The deseasonalized temperature is given by the AR(4) process $X(t)$ in Eq. (II.13), with random error terms (residuals) $e(t)$. Therefore, by use of least squares, an AR(4) model is fit to the deseasonalized stratospheric temperature data in $\mathcal{S}_d$, and then subtracted to find the residuals dataset $\mathcal{E}$. Mathematically, the residuals are given by

$$e(t) = X(t) - \sum_{k=1}^{4} \beta_k X(t-k). \tag{II.14}$$

In Sect. II.3.5, yearly heteroskedasticity is observed in the squared residuals. This means that the daily variance values (over the year) of the dataset $\mathcal{E}$ are time-dependent. Therefore, a time-varying volatility function $\sigma(t)$ is approximated and divided on the residuals in $\mathcal{E}$ to obtain the $\sigma(t)$-scaled residuals

$$\epsilon(t) = \frac{e(t)}{\sigma(t)}. \tag{II.15}$$

That is, $\epsilon(t)$ represents the data in $\hat{\mathcal{E}}$. Recall from Sect. II.2.2 (Eq. (II.5)), that $\epsilon(t)$ are i.i.d. random variables. The mean value of residuals each day d during the year, $d \in [1, 365]$ (see Sect. II.3.2), is assumed to be constant. Therefore, the variance each day during the year is given by

$$\mathrm{Var}(e_d(t)) = \left(E[e_d^2(t)] - E[e_d(t)]^2\right), \tag{II.16}$$

where $E[e_d(t)]$ represents the empirical mean value of residuals at day d. The magnitude of $E[e_d(t)]^2$ is insignificant compared to $E[e_d^2(t)]$, see Fig. II.3 for an illustration of this. Hence, the approximation

$$\mathrm{Var}(e_d(t)) \simeq E[e_d^2(t)], \tag{II.17}$$

is used to fit an appropriate time-varying variance function, $V(t)$, for $t \in [1, 365]$. See Sect. II.3.5 for a thorough explanation of how to compute $E[e_d^2(t)]$ empirically. When $E[e_d^2(t)]$ is computed for each d, the function $V(t)$ is fit to the values by use of three heavily truncated Fourier series (by least squares), which are connected by two sigmoid functions. The time-varying volatility function is finally computed as $\sigma(t) = \sqrt{V(t)}$. When $\hat{\mathcal{E}}$ is obtained, an appropriate probability density function (pdf) describing the distribution of the $\sigma(t)$-scaled residuals has to be found. Finally, the last step is to introduce a stochastic process which is able to replicate the behaviour of the particular pdf. The $\sigma(t)$-scaled residuals function $\epsilon(t)$ is represented by this stochastic process in the CAR model.

From this analysis, an appropriate driving stochastic process for the CAR(4) model is obtained. However, at this point (due to doing time series analysis) the model is given by Eq. (II.13), and is thus a discrete model. The CAR(4) model, which is given in Eq. (II.4), is found by applying the transformation relation in Eq. (II.7). A detailed description of this data analysis methodology applied to the ERA-Interim stratospheric temperature reanalysis data (see Sect. II.3.2) is given in Sects. II.3.3-II.3.5.

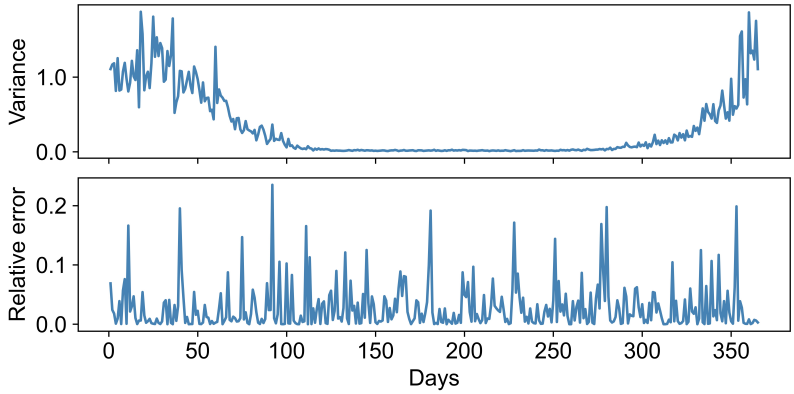

Figure II.3: Variance each day of the year computed with the approximation in Eq. (II.17), and the corresponding relative error when compared with the definition of variance (Eq. (II.16)). The mean absolute percentage error is 2.8%

II.3.2 The Zonal Mean Stratospheric Temperature Dataset

The aim of this section is to describe the stratospheric temperature dataset analyzed in the remaining of this paper.

Define a spherical coordinate system such that $(r_{\text{tot}}, \theta, \varphi)$ represents a point in the atmosphere. Let $r_{\text{tot}} = r_E + r$ represent the altitude from the center of the Earth, where r_E is the radius of the Earth and r is the distance from Earth's surface to the atmospheric point of interest. Further, θ represents the longitude and φ the latitude. With the presented notation, the region of interest in this

paper can be defined as

$$R \triangleq \big\{(r_{\text{tot}}, \theta, \varphi) | r = 10 \text{ hPa} \simeq 30 \text{ km}, \theta \in [-180^\circ\text{E}, 180^\circ\text{E}), \varphi = 60^\circ\text{N}\big\}.$$

The region R is an area bounded by a circumpolar line in the extra-tropical stratosphere. The pressure level 10 hPa corresponds roughly to 30 km altitude. Stratospheric dynamics in this region are highly variable, and they depend on the state of the stratospheric polar vortex.

Enhanced probing and representation of the stratosphere in atmospheric models and numerical weather prediction systems has potential to enhance surface weather predictions on weekly to monthly timescales (e.g., [36]; [32]; [21]). Maybe the most striking example of stratospheric influence on the surface is the extreme event of sudden stratospheric warmings (SSWs), where an abrupt disruption in the stratospheric winter circulation occurs, accompanied by a stratospheric temperature increase of several tens of degrees. SSWs are detectable in the region R. Through stratosphere-troposphere coupling, the effects of SSWs can extend to the troposphere, with increased probability of shifts in the jet stream and storm tracks, further affecting the expected precipitation and surface temperatures. This phenomenon can, for example, be manifested as harsher winter weather regimes on continental North America and Eurasia [3]. This may have impact on several sectors in society and industry.

With the purpose of deriving a stochastic stratospheric temperature model, a dataset $\mathcal{D}$ from the ERA-Interim reanalysis model product is retrieved from ECMWF [16], such that each temporal data point $d_i \in \mathcal{D}$ represents the spatial mean stratospheric temperature over R. As the spatial mean is taken over the full circumpolar interval, this is denoted as the zonal mean. The zonal mean properties of the stratosphere at the 10 hPa pressure level is commonly considered in stratospheric diagnostics, and when studying stratospheric events like SSWs and beyond [22]. The subscript i represents a measurement every six hours from midnight, and the zonal mean is taken over θ at a 0.5° spacing. That is, $\mathcal{D}$ contains four zonal mean temperature measurements every day within the interval $T \in [1 \text{ January } 1979, 31 \text{ December } 2018]$. For computational convenience, all data from 29 February each leap year are excluded from $\mathcal{D}$, such that the length of each year is constant. All stated specifications of $\mathcal{D}$ are collected in Tab. II.1. Further, define the dataset

$$\mathcal{S} \triangleq \big\{S_k : S_k = E[d|D_k]\big\},$$

where D_k are subsets of $\mathcal{D}$ containing four data points every given day k in the time interval T (except days 29 February), and $E[d|D_k]$ is the empirical mean. That is, $\mathcal{S}$ contains daily-zonal mean stratospheric temperatures over the region R for days in the time interval T. This is the time series analyzed in the remaining of this paper. As 29 February is excluded each leap year, the total number of data points in $\mathcal{S}$ is $14,600$. A plot of $\mathcal{S}$ for the last ten years (from 1 January 2009 to 31 December 2018) with a fitted seasonality function was shown in Fig. II.1.

Table II.1: Specifications of the stratospheric temperature dataset $\mathcal{D}$

Date	Grid	Pressure level	Time	Area	Unit
1 January 1979 to 31 December 2018	0.5°	10 hPa	00:00, 06:00, 12:00, 18:00	60°N and [−180°E, 180°E)	Kelvin

II.3.3 Fitting a Seasonality Function to Stratospheric Temperature Data

In this section, seasonality in stratospheric temperature data is analyzed. Seasonality in this setting means (deterministic) periodically repetitive patterns of temperature dynamics over time. A deterministic seasonality function will be fit to the dataset $\mathcal{S}$, with the aim of further analyzing deseasonalized temperature data where these periodically repetitive patterns are removed. Although the stratosphere is typically characterized by variations on longer timescales than the troposphere, there are oscillation, or atmospheric tide, patterns present at these altitudes as well. In addition to the directly forced cycles causing seasonal effects, for example, the phenomenon of quasi-biennial oscillations (QBO) is a nearly periodic phenomenon in the stratosphere. The QBO period is variable, but averages to about 28 months. This is a phenomenon occurring in the equatorial stratosphere. Still, the QBO can affect stratospheric conditions from pole to pole, and even has effects on the breaking of wintertime polar vortices, leading to SSWs ([39]; [4]).

Seasonal effects complicate stochastic modeling because they cause non-stationarity. In the current study, daily-zonal mean stratospheric temperatures over 40 years are considered, meaning that the periodic phenomena of interest are the yearly cycle and the QBO. Non-stationarity can also result from long-term effects of greenhouse gases and ozone, anthropogenic forcings that cause a stratospheric cooling trend ([24]; [25]; [38]). The first step in deriving a stochastic stratospheric temperature model is to fit a seasonality function to the data, and then to subtract this to remove the non-stationary effects.

As the yearly cycle is the most pronounced phenomenon (Figs. II.1 and II.2a), a Fourier series with a period of 365 days is chosen as seasonality function. Further, the long-term decreasing trend in stratospheric temperature is approximately linear, meaning that a linear function should be present in the seasonality function as well. Based on these considerations, a seasonality function $\Lambda(t)$ is defined as in Eq. (II.18).

In the following, the continuous version of daily-zonal mean stratospheric temperature data $S_i \in \mathcal{S}$ (as described in Sect. II.3.2) is denoted by $S(t)$, where $t \in \mathbb{R}^+$. Let $S(t)$ be given by the stochastic model in Eq. (II.1) with seasonality function

$$\Lambda(t) = c_0 + c_1 t + \sum_{k=1}^{n} \left(c_{2k} \cos(k\pi t/365) + c_{2k+1} \sin(k\pi t/365) \right), \tag{II.18}$$

where $c_0, c_1, c_2, \ldots, c_{2n+1}$ are constants. The choice of $\Lambda(t)$ is made based on the discussion above, where c_1 captures the slope of the long-term cooling of the stratosphere (corresponding to global warming of the troposphere), and where the constant term c_0 represents the average level at the beginning of the time series $\mathcal{S}$. The constants $c_2, \ldots, c_{2k+1}$ describe the yearly cycle as weights in the truncated Fourier series.

The seasonality function $\Lambda(t)$ is fit to the time series in $\mathcal{S}$ with $n = 10$ (using least squares), with resulting parameters given in Tab. II.2. Figure II.1 displays the fitted seasonality function $\Lambda(t)$ together with the ten last years of the times series in $\mathcal{S}$. The value of c_0 in Tab. II.2 indicates that the daily-zonal mean stratospheric temperature over the region R (see Sect. II.3.2) was approximately 226.15 K (−47.00°C) in 1979. The negative value of c_1 confirms the long-term cooling effect of the stratosphere. The c_1 value found corresponds to a daily-zonal mean stratospheric temperature decrease of approximately 1.05 K (equivalent to a change of 1.05°C) over the last 40 years at 60°N and 10 hPa. This is consistent with [38], estimating an overall cooling of the stratosphere of about 1-3 K over the same time span.

Table II.2: Seasonality function, $\Lambda(t)$, parameters (see Eq. (II.18)) for daily-zonal mean stratosphe ric temperature at 60°N and 10 hPa between 1 January 1979 and 31 December 2018

c_0	c_2	c_4	c_6	c_8	c_{10}	c_{12}	c_{14}	c_{16}	c_{18}	c_{20}
226.15	−0.05	−12.09	0.23	1.88	0.33	0.16	0.13	−0.09	−0.15	−0.01
c_1	c_3	c_5	c_7	c_9	c_{11}	c_{13}	c_{15}	c_{17}	c_{19}	c_{21}
−0.000072	−0.11	1.63	−0.23	2.81	−0.04	1.54	0.14	0.45	0.05	0.11

II.3.4 Fitting an AR Model to Deseasonalized Stratospheric Temperature Data

Having deseasonalized the stratospheric temperature dataset $\mathcal{S}$, the next step is to fit an AR model to the deseasonalized dataset $\mathcal{S}_d$. Temperature tends to having a mean-reverting property over time, a property that can be modeled by an AR(p) process [12]. Based on the discussion in Sect. II.2.1, suppose that the deseasonalized stratospheric temperature $Y(t) = S(t) - \Lambda(t)$ can be modeled by an AR(p) process as represented in Eq. (II.5), where the random error terms $e(t)$ represent the model residuals. The empirical ACF and PACF of the deseasonalized stratospheric temperature data illustrated in Figs. II.2b and II.2c confirm that it is appropriate to model $Y(t)$ by an AR(p) process, and indicate that $p = 4$ is needed to explain the time series evolution (see [34]). An AR(4) model is fit to the deseasonalized stratospheric temperature data in $\mathcal{S}_d$ by use of least squares. The resulting AR(4) model parameters are presented in Tab. II.3. By use of Eq. (II.7) the corresponding CAR(4) process is calculated, and the resulting model parameters for this continuous model are presented in Tab. II.3 as well. Based on the reasoning in [12], preservation of stationarity of

the CAR(4) model depends on the properties of the time-dependent volatility function $\sigma(t)$. However, as long as all eigenvalues of the matrix A have negative real part, it is ensured that the modeled temperature on average will coincide with the seasonality function $\Lambda(t)$ when time approaches infinity. This is because, as will be shown in Sect. II.3.5, the Lévy-driven CAR(4) model generates NIG distributed random variables with mean zero, a property which is preserved for the model in the long run when the eigenvalues have negative real part. The eigenvalue equation

$$\lambda^4 + \alpha_1\lambda^3 + \alpha_2\lambda^2 + \alpha_3\lambda + \alpha_4, \tag{II.19}$$

has roots $\lambda_{1,2} = -1.01 \pm 0.43i$, $\lambda_3 = -0.36$ and $\lambda_4 = -0.07$, and the stationarity condition is therefore satisfied.

Table II.3: AR(4) model parameters, and parameters of its continuous counterpart, when fitted to daily-zonal mean stratospheric temperature over 60°N and 10 hPa in the period 1 January 1979 to 31 December 2018

AR(4) parameters	β_1	β_2	β_3	β_4
	1.55	−0.75	0.28	−0.11
CAR(4) parameters	α_1	α_2	α_3	α_4
	2.45	2.10	0.56	0.03

II.3.5 Analyzing the Residuals

In this section, the residuals (random error terms) in the dataset $\mathcal{E}$ are analyzed to determine the appropriate stochastic driving process of the CAR(4) model for stratospheric temperature.

In computing the parameters of the CAR(4) model in Sect. II.3.4, the deterministic mean-reverting property of the stratospheric temperature is found. A suitable stochastic driving process for the model residuals, corresponding to the random error terms in Eq. (II.5), still remains to be found. As derived in Sect. II.3.1, the model residuals are given by

$$e(t) = X(t) - \sum_{k=1}^{4} \beta_k X(t-k). \tag{II.20}$$

The approach to find a suitable stochastic driving process is therefore to empirically determine the stratospheric temperature model residual distribution in $\mathcal{E}$. In [34], there is a statement that residuals of AR(p) models approach white noise for larger p. Therefore, it is reasonable as a first guess to assume that $e(t)$ is distributed as i.i.d. $N(0,1)$. A normal fit is performed on $\mathcal{E}$, however, by Fig. II.4a it is clear that the data is not normally distributed. Further, Fig. II.4b indicate a seasonally varying empirical ACF of squared residuals. Since the distributional mean value is close to zero, this is a sign of seasonal heteroskedasticity in

the distributional variance (see Sect. II.3.1). A similar seasonal pattern in the empirical ACF of squared residuals was observed by [12] in daily average surface temperature data in Sweden.

Still assuming the stratospheric temperature model residuals to be normally distributed random variables, however with a time-varying variance rather than the constant 1, $e(t)$ is rewritten as

$$e(t) = \sigma(t)\epsilon(t). \tag{II.21}$$

Here, $\epsilon(t)$ are distributed as i.i.d. $N(0,1)$, and $\sigma(t)$ is a yearly (see Fig. II.4b) time-varying deterministic function. To adjust for the heteroskedasticity, the volatility function $\sigma(t)$ must be defined explicitly. To do so, the same approach as in [12] is used: Daily residuals over 40 years are organized into 365 groups, one group for each day of the year. This means that all observations on 1 January are collected into group 1, all observations on 2 January into group 2, and so on until all days of all years are grouped together. Recall that observations on 29 February were removed each leap year, such that each year contains 365 data points. By computing the empirical mean of the squared residuals in each group, an estimate of the expected squared residual each day of the year is found, corresponding to an estimate of the daily variance, as explained in Sect. II.3.1 (Eq. (II.17)). The resulting 365 estimates of daily variance yields an estimate of the time-varying variance function, $V(t)$, over the year. This is illustrated in Fig. II.5. The yearly heteroskedasticity is clearly visible. Recall that, by definition, the volatility

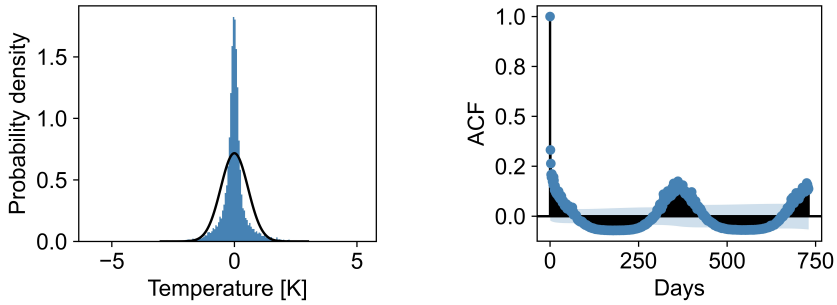

(a) Distribution of $e(t)$

(b) ACF of $e^2(t)$

Figure II.4: The distribution of stratospheric temperature model residuals $e(t)$ (Eq. (II.20)) with a fitted normal distribution, and ACF of the squared model residuals $e^2(t)$

function $\sigma(t)$ is the square root of the time-varying variance function. With the aim of obtaining $\sigma(t)$, an analytic function is fit to the empirically computed expected value of squared residuals, to find a proper function $V(t)$. Figure II.5 illustrate that the volatility in the stratospheric temperature variance is much higher in winter time than in summer time, as seen in [28]. This, as well as the shape of the estimated daily variance (expected squared residuals) over the year, makes function estimation with Fourier series more challenging than simply

fitting a single Fourier series. To properly fit a function $V(t)$, the year is split into three parts. Each part represents the winter/spring season, summer season and autumn/winter season, respectively. A local variance test is performed to find appropriate seasonal endpoints. That is, the summer season variance is low and stable compared to the two other seasons, and so the summer season endpoints are set where the local variance hits a given limit, δ. Define the local variance as

$$v(n) \triangleq \frac{1}{2n-1} \sum_{i=0}^{2n-1} (x_i - \mu)^2,$$

where n represents the degree of locality. The number of elements included in the sum is odd, $2n-1$, such that the local variance for each element is based on a symmetric number of neighbours on each side. The test is performed as follows: First, the limit δ is defined such that mid-summer local variances do not exceed δ. Second, with estimated expected squared residuals given as $[V_1, V_2, \ldots, V_{364}, V_{365}]$, the local variance $v(n)_k$ is computed for each point V_k in $[V_n, V_{n+1}, \ldots, V_{364-n}, V_{365-n}]$ (each endpoint is cut with $n-1$ elements for computability). Third, an array $K = [k_i \in \{n, n+1, \ldots, 365-n\} : \ v(n)_{k_i} < \delta]$ is constructed (sequentially in time), such that the index (that is, day) of elements with satisfactory small local variance is known. Fourth, based on the array K, a collection $\mathcal{K} = \{(k_i - k_{i-1}, k_i) \in \mathbb{N} \times \{n, n+1, \ldots, 365-n\} : \ \forall \ k_i \in K\}$ is constructed for stability purposes. Finally, all pairs in $\mathcal{K}$ where $k_i - k_{i-1} > 1$ (day) are printed such that stability of the condition $v(n)_k < \delta$ can be evaluated manually.

The analysis is performed with $n = 5$ and $\delta = 0.0002$, and gives cutoff at days 115 and 288, corresponding to 25 April and 15 October, respectively. For simplicity, the cutoffs are set at the following whole month. That is, the three seasons winter/spring, summer and autumn/winter are defined to be in the intervals [1 January, 30 April], [1 May, 31 October] and [1 November, 31 December], respectively. A function is fit to the estimate of $V(t)$ for each of the three seasons by use of the truncated Fourier series

$$w_f(t) = d_0 + \sum_{k=1}^{2} \left(d_{2k-1} \cos(fk\pi t/365) + d_{2k} \sin(fk\pi t/365) \right), \qquad \text{(II.22)}$$

where $d_0, ..., d_4$ are constants and f is a given parameter adjusting the series frequency. By manual inspection, the function $w_f(t)$ for each of the three seasons are chosen as $w_{0.44(1)}(t)$, $w_{2.0}(t)$ and $w_{0.44(2)}(t)$ respectively, and Tab. II.4 displays the fitted parameters.

The transitions from winter/spring to summer and from summer to autumn/winter should be smooth in order to obtain a smooth yearly time-varying volatility function $\sigma(t) : [1, 365] \to \mathbb{R}$. This is achieved by connecting the three functions $w_{0.44(1)}(t)$, $w_{2.0}(t)$ and $w_{0.44(2)}(t)$ with two sigmoid functions as in [33]. The sigmoid function $\omega(x)$ and the connective function $\xi(x)$ are given by

$$\omega(x) = \frac{1}{1 + \exp\left(-(\frac{x-a}{b})\right)} \quad \text{and} \quad \xi(x) = \big(1 - \omega(x)\big) f_1(x) + \omega(x) f_2(x),$$

where a and b are shift and scaling constants respectively, and $f_1(x)$ and $f_2(x)$ are two functions that are to be connected. By connecting the functions $w_{0.44(1)}(t)$ and $w_{2.0}(t)$ with $a = 120$ and $b = 2$, and connecting the functions $w_{2.0}(t)$ and $w_{0.44(2)}(t)$ with $a = 304$ and $b = 5$, a smooth function $\sigma(t)$ is found. The resulting volatility function is illustrated as $\sigma^2(t)$ (or $V(t)$) in Fig. II.5, together with the estimated daily variances during the year. With an explicit expression

Table II.4: Parameters of fitted Fourier series, $w_f(t)$ (see Eq. (II.22)), to each of the three seasons winter/spring, summer and autumn/winter

Winter/spring ($f = 0.44$)	d_0	d_1	d_2	d_3	d_4
	-507.58	633.29	269.90	-124.82	-130.75
Summer ($f = 2.0$)	d_0	d_1	d_2	d_3	d_4
	0.092	0.107	0.023	0.034	0.015
Autumn/winter ($f = 0.44$)	d_0	d_1	d_2	d_3	d_4
	13.36	-263.03	86.00	91.21	102.50

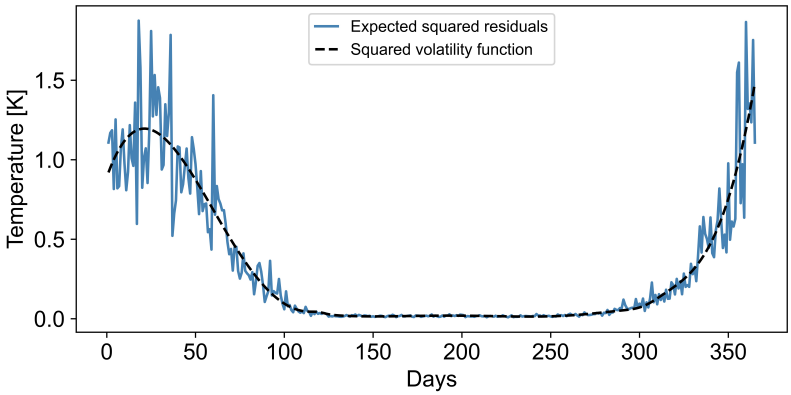

Figure II.5: Estimation of expected squared residuals (estimated variance) each day of the year illustrated together with a fitted function

for the volatility function $\sigma(t)$, the $\sigma(t)$-scaled residuals $\epsilon(t)$ (as described in Eq. (II.21)) can be studied. The distribution of the $\sigma(t)$-scaled stratospheric temperature model residuals in $\hat{\mathcal{E}}$ is compared to the normal distribution with a QQ-plot in Fig. II.6a. The above hypothesis about $\epsilon(t)$ being i.i.d. $N(0, 1)$ random variables does not hold, as the QQ-plot illustrate heavy tails and a slightly skewed distribution. Also, the Kolmogorov-Smirnov (KS) test with statistic 0.027 and p-value $1.57 \cdot 10^{-9}$ gives significance for rejecting the hypothesis about $\epsilon(t)$ being standard normal. A fit with the NIG distribution is further performed, and the resulting pdf is illustrated in Fig. II.6b. The KS test with statistic 0.0064 and p-value 0.57 does not reject the null-hypothesis that $\epsilon(t)$ represents NIG distributed

random variables. Note that the KS-test is meant to provide indicative results, rather than concluding results from a carefully planned statistical experiment.

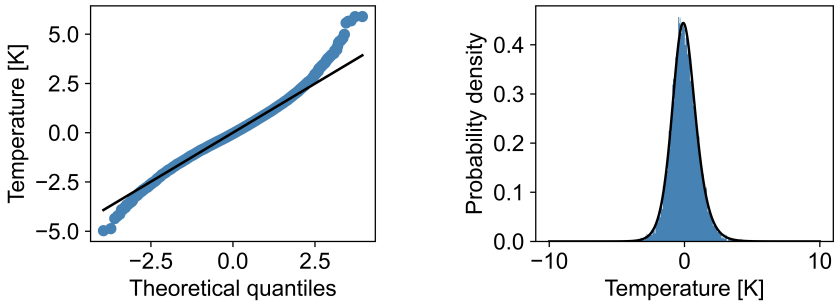

(a) Normal QQ-plot of $\epsilon(t)$ (b) NIG fit of $\epsilon(t)$

Figure II.6: Fitted distributions to the $\sigma(t)$-scaled stratospheric temperature model residuals $\epsilon(t)$, see Eq. (II.21)

The result of $\epsilon(t)$ representing NIG distributed random variables supports the hypothesis of using a Lévy process as the driving process for the stratospheric temperature model, as proposed in Sect. II.2.2. However, as shown in Figs. II.7a and II.7b, the squared $\sigma(t)$-scaled residuals are partially autocorrelated in approximately 5 lags, meaning increments of $\epsilon(t)$ fail to be independently distributed. These memory effects indicate using a stochastic volatility function as described in [9], rather than a deterministic yearly time-varying volatility function. To generalize the proposed model in Sect. II.2.2, a possibility would be to model $e(t)$ as a normal variance-mean mixture with an inverse Gaussian stochastic volatility, as this process is approximately NIG distributed ([7]; [14], Sect. 4). However, as the memory effects are rather small (except in the first lag), it could be appropriate to assume that there are no significant memory effects in the variance. A possibility is therefore to assume a deterministic volatility function, where the driving process for the stratospheric temperature model is a NIG Lévy process (e.g., [5]; [6]; [7]). Further studying of this aspect is beyond the scope of the current paper, and is left as a topic for further research.

II.4 Analyzing the Speed of Mean Reversion

In this section, it is shown that the assumption of constant speed of mean reversion for stratospheric temperature is erroneous. A generalization of the proposed stratospheric temperature model dynamics in Eq. (II.2), correcting this erroneous assumption, is presented. More specifically, a special case of the dynamics in Eq. (II.10) is proposed as a replacement to drive the stratospheric temperature model in Eq. (II.4).

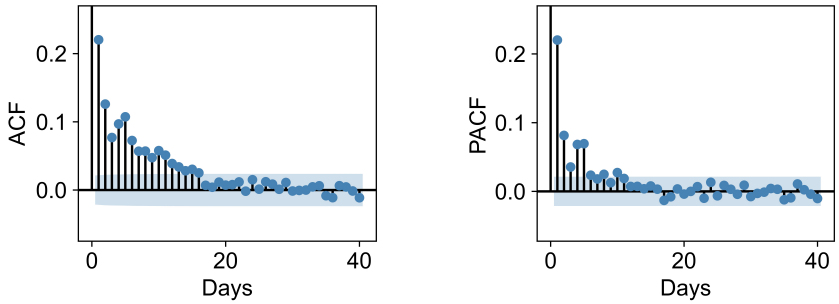

(a) ACF of $\epsilon^2(t)$ (b) PACF of $\epsilon^2(t)$

Figure II.7: ACF and PACF of the squared $\sigma(t)$-scaled stratospheric temperature model residuals $\epsilon^2(t)$, see Eq. (II.21)

II.4.1 Methodology for Analyzing Speed of Mean Reversion

In the previous sections, it was shown that the deseasonalized stratospheric temperature, $Y(t)$, follows a mean-reverting stochastic process. That is, deseasonalized stratospheric temperature dynamics is given by the OU process in Eq. (II.2). The matrix A holds parameters of speed of mean reversion, meaning that the rate at which the stratospheric temperature reverts back to its long-term mean is given by the elements of A, see Sect. II.2.1 (Eq. (II.8) and Eq. (II.9)). In the previous sections the speed of mean reversion was assumed to be constant, and thus independent of time. To check the validity of this assumption, a similar stability analysis of speed of mean reversion as in [11] will be performed in the following. The stability analysis exploits the transformation relation between CAR and AR models (see Sect. II.2.2), meaning that it is applied on computed AR parameters $\beta(t)$. That is: The mean value, $E[\beta(t)]$, and standard deviation, $\sqrt{\text{Var}(\beta(t))}$, of fitted AR($p$) parameters are computed empirically over each available year and month. Based on this, the yearly and monthly variation coefficients are found as

$$\Delta = \frac{\sqrt{\text{Var}(\beta(t))}}{E[\beta(t)]}. \tag{II.23}$$

The yearly and monthly variation coefficients reflect the stability of the speed of mean reversion over years and months, respectively. As the stratospheric temperature model is derived with lags in four days, this analysis will be performed with $p = 4$ for all computed AR parameters. The methodology for analyzing the yearly stability of speed of mean reversion is as follows: 1; Loop through the 40 years in $\mathcal{S}_d$ and collect deseasonalized daily-zonal mean stratospheric temperatures 365 days at a time, such that data for 1 January 1979 to 31 December 1979 are collected in one array, data for 1 January 1980 to 31 December 1980 in one array, and so on until the last array containing data for 1 January 2018 to 31 December 2018. Then, 2; Collect the 40 arrays containing all data each year in a single array to form the nested array $\boldsymbol{y}$, so

$\dim(\boldsymbol{y}) = 1 \times 40 \times 365$. 3; Loop through the 40 arrays in $\boldsymbol{y}$, where an AR(4) model is fit to each of the years 1979 to 2018. The result is 40 arrays of AR parameters $(\beta_1^y, \beta_2^y, \beta_3^y, \beta_4^y)$, $y \in \{1, 2, \ldots, 40\}$. 4; Collect all 40 AR parameters corresponding to the same lag in one array and compute the statistics. That is, make the arrays $\boldsymbol{\beta}_1^y = (\beta_1^1, \beta_1^2, \ldots, \beta_1^{40}), \ldots, \boldsymbol{\beta}_4^y = (\beta_4^1, \beta_4^2, \ldots, \beta_4^{40})$, and compute the empirical mean, standard deviation, and finally the variation coefficients defined in Eq. (II.23), for each array $\boldsymbol{\beta}_1^y$, $\boldsymbol{\beta}_2^y$, $\boldsymbol{\beta}_3^y$ and $\boldsymbol{\beta}_4^y$. The results from this yearly stability analysis are presented in Tab. II.5. Further, the methodology for the monthly stability analysis of speed of mean reversion is: 1; Define one array for each month: $\boldsymbol{Jan}, \boldsymbol{Feb}, \boldsymbol{Mar}, \ldots, \boldsymbol{Dec}$. 2; Loop through the 40 arrays in $\boldsymbol{y}$ (which is constructed in point 2 for the yearly stability analysis). For all 40 arrays, collect elements 0 to 30 in $\boldsymbol{Jan}$, elements 31 to 58 in $\boldsymbol{Feb}$, elements 59 to 89 in $\boldsymbol{Mar}$, and so on until you reach elements 334 to 364 which are collected in $\boldsymbol{Dec}$. The resulting arrays are nested arrays of the form

$$\boldsymbol{Jan} = \left[\boldsymbol{Jan}^1, \ldots, \boldsymbol{Jan}^{40}\right], \boldsymbol{Feb} = \left[\boldsymbol{Feb}^1, \ldots, \boldsymbol{Feb}^{40}\right], \ldots, \boldsymbol{Dec} = \left[\boldsymbol{Dec}^1, \ldots, \boldsymbol{Dec}^{40}\right].$$

Each array has dimension $1 \times 40 \times n$, where n corresponds to the number of days in that particular month. That is, $n = 31$ for $\boldsymbol{Jan}$, $n = 28$ for $\boldsymbol{Feb}$ and so on. 3; Collect the arrays $\boldsymbol{Jan}, \ldots, \boldsymbol{Dec}$ in a nested array $\boldsymbol{m}$: $\dim(\boldsymbol{m}) = 1 \times 12 \times 40 \times n$. Loop through each of the 480 months in $\boldsymbol{m}$, and fit an AR(4) model to each of the Januaries of the years 1979 to 2018, to each of the Februaries of the years 1979 to 2018, and so on until the last fit is performed on the data of December of 2018. The result is 480 arrays of AR parameters $(\beta_1^m, \beta_2^m, \beta_3^m, \beta_4^m)$, $m \in \{1, 2, \ldots, 480\}$. 4; Make the arrays $\boldsymbol{\beta}_1^m = (\beta_1^1, \beta_1^2, \ldots, \beta_1^{480}), \ldots, \boldsymbol{\beta}_4^m = (\beta_4^1, \beta_4^2, \ldots, \beta_4^{480})$, and for each of them compute the variation coefficient as defined in Eq. (II.23). Further, because of the constructed order of the parameters, the arrays $\boldsymbol{\beta}_1^m$, $\boldsymbol{\beta}_2^m$, $\boldsymbol{\beta}_3^m$ and $\boldsymbol{\beta}_4^m$ can be used to analyze the seasonal behaviour of speed of mean reversion. The computed results from this monthly stability analysis are presented in Tab. II.5, where the variability coefficients will reveal any monthly instability of speed of mean reversion. With the intention of detecting any monthly seasonal behaviour in the four AR parameters, $\boldsymbol{\beta}_1^m$, $\boldsymbol{\beta}_2^m$, $\boldsymbol{\beta}_3^m$ and $\boldsymbol{\beta}_4^m$ are plotted in Figs. II.8a-II.8d.

II.4.2 Interpretations of the Monthly Stability Analysis

The monthly variation coefficients are more extreme than the yearly ones. Therefore, the remaining of this section will focus on interpreting results from the monthly stability analysis, as well as to incorporate the observed time-varying behaviour of the speed of mean reversion, into the stratospheric temperature model dynamics in Eq. (II.10).

The magnitudes of the monthly variation coefficients (see Tab. II.5) for all four AR parameters, indicate that the assumption of constant speed of mean reversion in the stratospheric temperature model dynamics (Eq. (II.2)) is insufficient. The monthly variation coefficient, Δ, of the first lag parameter, β_1, is small compared to Δ of the three other lag parameters. However, as seen in Figs. II.8a-II.8d, the

magnitude of β_1 is up to many times larger than the magnitudes of β_2, β_3 and β_4 (where the magnitudes of β_1, β_2, β_3 and β_4 are assessed over the contents of $\boldsymbol{\beta}_1^m$, $\boldsymbol{\beta}_2^m$, $\boldsymbol{\beta}_3^m$ and $\boldsymbol{\beta}_4^m$ respectively). This means that larger variability in the latter lag parameters affect the estimated stratospheric temperature less. Despite this observation, all variability coefficients are too large to be ignored, meaning that time-dependent AR parameters should be used rather than constant ones. By the transformation relation between CAR(4) and AR(4) models in Eq. (II.7), it is clear that the stratospheric temperature model dynamics should be given by the OU process in Eq. (II.10), rather than the one in Eq. (II.2).

It is not only the monthly variability coefficients of the AR parameters that suggest time-varying speed of mean reversion. The sequential patterns of $\boldsymbol{\beta}_1^m$ and $\boldsymbol{\beta}_2^m$ in Figs. II.8a and II.8b clearly show that the AR parameters β_1 and β_2 are seasonally varying. Both the first, β_1, and the second, β_2, AR parameters are smaller in magnitude in summer time than in winter time. This means that summer time stratospheric temperature is less dependent on the stratospheric temperature the last two days, than winter time stratospheric temperature. This tendency is also (however less) evident for the third, β_3, and fourth, β_4, AR parameters in Figs. II.8c and II.8d. To the best of our knowledge

Table II.5: Mean value, standard deviation and absolute value of variability coefficient for the four parameters of an AR(4) process with yearly and monthly varying parameters, respectively

	Parameter	β_1	β_2	β_3	β_4
Yearly	Mean value	1.54	−0.74	0.28	−0.12
	Standard deviation	0.12	0.22	0.18	0.09
	abs(Δ)	7.8%	29.9%	64.3%	72.6%
	Parameter	β_1	β_2	β_3	β_4
Monthly	Mean value	1.29	−0.48	0.19	−0.06
	Standard deviation	0.34	0.45	0.32	0.20
	abs(Δ)	26.6%	94.8%	170.7%	312.9%

there is no previous research specifically on the mean reverting property of stratospheric temperature. In [40], daily values of speed of mean reversion for surface temperature are estimated by use of a neural network, revealing strong time-dependence. Even though daily variation in speed of mean reversion is not studied in the current paper, a similar conclusion is reached: Speed of mean reversion of stratospheric temperature is dependent on time. However, [40] found no signs of seasonal patterns, unlike the current study for stratospheric temperature where a clear seasonal pattern is observed in the monthly estimated AR parameters. In response to the observation of time-dependence in speed of mean reversion of surface temperature, [8] presented a generalized version of the state-of-the-art stochastic models for surface temperatures applied in mathematical finance (see Sect. II.2.2), where the speed of mean reversion of the driving (standard) OU process is a stochastic process. A simplified version

of this generalized process (however multidimensional, and Lévy-driven rather than Brownian motion-driven) is presented in the current paper to incorporate time variability in speed of mean reversion. That is, the matrix $A(t)$ holding parameters of speed of mean reversion is assumed to be time-dependent and deterministic as presented in Thm. II.2.1.

Before presenting an explicit time-dependent and deterministic matrix $A(t)$ representing the speed of mean reversion of stratospheric temperature, its time-varying behaviour will be discussed. As already mentioned, the monthly AR parameters (which the speed of mean reversion depends directly upon) have large variability coefficients, Δ, as well as a seasonal behaviour. From the definition of Δ in Eq. (II.23), one can see that the seasonal behaviour increases the computed variability coefficients considerably. By removing the seasonal behaviour in the AR parameters (see below) noise is still present, indicating that the speed of mean reversion could be modeled by a stochastic process. However, this is beyond the scope of this paper, and the noise is assumed to be negligible. For this reason, time-dependence in speed of mean reversion is assumed to come solely from the seasonal variations.

As discussed in Sect. II.3.3, the only long-term (perfectly) periodic phenomenon in the stratosphere is the yearly cycle. This is clearly seen in the stratospheric temperature data presented in Fig. II.1. Further, as seen in Fig. II.5, this phenomenon affects the variability, as well as volatility in variability, of stratospheric temperature. Physical explanations of this behaviour are discussed in [28], where the winter time stratosphere is said to be more disturbed than the summer time stratosphere. Based on this, together with the above discussion concluding stronger speed of mean reversion in winter time than in summer time, it might be reasonable to assume that the yearly cycle affects the speed of mean reversion of stratospheric temperature as well. Stated in another way: Large values of stratospheric temperature variance seem to generate larger dependence on stratospheric temperature the last couple of days. This is a topic for further research.

An explicit deterministic matrix $A(t)$ representing speed of mean reversion of stratospheric temperature is proposed in the following. By introducing time-varying AR(4) parameters such that each month of the year holds fixed parameters, seasonal variability will be adjusted for on a monthly basis. The result of the monthly variation analysis is exploited to define such time varying AR(4) parameters. That is, define monthly parameter values as (remember that the initial dataset $\mathcal{S}$ contains stratospheric temperature values over 40 years)

$$\beta_k^M \triangleq \begin{cases} \beta_k^1 \\ \beta_k^2 \\ \vdots \\ \beta_k^{12} \end{cases} = \begin{cases} E[\boldsymbol{\beta}_k^m], & \text{for } m \in [1, 40] \\ E[\boldsymbol{\beta}_k^m], & \text{for } m \in [41, 80] \\ \quad \vdots \\ E[\boldsymbol{\beta}_k^m], & \text{for } m \in [441, 480], \end{cases}$$

where $M \in \{1, 2, \ldots, 12\}$ represents January to December respectively, $k \in \{1, 2, 3, 4\}$ and $E[\cdot]$ represents the empirical mean. The computed values of

β_1^M, β_2^M, β_3^M and β_4^M are marked in Figs. II.8a-II.8d, respectively. Building on the theory in Sect. II.2.2, the corresponding CAR(4) model is given by the multidimensional OU process in Eq. (II.10) (Thm. II.2.1). Time-dependence in the functions $\alpha_1(t), \dots \alpha_4(t)$ does not matter for the transformation relation between CAR and AR models as long as the discretization scheme is chosen properly ([29]; [12]). That is, in this specific case, the discretization scheme has to be constructed such that the two time points which define the current scheme time step, never belongs to two different months. Hence, the continuous parameter counterparts, $\alpha_k(t)$, of the β_k^M's can be computed by the transformation relation in Eq. (II.7). The $\alpha_k(t)$'s can be considered as 12 level step functions, where each step represents a month of the year. The roots of the eigenvalue equation (Eq. (II.19)) of each of the 12 steps in each of the functions $\alpha_k(t)$ are computed, and their real parts are shown in Fig. II.9. As all the roots have negative real part the stationarity condition of CAR processes is secured. Repeating the

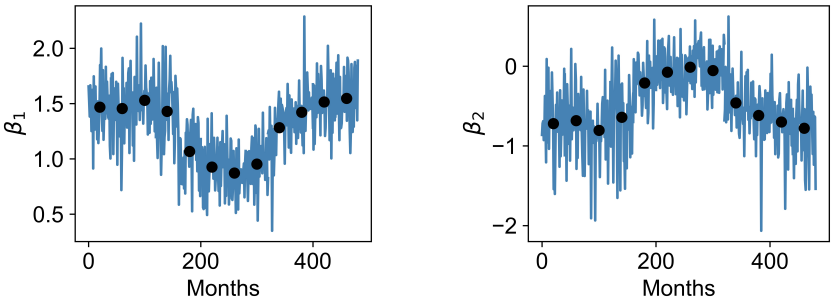

(a) Monthly variability in β_1

(b) Monthly variability in β_2

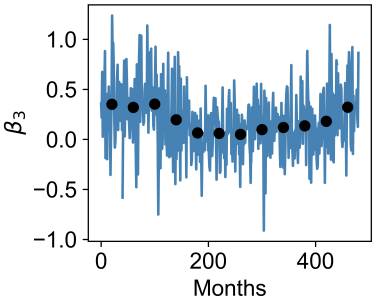

(c) Monthly variability in β_3

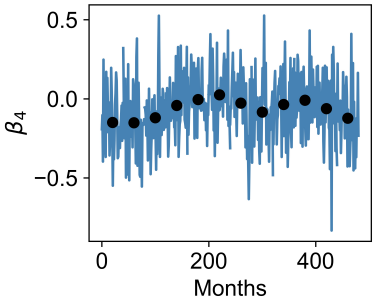

(d) Monthly variability in β_4

Figure II.8: Monthly variability in the four AR parameters of the stratospheric temperature model

analysis in Sect. II.3.5 with model residuals

$$e(t) = X(t) - \sum_{k=1}^{4} \beta_k^M X(t-k),$$

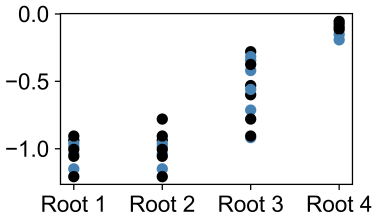

Figure II.9: Real part of the roots of the eigenvalue equations (Eq. (II.19)) of the monthly varying CAR(4) parameters

also gives residuals on the form $e(t) = \sigma(t)\epsilon(t)$, with $\epsilon(t)$ being NIG distributed random variables with memory effects. This confirms that the proposed CAR(4) model from Sect. II.2.2 is suitable to model stratospheric temperature dynamics when driven by the multidimensional OU dynamics in Eq. (II.10), see Thm. II.2.1.

II.5 Conclusions and Further Work

In this paper, a novel stochastic model for stratospheric temperature is proposed. By time series analysis, it was shown that stratospheric temperature can be approximated by an AR(4) process added to a deterministic seasonality function. The seasonality function captures periodical (yearly seasonal) effects as well as a long-term trend to model stratospheric cooling. The scaled model residuals were shown to be NIG distributed. By exploiting the connection between AR and CAR processes, a continuous time model for stratospheric temperature was developed. It was shown that a Lévy driven CAR(4) process with time-dependent volatility is well suited as a continuous time, stochastic model for deseasonalized stratospheric temperature.

Some ideas for future work include incorporating a volatility which is stochastic, not just time-dependent, into the model. Furthermore, it may be of interest to analyze further why large values of variance in the stratospheric temperature seem to generate a larger dependency on stratospheric temperature the previous days. Developing a continuous time, stochastic model for stratospheric wind, potentially as a joint model with stratospheric temperature, is also relevant. In addition, based on the model presented in the current paper, one may exploit stratosphere-troposphere coupling in order to develop improved methods for pricing of weather derivatives (on surface-level). A current work in progress is to develop a dual model for stratospheric temperature, where winter season and summer season temperatures are studied separately. Such a model is particularly useful when analyzing, for example, pure winter phenomena, such as sudden stratospheric warmings.

Acknowledgements. The PhD grant of M. D. Eggen is funded by NORSAR. This work was supported by the Research Council of Norway, FRIPRO Young Research Talent SCROLLER project, grant number 299897, as well as the

Research Council of Norway FRIPRO/FRINATEK project MADEIRA, grant number 274377.

References

[1] Baldwin, M. P. and Dunkerton, T. J. "Stratospheric harbingers of anomalous weather regimes". In: *Science* vol. 294, no. 5542 (2001), pp. 581–584.

[2] Baldwin, M. P. et al. "100 years of progress in understanding the stratosphere and mesosphere". In: *Meteorological Monographs* vol. 59, no. 1 (2019), pp. 27.1–27.62.

[3] Baldwin, M. P. et al. "Sudden stratospheric warmings". In: *Reviews of Geophysics* vol. 59, no. 1 (2021).

[4] Baldwin, M. P. et al. "The quasi-biennial oscillation". In: *Reviews of Geophysics* vol. 39, no. 2 (2001), pp. 179–229.

[5] Barndorff-Nielsen, O. E. "Normal inverse Gaussian distributions and stochastic volatility modelling". In: *Scandinavian Journal of Statistics* vol. 24, no. 1 (1997), pp. 1–13.

[6] Barndorff-Nielsen, O. E. "Processes of normal inverse Gaussian type". In: *Finance and Stochastics* vol. 2, no. 1 (1997), pp. 41–68.

[7] Barndorff-Nielsen, O. E. and Shephard, N. "Non-Gaussian Ornstein-Uhlenbeck-based models and some of their uses in financial economics". In: *Journal of the Royal Statistical Society. Series B, Statistical Methodology* vol. 63, no. 2 (2001), pp. 167–241.

[8] Benth, F. E. and Khedher, A. "Weak Stationarity of Ornstein-Uhlenbeck Processes with Stochastic Speed of Mean Reversion". In: *The Fascination of Probability, Statistics and their Applications*. Ed. by Podolskij, M. et al. Cham: Springer International Publishing, 2015, pp. 153–189.

[9] Benth, F. E. and Šaltytė Benth, J. "Dynamic pricing of wind futures". In: *Energy Economics* vol. 31, no. 1 (2009), pp. 16–24.

[10] Benth, F. E. and Šaltytė Benth, J. *Modeling and Pricing in Financial Markets for Weather Derivatives*. World Scientific, 2013.

[11] Benth, F. E. and Šaltytė Benth, J. "Stochastic modelling of temperature variations with a view towards weather derivatives". In: *Applied Mathematical Finance* vol. 12, no. 1 (2005), pp. 53–85.

[12] Benth, F. E., Šaltytė Benth, J., and Koekebakker, S. *Stochastic Modelling of Electricity and Related Markets*. Vol. 11. World Scientific, 2008.

[13] Benth, F. E. and Taib, C. M. I. C. "On the speed towards the mean for CARMA processes with applications to energy markets". In: *Available at http://www.iot.ntnu.no/ef2012/backup/files/papers/37.pdf* (2012).

[14] Benth, F. E. and Taib, C. M. I. C. "On the speed towards the mean for continuous time autoregressive moving average processes with applications to energy markets". In: *Energy Economics* vol. 40 (2013), pp. 259–268.

[15] Benth, F. E. et al. "Futures pricing in electricity markets based on stable CARMA spot models". In: *Energy Economics* vol. 44 (2014), pp. 392–406.

[16] Berrisford, P. et al. "The ERA-Interim archive Version 2.0". In: *Available at https://www.ecmwf.int/en/elibrary/73682-era-interim-archive-version-20* (2011).

[17] Brockwell, P. J. "Lévy-driven CARMA processes". In: *Annals of the Institute of Statistical Mathematics* vol. 53, no. 1 (2001), pp. 113–124.

[18] Brockwell, P. J. "Recent results in the theory and applications of CARMA processes". In: *Annals of the Institute of Statistical Mathematics* vol. 66, no. 4 (2014), pp. 647–685.

[19] Brockwell, P. J. "Representations of continuous-time ARMA processes". In: *Journal of Applied Probability* vol. 41, no. A (2004), pp. 375–382.

[20] Brockwell, P. J. and Lindner, A. "Prediction of Lévy-driven CARMA processes". In: *Journal of Econometrics* vol. 189, no. 2 (2015), pp. 263–271.

[21] Butler, A. et al. "Sub-Seasonal Predictability and the Stratosphere". In: *Sub-Seasonal to Seasonal Prediction*. Ed. by Robertson, A. and Vitart, F. Elsevier, 2019, pp. 223–241.

[22] Butler, A. H. et al. "Defining sudden stratospheric warmings". In: *Bulletin of the American Meteorological Society* vol. 96, no. 11 (2015), pp. 1913–1928.

[23] Clewlow, L. and Strickland, C. *Energy Derivatives-Pricing and Risk Management*. Lacima Publishers, 2000.

[24] Cnossen, I., Laštovička, J., and Emmert, J. T. "Introduction to special issue on "Long-term changes and trends in the stratosphere, mesosphere, thermosphere and ionosphere"". In: *Journal of Geophysical Research: Atmospheres* vol. 120, no. 22 (2015), pp. 11401–11403.

[25] Danilov, A. D. and Konstantinova, A. V. "Long-term variations in the parameters of the middle and upper atmosphere and ionosphere (review)". In: *Geomagnetism and Aeronomy* vol. 60, no. 4 (2020), pp. 397–420.

[26] Dee, D. P. et al. "The ERA-Interim reanalysis: configuration and performance of the data assimilation system". In: *Quarterly Journal of the Royal Meteorological Society* vol. 137, no. 656 (2011), pp. 553–597.

[27] Fu, Q., Solomon, S., and Lin, P. "On the seasonal dependence of tropical lower-stratospheric temperature trends". In: *Atmospheric Chemistry and Physics* vol. 10, no. 6 (2010), pp. 2643–2653.

[28] Haynes, P. "Stratospheric dynamics". In: *Annual Review of Fluid Mechanics* vol. 37, no. 1 (2005), pp. 263–293.

[29] Iacus, S. M. *Simulation and Inference for Stochastic Differential Equations: With R Examples*. Springer New York, 2008.

[30] Intergovernmental Panel on Climate Change. *Climate Change 2013 – The Physical Science Basis: Working Group I Contribution to the Fifth Assessment Report of the Intergovernmental Panel on Climate Change*. Cambridge University Press, 2014.

[31] Jones, P. D. and Wigley, T. M. L. "Global warming trends". In: *Scientific American* vol. 263, no. 2 (1990), pp. 84–91.

[32] Karpechko, A., Tummon, F., and WMO Secretariat. "Climate predictability in the stratosphere". In: *WMO Bulletin* vol. 65, no. 1 (2016).

[33] Kitchin, J. "Smooth transitions between discontinuous functions". In: *Available at https://kitchingroup.cheme.cmu.edu/blog/2013/01/31/Smooth-transitions-between-discontinuous-functions/* (2013). (accessed: 09.11.2020).

[34] Levendis, J. D. *Time Series Econometrics: Learning Through Replication*. Springer International Publishing: Imprint: Springer, 2018.

[35] McCormack, J. P. and Hood, L. L. "Apparent solar cycle variations of upper stratospheric ozone and temperature: Latitude and seasonal dependences". In: *Journal of Geophysical Research: Atmospheres* vol. 101, no. D15 (1996), pp. 20933–20944.

[36] Pedatella, N. et al. "How sudden stratospheric warming affects the whole atmosphere". In: *Eos* vol. 99 (2018).

[37] Sévellec, F. and Drijfhout, S. S. "A novel probabilistic forecast system predicting anomalously warm 2018-2022 reinforcing the long-term global warming trend". In: *Nature Communications* vol. 9, no. 1 (2018), pp. 3024–3024.

[38] Steiner, A. K. et al. "Observed temperature changes in the troposphere and stratosphere from 1979 to 2018". In: *Journal of Climate* vol. 33, no. 19 (2020), pp. 8165–8194.

[39] Vallis, G. K. "The Stratosphere". In: *Atmospheric and Oceanic Fluid Dynamics: Fundamentals and Large-Scale Circulation*. Cambridge University Press, 2017, pp. 627–671.

[40] Zapranis, A. and Alexandridis, A. "Modelling the temperature time-dependent speed of mean reversion in the context of weather derivatives pricing". In: *Applied Mathematical Finance* vol. 15, no. 4 (2008), pp. 355–386.

Appendix A

A brief survey of topics in linear functional analysis

In this work it is assumed that the reader is familiar with basic real analysis theory and terminology. The following is meant as a reminder of important concepts within the field of linear functional analysis, as well as an introduction of relevant notation for this thesis. A final goal is to recall theory needed in order to discuss numerical estimation methods of SPDEs. The theory presented in this appendix is exclusively based on [1], [2], [3] and [4], and is not meant as a stand-alone chapter produced by the author.

A.1 Banach spaces

To discuss linear functional analysis we need to prescribe in what space given functions are situated, giving basic and sometimes necessary properties. First, recall that a metric space (M, d) is defined by some set M on which a function (metric) $d : M \times M \to \mathbb{R}$ is defined. Equip a vector space V with a norm, that is a function $\|\cdot\|_V : V \to \mathbb{R}$. Norms induces metrics, hence $(V, \|\cdot\|_V)$ is a normed vector space as well as a metric space. In this work we will usually work under $(\mathbb{R}^n, \|\cdot\|_2)$, for some $n \in \mathbb{N}$, where $\|\cdot\|_2$ is the Euclidean norm. Further, complete normed vector spaces, also called Banach spaces, play an important role in applications. Note that $(\mathbb{R}^n, \|\cdot\|_2)$ is a Banach space. With a notion of what a Banach space is, we will further introduce some concepts useful for the study of SPDEs in infinite-dimensional spaces.

We follow [2], and denote by $\mathcal{D}_j \coloneqq \partial/\partial x_j$ the partial derivative with respect to an element x_j, $j \in \mathbb{N}$. Given a multi-index $\alpha = (\alpha_1, \ldots, \alpha_n)$ with $\|\alpha\|_1 \coloneqq \alpha_1 + \cdots + \alpha_n$, we define

$$\mathcal{D}^\alpha \coloneqq \mathcal{D}_1^{\alpha_1} \cdots \mathcal{D}_n^{\alpha_n}, \quad \mathcal{D}^\alpha u = \frac{\partial^{\|\alpha\|_1} u}{\partial x_1^{\alpha_1} \cdots \partial x_n^{\alpha_n}}, \quad u \in B. \tag{A.1}$$

Furthermore, given a Banach space $(B, \|\cdot\|_B)$ and a bounded domain $D \in \mathbb{R}^n$, define the set of continuous functions $u : D \to B$ as $C(D, B)$, and equip it with the norm

$$\|u\|_\infty \coloneqq \sup_{x \in \bar{D}} \|u(x)\|_B.$$

Similarly define $C^r(D, B)$, $r \in \mathbb{N}$, as the set of functions u satisfying $\mathcal{D}^\alpha u \in C(D, B)$, where $\|\alpha\|_1 \leq r$, and equip it with the norm

$$\|u\|_{C^r(\bar{D}, B)} \coloneqq \sum_{0 \leq \|\alpha\|_1 \leq r} \|\mathcal{D}^\alpha u\|_\infty.$$

The defined sets $C(D, B)$ and $C^r(D, B)$ with their respective norms are Banach spaces [2]. These spaces are convenient to use in the field of partial differential equations, as they reflect regularity of functions.

As we are considering stochastic partial differential equations in this thesis, some results on integral theory are introduced. We start by defining Bochner's integral.

Definition A.1.1 ([4], Definition on page 132)**.** A function $u(z)$ defined on a measure space $(Z, \mathcal{B}, m)$ with values in a Banach space B is said to be Bochner m-integrable, if there exists a sequence of finitely-valued functions $\{u_n(z)\}$ which z-converges to $u(z)$ m-a.e. in such a way that

$$\lim_{n\to\infty} \int_Z \|u(z) - u_n(z)\|_B m(dz) = 0, \quad z \in Z.$$

For any set $F \in \mathcal{B}$, the Bochner m-integral of $u(z)$ over F is defined by

$$\int_F u(z)m(dz) = \lim_{n\to\infty} \int_Z C_F(z)u_n(z)m(dz), \quad z \in Z,$$

(with z-convergence) where C_F is the defining function of the set F.

We will usually work under appropriate measure spaces $(\Omega, \mathcal{F}, \mu)$, where Ω is a set, $\mathcal{F}$ is a class of subsets being a Borel σ-algebra, and the function $\mu : \mathcal{F} \to \bar{\mathbb{R}}^+$ is a measure. Given the measure space $(\Omega, \mathcal{F}, \mu)$ and a Banach space $(B, \|\cdot\|_B)$, define by $L^p(\Omega, B)$ the set of $\mathcal{F}$-measurable functions $u : \Omega \to B$ such that $\|u\|_{L^p(\Omega,B)} < \infty$, where

$$\|u\|_{L^p(\Omega,B)} \coloneqq \left(\int_\Omega \|u(\omega)\|_B^p d\mu(\omega) \right)^{1/p}, \quad \omega \in \Omega,$$

for $1 \leq p < \infty$. In this case $L^p(\Omega, B)$ is a Banach space.

A.2 Hilbert spaces

In the last section we recalled the definition of Banach spaces and introduced some relevant examples. Note that Banach spaces are equipped with a norm that generalizes the concept of vector lengths, classically thought of as the Euclidean norm $\|\cdot\|_2$. Another useful geometric concept is the angle, classically given by the scalar product as $\langle u, v\rangle_2 = \|u\|_2\|v\|_2 \cos\theta$, where we have the relation $\|u\|_2 = \sqrt{\langle u, u\rangle_2}$. As for the norm, the analogue generalization to the scalar product is the inner product, being a function $\langle\cdot,\cdot\rangle_V : V \times V \to \mathbb{R}$ (or $\mathbb{C}$) with fixed properties on a real (complex) vector space V. A Banach space equipped with a real (complex) inner product is called a real (complex) Hilbert space.

A.2.1 Orthonormal basis

The advantage with Hilbert spaces is that they can be spanned using orthogonality. That is, given a Hilbert space H, vectors from a sequence

$\{v_i : i \in \mathbb{N}\} \subset H$ are said to be orthogonal when $\langle v_i, v_j \rangle_H = 0$ for $i, j \in \mathbb{N}$, $i \neq j$. With the additional property $\|v_i\|_H = 1$, for all $i \in \mathbb{N}$, $\{v_i : i \in \mathbb{N}\}$ is said to be an orthonormal sequence, and we often write $e_i \coloneqq v_i$, $i \in \mathbb{N}$, in that case. Finally, $\{e_i : i \in \mathbb{N}\}$ forms an orthonormal basis for H when $\overline{\text{Sp}}\{e_i : i \in \mathbb{N}\} = H$. Given an orthonormal basis, any vector $v \in H$ can be decomposed as $v = \sum_{i=1}^{\infty} \langle v, e_i \rangle_H e_i$. Recall that such decomposition holds for finite-dimensional Hilbert spaces as well. An important difference between finite and infinite dimensions is that infinite-dimensional Hilbert spaces are separable if and only if they have an orthonormal basis, however, all finite-dimensional Hilbert spaces are separable.

A.2.2 The L^2 space

With the above introduction, it is straight forward to see that the inner product space $(\mathbb{R}^n, \|\cdot\|_2, \langle \cdot, \cdot \rangle_2)$ is a real Hilbert space with inner product $\langle u, v \rangle_2 \coloneqq u_1 v_1 + u_2 v_2 + \cdots + u_n v_n$, $u, v \in \mathbb{R}^n$. We now introduce another important example of Hilbert spaces. Let $(\Omega, \mathcal{F}, \mu)$ be a measure space as defined in Section A.1, and let $(H, \|\cdot\|_H)$ be a Hilbert space with $\|\cdot\|_H$ induced by the inner product $\langle \cdot, \cdot \rangle_H$[1]. Then the set $L^2(\Omega, H)$ is a Hilbert space with inner product

$$\langle u, v \rangle_{L^2(\Omega,H)} \coloneqq \int_\Omega \langle u(\omega), v(\omega) \rangle_H d\mu(\omega), \quad \omega \in \Omega.$$

The L^2 space plays an important role in considerations of stochastic processes.

A.2.3 Stochastic processes in Hilbert space

We will present random variables taking values in a Hilbert space equipped with the corresponding Borel σ-algebra, that is the measurable space $(H, \mathcal{B}(H))$. An important feature is that families of such random variables with well-defined moments form Banach and Hilbert spaces.

The most important family of spaces in this thesis is the Banach spaces $L^p(\Omega, H)$. That is, given a probability space $(\Omega, \mathcal{F}, P)$ and a Hilbert space $(H, \|\cdot\|_H)$, $L^p(\Omega, H)$ with $1 \leq p < \infty$ is the space of H-valued $\mathcal{F}$-measurable random variables $X : \Omega \to H$ satisfying $E[\|X\|_H^p] < \infty$, with norm

$$\|X\|_{L^p(\Omega,H)} \coloneqq \left(\int_\Omega \|X(\omega)\|_H^p dP(\omega) \right)^{1/p} = E\left[\|X\|_H^p\right]^{1/p}.$$

Note that the case $p = 2$ forms a Hilbert space with inner product

$$\langle X, Y \rangle_{L^2(\Omega,H)} \coloneqq \int_\Omega \langle X(\omega), Y(\omega) \rangle_H dP(\omega) = E\left[\langle X, Y \rangle_H\right],$$

[1] In this thesis we usually denote the norm and inner product on H as $|\cdot|$ and $\langle \cdot, \cdot \rangle$ respectively.

where $\langle \cdot, \cdot \rangle_H$ is the inner product on H.

We give the definition of the specific case when a random variable is H-valued Gaussian random variable.

Definition A.2.1 ([2])**.** Let H be a real Hilbert space. An H-valued random variable X is Gaussian if $\langle X, \phi \rangle$ is a real valued Gaussian random variable for all $\phi \in H$.

For the multivariate case we have to introduce a covariance operator. When H is a separable Hilbert space and X is an H-valued Gaussian with mean $\mu = E[X]$, we have that $X \in L^2(\Omega, H)$. The associated covariance operator is the linear operator $\mathcal{C} : H \to H$ satisfying

$$\langle \mathcal{C}\phi, \psi \rangle \coloneqq \mathrm{Cov}\left(\langle X, \phi \rangle, \langle Y, \psi \rangle\right), \quad \forall \phi, \psi \in H.$$

The covariance operator is a well-defined symmetric, non-negative trace class operator on X. Also note that $\langle \mathcal{C}\phi, \phi \rangle = \mathrm{Var}\langle X, \phi \rangle$ for any $\phi \in H$. We say that X is distributed as $X \sim N(\mu, \mathcal{C})$.

Finally, we have what we need introduce stochastic processes in Hilbert space. Suppose given a set $T \subset \mathbb{R}$. An H-valued random variable is a function $X : T \times \Omega \to H$. We often write $X(t) \coloneqq X(t, \omega)$, with $t \in T, \omega \in \Omega$. The set $\{X(t)\}_{t \in T}$ is referred to as an H-valued stochastic process. For a fixed $\omega \in \Omega$, $X(\cdot, \omega)$ is called a sample path as usual. A special case of Gaussian random processes in Hilbert space, that is the Q-Wiener process, is introduced in Section. 1.3.2.

A.3 Linear operators

Notation and some concepts for bounded linear operators, including some important examples, are presented in Section A.3.1. An important example of bounded linear operators are the Hilbert-Schmidt operators. This class of operators is defined in Section A.3.2. Finally, Section A.3.3 introduces unbounded linear operators, and we consider a specific class of unbounded operators with well-defined powers.

A.3.1 Bounded linear operators

Given two normed linear spaces X and Y, we denote by $\mathcal{L}(X, Y)$ the normed linear space of all bounded linear operators $T : X \to Y$, meaning that T satisfies

$$\|T\|_{\mathrm{op}} \coloneqq \sup\{\|T(x)\|_Y : \|x\|_X \leq 1\}.$$

Note that $\|\cdot\|_{\mathrm{op}} : \mathcal{L}(X, Y) \to \mathbb{R}$ is a norm on $\mathcal{L}(X, Y)$, and recall that all bounded linear operators are continuous. When in addition Y is complete, that is when Y is a Banach space, $\mathcal{L}(X, Y)$ is also a Banach space. Furthermore, when $Y = \mathbb{R}$, we say that $T : X \to \mathbb{R}$ is a bounded linear functional, and in this case we refer to $\mathcal{L}(X) \coloneqq \mathcal{L}(X, \mathbb{R})$ as the dual space of X. Often, the dual space of X is denoted X'. Riesz representation theorem is an important theorem about characterization of bounded linear functionals.

Theorem A.3.1 ([2], Theorem 1.57)**.** *Let H be a Hilbert space with inner product $\langle \cdot, \cdot \rangle$ and let φ be a bounded linear functional on H. There exists a unique $v_\varphi \in H$ such that*

$$\langle v_\varphi, v \rangle = \varphi(v), \quad \forall v \in H.$$

Riesz representation theorem (Theorem A.3.1) provides existence and uniqueness of a vector v_φ representing a given bounded linear functional φ.

We continue with defining projections in Hilbert spaces and state their properties. First, we recall a result about linear subspaces.

Lemma A.3.2 ([3], Lemma 3.25)**.** *If H is a Hilbert space and $Y \subset H$ is a linear subspace, then Y is a Hilbert space if and only if Y is closed in H.*

Now, given a separable Hilbert space H with orthonormal basis $\{e_i : i \in \mathbb{N}\}$ and a linear subspace $Y \coloneqq \{e_1, \dots e_N\}$, there exists a projection from H to Y. That is, given a vector $v \in H$ and an orthogonal projection $P : H \to Y$ we have

$$Pv = \sum_{i=1}^{N} \langle v, e_i \rangle e_i,$$

with properties $P^2 = P$, $|Pv| \leq |v|$ and $|v - Pv| \to 0$ as $N \to \infty$. Finally, we know from Lemma A.3.2 that $\bar{Y}$ is a finite-dimensional Hilbert space.

Finally, the class of symmetric linear operators is defined for the special case of bounded linear operators on a Hilbert space.

Definition A.3.3 ([2], Definition 1.69)**.** $T \in \mathcal{L}(H)$ is symmetric on a Hilbert space H if

$$\langle Tu, v \rangle = \langle u, Tv \rangle, \quad \text{for any } u, v \in H.$$

A.3.2 Hilbert-Schmidt operators

The Hilbert-Schmidt operators are bounded linear operators, and defined as follows.

Definition A.3.4 ([2], Definition 1.60)**.** Let H, U be separable Hilbert spaces with norms $|\cdot|$, $\|\cdot\|_U$ respectively. For an orthonormal basis $\{e_j : j \in \mathbb{N}\}$ of U, define the Hilbert-Schmidt norm

$$\|T\|_{\mathrm{HS}(U,H)} \coloneqq \left(\sum_{j=1}^{\infty} \|Te_j\|_U^2 \right)^{1/2}.$$

The set $\mathrm{HS}(U, H) \coloneqq \{T \in \mathcal{L}(U, H) : \|T\|_{\mathrm{HS}(U,H)} < \infty\}$ is a Banach space with the Hilbert-Schmidt norm. An operator $T \in \mathrm{HS}(U, H)$ is known as a Hilbert-Schmidt operator. We write $\|T\|_{\mathrm{HS}} \coloneqq \|T\|_{\mathrm{HS}(H,H)}$ if $U = H$.

In the study of SPDEs we are interested in integral operators. Given a domain D, an integral operator T on $L^2(D)$ with kernel $G \in L^2(D \times D)$ is given by

$$(Tu)(x) \coloneqq \int_D G(x,y)u(y)dy, \tag{A.2}$$

for $x, y \in D$ and $u \in L^2(D)$. The integral operator in Eq. (A.2) is a Hilbert-Schmidt operator on $L^2(D)$, and any Hilbert-Schmidt operator on $L^2(D)$ can be written as Eq. (A.2), meaning that $\|T\|_{\text{HS}} = \|G\|_{L^2(D\times D)}$.

A.3.3 Unbounded linear operators and powers

Unbounded linear operators occur in the study of (S)PDEs, as the differential operators are unbounded. We denote a linear operators as A, and for a given Hilbert space H we introduce the domain of linear operators, $\mathcal{D}(A)$, as $A : \mathcal{D}(A) \subset H \to H$. The following assumption is sufficient for defining powers of linear operators.

Assumption A.3.5. *Assume that A has an orthonormal basis of eigenfunctions $\{e_i : i \in \mathbb{N}\}$ with corresponding eigenvalues $\lambda_i > 0$ ordered so that $\lambda_{i+1} \geq \lambda_i$. That is, the relation $(\lambda_i - A)e_i = 0$ holds, where $0 \neq e_i \in \mathcal{D}(A)$.*

In the current setup we have that $Au = \sum_{i=1}^{\infty} \lambda_i \langle u, e_i\rangle e_i$ for $u \in \mathcal{D}(A)$. This further implies that A is self-adjoint, meaning that $\langle Au, v\rangle = \langle u, Av\rangle$ holds for all $u, v \in \mathcal{D}(A)$. A second property we can introduce for A in the given setting is the fractional power

$$A^\alpha u \coloneqq \sum_{i=1}^{\infty} \lambda_i^\alpha u_i e_i, \tag{A.3}$$

for constant $\alpha \in \mathbb{R}$ and functions $u = \sum_{i=1}^{\infty} u_i e_i$, where $u_i \in \mathbb{R}$. The corresponding domain $\mathcal{D}(A^\alpha)$ is defined as the set of functions u for which $A^\alpha u \in H$ holds. Further, $\mathcal{D}(A^\alpha)$ is a Hilbert space with inner product $\langle u, \nu\rangle_\alpha \coloneqq \langle A^\alpha u, A^\alpha \nu\rangle$. In [2], precise statements about regularity of solutions are made made using fractional power norms.

Finally, we recall a result from Lemma 1.89 in [2]. This result is useful in the study of weak solutions of SPDEs.

Lemma A.3.6 ([2], Lemma 1.89 (ii))**.** *Let Assumption A.3.5 hold. Then*

$$\langle A^{1/2}u, A^{1/2}\nu\rangle = \langle Au, \nu\rangle$$

for $u \in \mathcal{D}(A)$ and $\nu \in \mathcal{D}(A^{1/2})$.

A.4 Sobolev spaces

As stated in [2]; just as $C^r(D, B)$ (see Section A.1) describes the regularity of continuous functions, Sobolev spaces describe the regularity of integrable

functions. In this section we introduce the Sobolev space for Lebesgue-integrable functions, as they are important within the theory of (stochastic) partial differential equations. Note that Definitions A.4.1 and A.4.2 in this section are simplified versions of analogous definitions in [2].

First we define the concept of weak derivatives, such that (stochastic) partial differential equations involving functions that are not differentiable in the traditional sense can be assessed. In the following, assume given a domain $D \in \mathbb{R}^n$.

Definition A.4.1 ([2], Definition 1.42)**.** We say a measurable function $\mathcal{D}^\alpha u : D \to \mathbb{R}$ is the α-th weak derivative of a measurable function $u : D \to \mathbb{R}$ if

$$\int_D \mathcal{D}^\alpha u(x) f(x) dx = (-1)^{\|\alpha\|_1} \int_D u(x) \mathcal{D}^\alpha f(x) dx, \quad \forall f \in C_c^\infty(D).$$

Note that $C_c^\infty(D)$ denotes the set of infinitely differentiable functions with compact support on D, and that $f \in C_c^\infty(D)$ is referred to as a test function. As noted in [2], test functions from this particular space are used because they are differentiable, zero outside the domain[2] and dense in $L^2(D)$.

Further, we define Sobolev spaces. We will see that functions in Sobolev spaces admit well-defined[3] weak solutions of (stochastic) partial differential equations.

Definition A.4.2 ([2], Definition 1.44)**.** Let D be a domain. For $p \geq 1$, the Sobolev space $W^{r,p}(D)$ is the set of functions whose weak derivatives up to order $r \in \mathbb{N}$ are in $L^p(D)$. That is,

$$W^{r,p}(D) \coloneqq \{u : \mathcal{D}^\alpha u \in L^p(D) \text{ if } \|\alpha\|_1 \leq r\}.$$

Recall that $r \in \mathbb{N}$ represents the maximum order of well-defined derivatives.

Important examples of Sobolev spaces are $W^{r,2}(D)$. The space $W^{r,2}(D)$ is a Hilbert space with inner product

$$\langle u, v \rangle_{H^r(D)} \coloneqq \sum_{0 \leq \|\alpha\|_1 \leq r} \langle \mathcal{D}^\alpha u, \mathcal{D}^\alpha v \rangle_{L^2(D)},$$

where $H^r(D) \coloneqq W^{r,2}(D)$.

When dealing with boundary-value problems, we have to work under Sobolev spaces incorporating the boundary conditions. We define the Sobolev space incorporating the boundary conditions used in thesis, that is the two-dimensional periodic boundary condition. First, the concept of completion is recalled.

Definition A.4.3 ([2], Definition 1.46)**.** X is the completion of Y with respect to $\|\cdot\|$ if X equals the union of the space Y and the limit points of sequences in Y with respect to $\|\cdot\|$.

The two-dimensional second order periodic boundary condition Sobolev space, H^2_{per}, is defined as follows.

[2] Not noted in [2], but is also used in the derivation of the result

[3] Away from the boundary

Definition A.4.4 ([2], Definition 1.47 (iii))**.** Let $D \coloneqq (a_1, b_1) \times (a_2, b_2) \subset \mathbb{R}^2$ be a domain. H^2_{per} is the completion with respect to the $H^2(D)$ norm of the set of $u \in C^\infty(\bar{D})$ such that

$$\frac{\partial^r}{\partial x_1^r} u(a_1, y) = \frac{\partial^r}{\partial x_1^r} u(b_1, y), \quad \frac{\partial^r}{\partial x_2^r} u(x, a_2) = \frac{\partial^r}{\partial x_2^r} u(x, b_2),$$

for $x \in (a_1, b_1)$, $y \in (a_2, b_2)$, and $r = 0, 1, 2$. It is a Hilbert space with the $H^2(D)$ inner product.

We will use the Hilbert space H^2_{per} in applications when considering the two-dimensional heat equation.

A.5 Strongly continuous operator semigroups

An introduction to strongly continuous semigroups is given, as they are essential in our assessment of the stochastic heat equation. That is, the spatial coordinate $x \in \mathbb{R}^d$ of the solution of the stochastic heat equation is suppressed, and the solution is interpreted as a function with values in a Hilbert space. The study of existence and uniqueness of solutions of such Hilbertian SODEs leads to a solution operator, $\mathcal{S}(t)$, also called a semigroup[4].

The definition of strongly continuous semigroups is as follows.

Definition A.5.1 ([1], Definition 1.1)**.** A family $\{\mathcal{S}(t)\}_{t \geq 0}$ of bounded linear operators on a Banach space B is called a strongly continuous (one-parameter) semigroup (or C_0-semigroup[5]) if it satisfies the function equation

$$\begin{cases} \mathcal{S}(t+s) = \mathcal{S}(t)\mathcal{S}(s) & \text{for all } t, s \geq 0, \\ S(0) = I, \end{cases}$$

where I is the identity operator on B, and is strongly continuous in the following sense. For every $v \in B$ the orbit maps

$$\xi_v : t \to \xi_v(t) \coloneqq \mathcal{S}(t)v$$

are continuous from $\mathbb{R}^+$ into B for every $v \in B$.

In this case B is considered the state space of a system, t as time, and $\mathcal{S}(t)$ as a map describing the change of the given state at $t = 0$ into the state $\mathcal{S}(t)v$ at time t. Note that the operator semigroup maps as $\mathcal{S}(t) : B \to B$.

On a dense subspace of the Banach space B on which the strongly continuous operator semigroup is defined the semigroups' so-called generator, A, can be defined. As we will see, the generators domain, $\mathcal{D}(A)$, is the subspace on which the orbit map $\xi_v : t \to \mathcal{S}(t)v \in B$ is differentiable.

[4] Semigroup for solutions in $\mathbb{R}^+$, group for solutions in $\mathbb{R}$

[5] Although we prefer the terminology 'strongly continuous', we point out that the symbol C_0 abbreviates 'Cesàro summable of order 0'

Definition A.5.2 ([1], Definition 1.2)**.** The generator $A : \mathcal{D}(A) \subseteq B \to B$ of a strongly continuous semigroup $\{\mathcal{S}(t)\}_{t\geq 0}$ on a Banach space B is the operator

$$Av \coloneqq \frac{d}{dt}\xi_v(0) = \lim_{h\to 0}\frac{1}{h}(\mathcal{S}(h)v - v),$$

defined for every v in its domain

$$\mathcal{D}(A) = \{v \in B : \xi_v \text{ is differentiable in } \mathbb{R}^+\}.$$

Note that it is proved in Lemma 1.1 of [1] that right differentiability of $\xi_v(\cdot)$ at $t = 0$ is equivalent to that $\xi_v(\cdot)$ is differentiable on $\mathbb{R}^+$. We state some important properties of generators of strongly continuous operator semigroups in the following lemma.

Lemma A.5.3 ([1], Lemma 1.3)**.** *For the generator $(A, \mathcal{D}(A))$ of a strongly continuous semigroup $\{\mathcal{S}(t)\}_{t\geq 0}$, the following properties hold.*

1) *$A : \mathcal{D}(A) \subseteq B \to B$ is a linear operator.*

2) *If $v \in \mathcal{D}(A)$, then $\mathcal{S}(t)v \in \mathcal{D}(A)$ and*

$$\frac{d}{dt}\mathcal{S}(t)v = \mathcal{S}(t)Av = A\mathcal{S}(t)v, \quad \text{for all } t \geq 0.$$

3) *For every $t \geq 0$ and $v \in B$, one has*

$$\int_0^t \mathcal{S}(s)v ds \in \mathcal{D}(A).$$

4) *For every $t \geq 0$, one has*

$$\begin{aligned}\mathcal{S}(t)v - v &= A\int_0^t \mathcal{S}(s)v ds \quad \text{if } v \in B\\ &= \int_0^t \mathcal{S}(s)Av ds \quad \text{if } v \in \mathcal{D}(A).\end{aligned}$$

In general the generator of a strongly continuous operator semigroup is unbounded, however, as stated in Theorem 1.4 of [1], A is closed and densely defined, and determines the semigroup uniquely. For the special case when A is a bounded linear operator, the following result shows that the generated semigroup has a particularly nice characterization. This special case of strongly continuous semigroups is referred to as uniformly continuous semigroups.

Corollary A.5.4 ([1], Corollary 1.5)**.** *For a strongly continuous semigroup $\{\mathcal{S}(t)\}_{t\geq 0}$ on a Banach space B with generator $(A, \mathcal{D}(A))$, the following assertions are equivalent.*

1) *The generator A is bounded; i.e., there exists $M > 0$ such that*

$$\|Av\| \leq M\|v\| \quad \text{for all } v \in \mathcal{D}(A).$$

2) *The domain* $\mathcal{D}(A)$ *is all of* B.

3) *The domain* $\mathcal{D}(A)$ *is closed in* B.

4) *The semigroup* $\{\mathcal{S}(t)\}_{t\geq 0}$ *is uniformly continuous.*

In each case, the semigroup is given by

$$\mathcal{S}(t) = e^{tA} = \sum_{k=0}^{\infty} \frac{t^k A^k}{k!}, \quad t \geq 0.$$

Note that $\|\cdot\|$ denotes the norm on B. Further, $\mathcal{S}(t) = e^{tA}$ is a well-defined bounded operator on B, and note that every uniformly continuous operator semigroup on a Banach space is on this form.

The following result shows that C_0-semigroups are bounded with respect to their operator norm $\|\cdot\|_{\text{op}}$. This is a convenient result when dealing with integrals of semigroups.

Proposition A.5.5 ([1], Proposition 1.4)**.** *For every strongly continuous semigroup* $\{\mathcal{S}(t)\}_{t\geq 0}$*, there exist constants* $w \in \mathbb{R}$ *and* $M \geq 1$ *such that*

$$\|\mathcal{S}(t)\|_{op} \leq Me^{wt},$$

for all $t \geq 0$.

As noted in [4], $\{\mathcal{S}(t)\}_{t\geq 0}$ is called a contraction semigroup of class C_0 if $\|\mathcal{S}(t)\|_{\text{op}} \leq 1$ holds for all $t \geq 0$. Contraction semigroups are used to derive results in this thesis. The next result shows that contraction semigroups are generated by dissipative operators, meaning $\langle Av, v\rangle \leq 0$ for any $v \in \mathcal{D}(A)$. We give a simplified version[6] of a theorem in [4], where the original result holds for Banach spaces.

Theorem A.5.6 ([4], page 250)**.** *Let* A *be a linear operator with domain* $\mathcal{D}(A)$ *and range* $\mathcal{R}(A)$ *both in a complex (or real) Hilbert space* H *such that* A *is dense in* H*. Then* A *generates a contraction semigroup of class* C_0 *in* H *if and only if* A *is dissipative (with respect to any inner product* $\langle u, v\rangle$*) and* $\mathcal{R}(I - A) = H$.

As explained in [1], operator semigroups naturally appear in the initial value problem

$$\begin{cases} \frac{d}{dt}u(t) = Au(t) & \text{for } t \geq 0, \\ u(0) = x, \end{cases}$$

where A is a linear operator on a Banach space B and $x \in B$. That is, if there exists a unique solution u (differentiable on $\mathbb{R}^+$) that holds for each initial value $x \in B$, then

$$\mathcal{S}(t)u \coloneqq u(t, x), \quad t \geq 0, x \in B,$$

defines an operator semigroup. This is the approach we use in this work when considering SPDEs as SODEs in Hilbert space.

[6] This simplified version is sufficient for our application

References

[1] Engel, K.-J. and Nagel, R. *A Short Course on Operator Semigroups*. Springer New York, 2006.

[2] Lord, G. J., Powell, C. E., and Shardlow, T. *An Introduction to Computational Stochastic PDEs*. Cambridge Texts in Applied Mathematics. Cambridge University Press, 2014.

[3] Rynne, B. and Youngson, M. A. *Linear functional analysis*. 2nd Ed. Springer Science & Business Media, 2008.

[4] Yosida, K. *Functional Analysis*. 6th ed. 1995. Classics in Mathematics. Berlin, Heidelberg: Springer Berlin Heidelberg : Imprint: Springer, 1995.